ROLES FOR THE TGF-BETA/BMP AND BETA-CATENIN SIGNALING PATHWAYS IN LUNG DEVELOPMENT AND REPAIR

by

Anna Christine Zemke

BS, Seattle Pacific University, 2001

Submitted to the Graduate Faculty of

The School of Medicine in partial fulfillment

of the requirements for the degree of

Doctor of Philosophy

University of Pittsburgh

2007

UNIVERSITY OF PITTSBURGH

SCHOOL OF MEDICINE

This dissertation was presented

by

Anna Christine Zemke

It was defended on

August 29, 2007

and approved by

Committee Chair: Stefan Schlatt, Associate Professor, Department of Cell Biology & Physiology

Jeffrey Brodsky, Professor, Department of Biological Science

Naftali Kaminski, Associate Professor, Department of Medicine

Tim Oury, Associate Professor, Department of Pathology

Dissertation Advisor: Barry Stripp, Associate Professor, Department of Cell Biology & Physiology

ROLES FOR THE TGF-BETA/BMP AND BETA-CATENIN SIGNALING PATHWAYS IN LUNG DEVELOPMENT AND REPAIR

Anna Christine Zemke, PhD

University of Pittsburgh, 2007

The conducting airway epithelium is lined with a heterogeneous population of secretory and ciliated cells. Inflammation and inhaled toxicants can damage the epithelial lining, which is rapidly repaired through a tissue stem cell-mediated process. Incomplete and disrupted repair contribute to the development of chronic lung disease. The signaling pathways that orchestrate airway epithelial repair are largely unknown, however roles for both Wnt/β-catenin and TGFβ/BMP signaling have been suggested. The TGFβ/BMP family of signaling molecules regulates lung branching morphogensis, epithelial repair and carcinogenesis. To determine the role of Smad4 in these processes, cell type specific deletion of Smad4 was used to block Smad-dependent signaling. Loss of Smad4-dependent signaling during embryogenesis markedly increased airway branching. These mice later developed adenomas, reflecting the role of Smad4 in lung tumor suppression. Epithelial repair was not influenced by loss of Smad-dependent signaling. These data indicated a role for Smad-dependent signaling in branching morphogenesis and tumor suppression, but not epithelial repair.

Next, the necessity for Wnt/β-catenin signaling in airway epithelial homeostasis and repair was determined. Wnt/β-catenin signaling regulates epithelial homeostasis in the intestine

and skin, but the role of this pathway in the airways is unknown. This hypothesis was tested through the generation of mice with airway-specific loss of β-catenin. A β-catenin null airway epithelium repaired normally in an *in vivo* injury model system. No defects in epithelial homeostasis or differentiation were seen in the absence of β-catenin. We concluded that β-catenin is not a principal regulator of airway homeostasis in the adult conducting airway epithelium. Finally, my dissertation research further characterized the molecular phenotype of the airway secretory cell population. Two ablation models were used to deplete secretory cells *in vivo*. Microarray analysis was performed following secretory cell ablation to identify genes that might be expressed within the secretory population. Four novel secretory cell markers were identified by this approach. In conclusion, this dissertation reports on the determination of roles for Wnt/β-catenin and TGFβ/BMP signaling in the airway epithelium and describes further characterization of the molecular repertoire of the airway secretory cell population.

TABLE OF CONTENTS

LIST OF TABLES

LIST OF FIGURES

ACKNOWLEDGEMENTS

Many people have contributed to the scientific work described here, my research training, and all the fun I have had the past several years.

Barry Stripp, my dissertation advisor, has been a superb mentor and dedicated teacher. He has provided enthusiasm, advice on experimental design, and a lot of encouragement.

Current and former Stripp Lab members have made science a lot of fun, and the Cellomics building a great place to eat lunch, including **Jeff, Ifeoma,** and **Carlos**. Fellow graduate students **Josh** and **Roxana** have provided good scientific discussion and encouragement. **Brian** provided technical assistance in the lab, and we had a lot of fun the past year. **Chris** provided assistance with mouse husbandry on a set of projects that involved many mice. Chris also introduced me to puppies, kittens, baby donkeys, a baby pony, assorted trick-performing poultry, assorted farm animals, a pair of recently hatched emus, one adorable fawn, killdeer, Ben-the-cat, crowds of Eastern toads, and a "baby" snapping turtle. **Sue** encouraged scientific rigor and helped keep these project focused.

Donna Beers-Stolz provided imaging assistance at the final hours after the lab had moved.

Various **Zemkes**, most especially my parents, have been a constant source of support. They have patiently listened to details about lab work and provided advice over the past 6 years in Pittsburgh. My mother, Diane Zemke, helped proofread pages upon pages of dissertation and papers

.

ABBREVIATIONS

AOX3: aldehyde oxidase 3APC: adenomatous polyposis coli

BMP: Bone morphogenic protein

Bmpr1a : Bone morphogenic protein receptor 1a

BrdU: Bromodeoxyuridine

CCSP: Clara cell secretory protein, Scgb1a1

CCSP-HSVtK: mice with CCSP driving HSVtK

CGRP: Calcitonin gene related peptide

Cldn10: Claudin 10

Cyp2f2: Cytochrome P 450 2f2

DAPI: 4, 6, diamidino-2-phenylindole

DPC: days post-coitum

E: embryonic

EMTU: Epithelial-mesenchymal trophic unit

FAP: familial adenomatous polyposis

Fmo3: Flavin monooxygenase 3

FoxJ1: Forkhead box J1

HSVtK: Herpes simplex virus thymidine kinase

LacZ: beta-D-galactosidase

MCM: mucous cell metaplasia

NEB: neuroepithelial body

P: Postnatal day

PAS: periodic acid Schiff stain

PNEC: pulmonary neuroendocrine cell

Pon1: Paraoxonase 1

SEM: standard error on the mean

SPC: Surfactant protein C

TA cell : Transit amplyfying cell

Tcf: T-cell factor

TGF-β: Transforming growth factor β

Wnt: Inhibitor of Wingless

X-gal: 5-bromo-4-chloro-3-indolyl-b-D-galactopyranoside

1.0 INTRODUCTION

This chapter contains introductory material about the airway epithelium at homeostasis, lung development, TGFβ/BMP signaling, Wnt/β-catenin signaling, and epithelial repair. Chapter 1 concludes with a description of the specific aims of this dissertation. The following three chapters are descriptions of individual projects. In Chapter 2, the requirement for β-catenin signaling in adult airway epithelial homeostasis and repair is tested. We found no evidence that β-catenin controls stem-cell mediated airway repair. Chapter 3 focuses on three functions of Smad4-dependent signaling in the lung: control of branching morphogenesis, tumor suppression, and regulation of airway epithelial repair. Loss of Smad4 during embryogenesis increases airway branching and causes adenoma formation. We found no evidence that Smad4 regulated homeostasis or repair in the adult conducting airways. As will be apparent from Chapters 2 and 3, one factor limiting our ability to study the airway epithelium, is the lack of molecular markers. Chapter 4 uses microarray analysis to further characterize the molecular repertoire of the Clara cell. A number of phase-1 metabolism enzymes were identified, as well as the novel Clara cell marker Claudin 10. Finally, in Chapter 5, the specific findings of the dissertation will be briefly summarized and put into the context of the field of lung research. One appendix is included, which contains the microarray data generated in Chapter 4.

1.1 GENERAL AIRWAY STRUCTURE AND FUNCTION

1.1.1 Lung anatomy

The lung provides a large surface for diffusion of oxygen and carbon dioxide between the atmosphere and the blood. There are two functional lung compartments: the respiratory zone and the conducting zone. The respiratory zone, consisting of alveoli, alveolar ducts and respiratory bronchioles, is the surface across which gas exchange occurs. The conducting zone is composed of a series of branching airways that carry air from the mouth to the respiratory surfaces. The research contained in this dissertation is focused exclusively on the conducting airway, so while much is known about the alveolar space and the pathology that afflicts it, this introduction will focus on the conducting airway in homeostasis, development, and recovery from acute injury.

1.1.2 Airway Histology

Beginning at the trachea, the airways branch to form bronchi, bronchioles, and eventually terminal bronchioles [1]. In the mouse, the transition between the conducting and respiratory zones is abrupt, with few respiratory bronchioles and alveolar ducts [2]. The cellular composition of the epithelium and airway wall vary with airway location and species [3, 4]. Thus, in the studies described in this dissertation, the particular airway location must be taken into account. From the lumen outward, the conducting airways consist of an epithelial lining, basement membrane, lamina propria, smooth muscle bundles, cartilage or fibrous connective tissue, and adventitia.

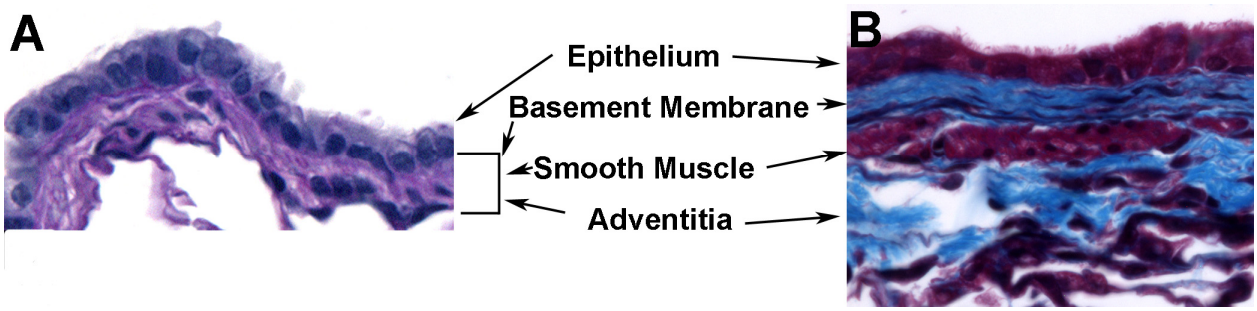

Figure 1: Mouse Airway Histology

Photomicrographs of mouse airway. In Panel A, a proximal mouse airway stained with PAS is seen. The basement membrane appears as a thin, magenta line below the epithelium. The smooth muscle and adventitia are relatively thin. Panel B demonstrates a severely remodeled mouse airway in which airway wall components can be more clearly seen (Trichrome stain). The basement membrane is much thicker and contains collagen (turquoise). Smooth muscle bundles are also more clearly seen. Original magnification of both panels: 40X.

The mouse airway epithelium is pseudostratified in the trachea, and becomes simple columnar within the bronchiolar airways. Beneath the epithelium, a layer of fibroblasts forms a very thin, nearly continuous sheath in close approximation to the epithelium [5]. Smooth muscle bundles which regulate the diameter of the airway are found along most of the conducting airway, becoming thinner distally. In addition, the airway wall is highly innervated, allowing the body to sense and respond to changes in the inspired atmosphere [6]. The functional relationship between these histological compartments is discussed in section 1.7.2.

1.1.3 Cellular Composition of the Airway Epithelium

The mouse airway epithelium is composed of four general categories of cell types: basal, ciliated, secretory, and neuroendocrine cells. The cellular composition and functional properties

of the airway epithelium change in response to injury, so it is important to briefly describe the various cell types found within the epithelium.

Basal cells are small, triangular cells that are found in the trachea and bronchi of healthy adult mice. With severe injury, basal cells with properties of basal cells can extend down into the primary bronchioles [7]. In the absence of injury, basal cells are typically located between the columnar epithelial cells and the basement membrane. Basal cells form the bulk of the proliferative population following tracheal injuries, and serve as the progenitor population for renewal of the proximal airway epithelium [7, 8]. These cells are usually identified by expression of cytokeratins 14 or reactivity to Griffonia simplicifonia isolectin B-4 (GSIB4), although CD151 and other cytokeratins have been used [7, 9].

Ciliated cells are most abundant in the primary bronchi where they make up 50% of all cells, but are found in lower numbers throughout the entire airway tree [3]. Immunoreactivity for acetylated tubulin or the transcription factor FoxJ1 can be used to identify airway ciliated cells [10]. The cells have numerous motile (9+2 microtubule arrangement) cilia on the apical surface. Synchronous ciliary beating moves the airway surface lining fluid proximally, toward the trachea. Particles and pathogens trapped in the airway lining fluid are thus moved out of the lung. Acquisition of FoxJ1 immunoreactive cells first appear at E15.5 days post-coitum (dpc) in the mouse. FoxJ1 triggers ciliogenesis, which takes another day of development to complete [11, 12]. Despite one report to the contrary by Park and colleagues, the preponderance of evidence shows that ciliated cells are post-mitotic [11, 13]. In the adult, bronchiolar epithelium, ciliated cells are derived from Clara cells [14]. Ciliated cells are very sensitive to oxidant injury, but generally resistant to most Clara cell toxins [14, 15].

Nonciliated cells are a mixed population of secretory cells that make up the bulk of cells lining the mouse airway. Secretory cells are categorized as goblet, serous, and Clara cells based on morphology and histochemistry. In homeostasis, goblet and serous cells are found only in the trachea, bronchi, and tracheal submucosal glands, while Clara cells are found in the terminal bronchioles. Goblet cells are terminally differentiated, mucus producing cells. They can be identified by flask shaped cytoplasm containing large PAS positive vesicles or electron-lucent secretory granules [16]. Goblet cells secrete high molecular weight glycoconjugates that regulate the viscoelastic properties of airway lining fluid [17]. Serous cells have electron dense secretory granules containing substances thought to contribute to host defense. Clara cells are the predominant secretory cell type in the mouse airway. The morphological and functional features of Clara cells are discussed extensively in part 1.7 and chapter 5. Briefly, Clara cells are non-ciliated secretory cells that make-up between 50-70% of cells lining the intrapulmonary airways. Clara cells contain abundant secretory vesicles, rough and smooth endoplasmic reticulum. The primary secretory product of the Clara cell is Secretoglobin 1a1 (also known as CCSP), although they produce a variety of other secretory products.

Pulmonary neuroendocrine cells (PNECs) are part of the diffuse endocrine system, which consists of neuroendocrine cells in many organs of the body. PNECs are infrequent cells that occur singly or in small clusters known as neuroepithelial bodies (NEBs). These cells are frequently innervated and secrete a variety of neuropeptides including serotonin, substance P, cholecystekinin, bombesin and calcitonin gene related peptidet (CGRP) [6]. In adulthood, PNECs act as chemosensors that communicate with the vagus nerve [6, 18]. PNECs proliferate in response to acute and chronic chemical injury and can become hyperplastic [19-22]. These cells serve as an airway stem cell niche (described in part 1.7).

1.1.4 Alterations to the airway epithelium in human disease states: Mucus Hypersecretion

Many diseases cause changes in the number and phenotype of various cell types in the airway epithelium. To limit the scope of the discussion, the illustrative example of mucus hypersecretion will be examined. This example will highlight how the signaling pathways associated with disease states can cause changes in the phenotype and representation of airway cells types leading to morbidity.

Diseases that include a strong inflammatory component, such as asthma, cystic fibrosis, and chronic bronchitis, are associated with increased mucus production. Mucus hypersecretion contributes to the airway plugging seen in end-stage cystic fibrosis and fatal asthma attacks. Excess pooled mucus is easily colonized with bacteria. The bacterial colonization causes inflammation which contributes to the downward spiral of exacerbation and airway remodeling seen in chronic bronchitis and cystic fibrosis.

Increased mucus production occurs through two basic mechanisms: expansion of submucosal glands and mucous cell metaplasia. In healthy humans, 90% of mucus in the lung is produced by submucosal glands [23]. These glands are found in the first 10 airway generations and contain 60% serous cells and 40% mucous (goblet) cells. In response to neural stimulation, the submucosal glands can produce large volumes of mucus. In cystic fibrosis, tracheal submucosal glands are larger and extend more distally than in normal lungs [24, 25]. Expanded submucosal glands are also a pathological feature of chronic obstructive pulmonary disease and asthma [26]. It is not clear if increased gland volume is a result of hypertrophy or hyperplasia, although in cystic fibrosis the extension of glands beyond the cartilaginous airways suggests that there is indeed growth of new glands.

All three diseases are also associated with an expansion of mucus secreting cells within the airway epithelium proper, caused by mucous cell metaplasia (MCM). In MCM, secretory cells change phenotypes so that Clara cells which do not normally produce mucins, begin to produce and secrete gel-forming mucins. *Muc5AC* and *Muc5B* are the primary mucins genes induced during MCM [27, 28]. The increase in mucins can be caused by a variety of cytokines and growth factors. Exposure to IL-13, generated by a T_H2 type immune response, increases *Muc5AC* gene transcription and can cause MCM [27, 29]. Epithelial growth factor (EGF) is also required for MCM, both *in vivo* and *in vitro* [30, 31]. Damaging stimuli, including cigarette smoke, mechanical damage, bacterial products, and the presence of inflammatory cells may all activate signaling through EGF (reviewed [32]).

Only the proximal to midlevel intrapulmonary airways are susceptible to mucous cell metaplasia in mouse models of allergic inflammation [33]. What makes the distal airway epithelium resistant to MCM is unknown. In mouse models of allergic inflammation, MCM rapidly resolves following removal of the inciting stimulus. Because MCM is a reversible change, therapies directed against the signaling pathways involved in MCM might be able to alleviate mucus hypersecretion and the associated morbidity.

1.2 FUNCTIONAL PROPERTIES OF THE AIRWAY EPITHELIUM

The airway epithelium is in direct contact with the outside world, and thus must maintain a barrier between the internal and external environments. Most physiologic functions of the airway epithelium are related to protection from chemical and infectious agents.

1.2.1 Physical Barrier function

The airways are lined by a continuous epithelial sheet held together with tight junctions, adherens junctions, and desmosomes [17]. These tight junctions provide a barrier where the movement of water, ions, and macromolecules can be regulated. Water permeability of the entire lung epithelium (alveolar and airway) is high relative to other organs, reflecting the importance of fluid clearance from the airway. Airway epithelial water permeability is regulated by aquaporins 3 and 4 [34]. Paracellullar ion transport is also highly regulated, principally by members of the claudin family [35]. Exposure to cytokines produced during chronic inflammation such as TNFα and INFγ increases airway permeability and may disrupt barrier function [36]. As described below, airway cells will rapidly flatten and migrate to cover physical breaks in the barrier.

1.2.2 Protection from Pathogens

Under normal conditions, the airways are nearly sterile because mucociliary clearance removes any inhaled pathogens. The conducting airways regulate fluid balance to maintain a thin layer of airway lining fluid. This fluid is progressively moved towards the mouth by mucociliary clearance. If mucociliary clearance is decreased, either from decreased ciliary movement or defective regulation of fluid volume, susceptibility to chronic respiratory infections increases [1].

In addition to providing a physical barrier to pathogens and mucociliary clearance, airway epithelial cells express pattern recognition molecules that can directly sense the presence of bacterial products. Pathogenic stimuli cause the airway epithelium to produce cytokines and chemotactic products that augment the immune response [37]. The airway lining fluid also

contains a number of antimicrobial proteins such as IgA, Surfactant Protein A, Surfactant Protein D, and lysozyme, many of which are secreted by Clara and serous cells [38]. The primary secretory product of Clara cells, secretoglobin 1a1 (CCSP) has an immunomodulatory function [39, 40]. The production of immunomodulatory and antibacterial proteins, in addition to cytokines, chemokines, and growth factors, makes the respiratory epithelium an integral part of the lung immune response.

1.2.3 Protection from Xenobiotics

With each breath we inhale a mixture oxygen, nitrogen, carbon dioxide, and water. Depending on the occupational or living environment, we also inhale organic compounds, heavy metals, and organic particulates. The entire cardiac output goes through the lung with each heart beat, where in addition of gas exchange, toxins can be rapidly absorbed into the blood. As witnessed by the effects of gaseous anesthetics, inhaled toxins can fatally depress the central nervous system in the space of a few breaths [41].

To protect against inhaled toxins, the airway and alveolar epithelia express a wide variety of phase-I and phase-II xenobiotic metabolizing enzymes. In particular, members of the cytochrome p450 monooxygenase system are expressed, either in a constitutive or inducible fashion [42-44]. While these enzymes may protect the rest of the body from the toxic effects of the parent compound, detoxifying reactions can produce free radicals or toxic metabolic intermediates that can kill the detoxifying cell [42, 45]. Thus, exposure to xenobiotics can cause necrosis of the respiratory epithelium due to bioactivation of the offending compound to highly reactive metabolites. Each species has unique sensitivities to inhaled toxin depending on which

specific Cyp450 isoforms are expressed in the lung. The unique cellular sensitivities of cells to toxicants based on their capacity to undergo phase I metabolism has been exploited experimentally to understand cellular mechanisms of epithelial repair [41]. Xenobiotic metabolism is discussed in greater detail in chapter 4.

1.3 REPAIR OF THE ADULT AIRWAY EPITHELIUM

The airway epithelium responds rapidly after an acute injury to maintain barrier function. If the response results in a histologically normal epithelium, the term "regeneration" is used. However, in most cases there are remaining areas of abnormality, and the term "repair" is more appropriate. Immediately following an airway injury, the remaining epithelial cells flatten to cover the basement membrane, there is a wave of epithelial proliferation, and finally the newly formed cells differentiate [46]. In addition to the epithelium, fibroblasts underlying the airway proliferate and there are changes in the inflammatory state of the lung. This section will discuss the contribution made by airway stem cells and transit-amplifying cells to epithelial repair, the concept of the epithelial-mesenchymal trophic unit, and two signaling pathways that might coordinate the epithelial response to injury.

1.3.1 Adult Airway Stem Cells

Two properties define a stem cell: the ability to self renew and give rise to more differentiated progeny [47, 48]. Once a stem cell is activated, it can divide asymmetrically to give rise to another stem cell and a more differentiated daughter cell. This daughter cell, termed a transit-

amplifying (TA) cell, is usually highly proliferative. In tissues with multiple cell types, the stem cell may generate TA cells that progressively differentiates into the different cell types found in the tissue. In some cases, a stem cell generates only one differentiated cell type. In this case, both the stem cell and TA cell have the same unipotential differentiation capacity, however the stem cell is capable of indefinite self-renewal while the TA cell is committed to producing more differentiated daughters [47]. The existence of an airway stem cell holds promise because a stem cell could theoretically give rise to an unlimited amount of fully differentiated airway epithelium that could be used to treat a variety of diseases.

1.3.1.1 Evidence for an Airway Stem Cell

The initial evidence for the existence of an airway stem cell came from the naphthalene model of airway injury and repair. Naphthalene exposure kills most of the Clara cells in mice, but a rare, naphthalene-resistant, CCSP-expressing population survives the exposure. The repair process following naphthalene exposure is focal. Small repairing regions are seen at airway bifurcations, near neuroepithelial bodies, and at terminal bronchioles. As these repairing regions enlarge, most regions will merge and the bulk of the epithelium returns to normal. Because of the focal nature of this process, it was possible to conclude that there are progenitor cells located at specific anatomical regions of the lung [49].

What is the phenotype of these progenitor cells? There were two lines of evidence that determined the molecular phenotype of the airway progenitor cells. First, there is much evidence that ciliated cells are post-mitotic. Evans and colleagues used ozone exposure (an oxidant which selectively kills ciliated cells), followed by transmission electron microscopy, to establish that mouse Clara cells proliferate, both to self-renew and generate post-mitotic ciliated cells [14].

More recently, Hogan's group has used lineage tagging to show that FoxJ1 expressing cells do not proliferate [50]. By exclusion, the progenitor population is not ciliated.

Following naphthalene exposure, proliferation is seen in both CCSP-expressing cells and neuroendocrine cells. The neuroepithelial bodies become quite hyperplastic [22]. Because repairing zones are seen surrounding neuroepithelial bodies, the possibility existed that neuroendocrine cells were the progenitor population for the airway epithelium. The alternative hypothesis was that a population of naphthalene-resistant, CCSP-expressing cells preserved within the NEB was responsible for repair. The next approach was to see if restoration of the airway could occur if all CCSP expressing cells were killed (and neuroendocrine cells left undisturbed). To do this, mice were generated that contained herpes viral thymidine kinase driven by the mouse CCSP promoter (termed CCSP-HSVtK mice). Administration of ganciclovir to these mice causes rapid death of all CCSP expressing cells. When mice were continuously given ganciclovir, no airway repair was seen although NEB hyperplasia developed. While this experiment showed that the NEB population was self-sustaining, it did not show that the progenitor population expressed CCSP. Theoretically, the progenitor could be generating daughter cells which are immediately killed when they begin to express CCSP. However, when mice were given a brief pulse of ganciclovir, a similarly severe injury resulted that was not followed by a repair response. From these experiments, it was concluded that the airway epithelial progenitor cell expresses CCSP [19, 21, 51]. The only caveat to this interpretation is that it is the CCSP expressing cells could be required for progenitor function, rather than being the progenitors *per se*.

1.3.1.2 Evolution from "lung progenitor" to "airway stem cell"

Are these progenitor cells actually airway stem cells? In the previous section, the more general word "progenitor" was used because the existence of an airway stem cell could not be determined from the data being discussed. Specifically, from the data discussed thus far, the self-renewal of the airway progenitor has not been demonstrated. There are additional features that usually characterize stem cells, including location in a specific microenvironment (or "niche"), pollution resistance, and relative quiescence. Because the airway cells progenitors described above share these characteristics, it is fair to describe these cells as airway stem cells.

Classical stem cells are located in a niche where cell-cell contacts regulate their behavior. In the *Drosophila* testis, germ stem cells are arranged in a circle around central hub cells. Contact with the hub cell regulates self-renewal to maintain germ cell identity [52]. Stem cell niches have also been identified for the intestine and hematopoietic system [47]. The naphthalene-resistant, CCSP-expressing cells discussed above are found specifically at terminal bronchioles and near NEBs, which provide a specific microenvironments.

It is thought that pollution resistance is a general property of stem cells. Hematopoietic stem cells can be identified by their ability to efflux Hoechst dyes using the P-glycoprotein transporter. This transporter can efflux a wide variety of potentially toxic substances [53]. The resistance to naphthalene toxicity of the CCSP-expressing progenitors is characteristic of a stem cell. The mechanism of naphthalene resistance is unknown. However, the development of full xenobiotic metabolism capacity occurs late in airway differentiation (discussed in chapter 4). Naphthalene resistance could also be considered a sign of relative undifferentiation, which is another characteristic feature of stem cells.

Stem cells are much more quiescent than most other cells within a tissue. Because the TA cells are so highly proliferative, few stem cell proliferation cycles can generate large numbers of progeny. Retention of a nuclear label (due to low proliferation rate) has been used to identify stem cells in the skin [54, 55]. In the airway, CCSP-expressing cells were found that retained a BrdU label in terminal bronchioles and around neuroendocrine bodies [51, 56]. Importantly, recent unpublished data from our laboratory has shown that these label-retaining cells are capable of re-entering the cell cycle in response to a second injury.

There are several limitations to our understanding of the airway stem cell. First, the most rigorous experiments in the hematopoietic system required that one cell be prospectively isolated, transplanted into an irradiated recipient and reconstitute the bone marrow of that recipient over the long term. It is then possible to isolate a hematopoietic stem cell from the recipient, and transplant it to a second irradiated donor. The ability to reconstitute recipients in serial transplantation assays defines the hematopoietic stem cell [57]. There are several problems applying this paradigm to the lung and other solid organs including the gut. First, the only functionally defined molecular marker for the airway stem cell is CCSP. This antigen can not be used for live cell prospective isolation because it is intracellular. It also lacks specificity, being expressed in at least 50% of all airway epithelial cells. Second, no transplantation assay exists. Third, no well established *in vitro* assays exist. *In vitro* colony forming assays were used to characterize the differentiation and proliferation potentials of stem cells in the hematopoietic system [58]. While colonies can be grown from isolated airway cells, the identity of the founder cells that initiate colony formation is unknown. This is particularly a concern because of the comparatively low purity of airway cell preparations.

In conclusion, an airway cell exists that behaves like a stem cell *in vivo*. Categorizing this cell as a stem cell is useful because it provides an experimental framework from which predictions can be made (as was done in chapter 2). It is well accepted that stem cells exist in the gut, despite failure to fulfill any of the criteria used in the hematopoietic system. The largest deficiency in the lung stem cell literature is failure to show that lung stem cells are capable of self-renewal. This is particularly important given the relatively low proliferation rate of the lung epithelium. While stem cell self-renewal has not been formally shown on the cellular level in the intestine, failure to self-renew would have a rapid and dramatic phenotype given the high mitotic index of gut epithelium. For the purposes of this dissertation, I consider the naphthalene resistant, CCSP expressing cell that is necessary for airway repair following naphthalene exposure to be a tissue stem cell.

1.3.1.3 Bronchoalveolar Stem Cells

A recent report by Kim and colleagues proposes the existence of a bronchoalveolar stem cell with the cell surface phenotype of Sca-1^{pos} CD45^{neg} Pecam^{neg} CD34^{pos}. These cells were described to be located at the bronchoalveolar duct junction, express both SPC and CCSP, and give rise to both alveolar and airway epithelium, although this description required inference between *in vitro* and *in vivo* data sets [59]. The possibility of a surface phenotype that would allow prospective isolation of airway stem cells caused great excitement in the field, because it would allow development of *in vitro* and *in vivo* assays to address many of the issue discussed in the previous section. However, there are many caveats to this data set. First, the association of the cell surface phenotype with the expression of CCSP and SPC was found in cells following a lengthy isolation procedure. It is possible that SPC expression was induced as a stress response and that this phenotype can not be translated to unperturbed airway cells *in vivo*. Likewise,

increased SPC production might be seen as a stress response *in vivo* following naphthalene treatments. Next, if a stem cell expressing CCSP and SPC can contribute to both the airway and alveoli, then one would expect recombination by CCSP-Cre to occur in both anatomic compartments. Clones that contain the recombined allele should be seen in the alveolar epithelium. As shown in Figure 8, no clones of recombinant cells are seen in alveolar cells with this Cre line. It is unlikely that a CCSP expressing stem cell contributes to both anatomic compartments. Finally, attempts in our lab and others have failed to confirm the utility of this cell surface phenotype. In particular, the percentage of airway cells with surface Sca1 is reported to be 0.4% by Kim and colleagues, while previously published work by our laboratory found at least 30% of all airway epithelial cells show surface Sca1 [60]. Until the cell surface phenotype is independently confirmed, I am reluctant to use the data set for the purposes of designing experiments described in this dissertation. Hopefully, further experimentation will clarify the cell surface phenotype of the airway stem cell.

1.3.2 The epithelial-mesenchymal trophic unit

Injury to the epithelium does not occur in isolation. This is strikingly seen after naphthalene exposure. As shown in the figure below, during the first week following naphthalene exposure, there is abundant proliferation in the underlying mesenchyme. The concept of the epithelial-mesenchymal trophic unit provides a conceptual framework to describe such cellular interactions following an injury. The epithelial-mesenchymal tropic unit (EMTU) is originally described as consisting of the epithelium, extracellular matrix, attenuated fibroblast sheath and associated innervation [61]. Injuries to any of the components of the EMTU will have effects on the other components. This interdependence makes the application of many

studies to a specific anatomic compartment difficult. For example, treatment of mice with a blocking antibody to TGFβ in the ovalbumin model of allergic inflammation decreases mucous cell metaplasia, smooth muscle proliferation, and peribronchiolar matrix deposition, without changing the cytokine profile [62]. However, it is not clear if the decreased mucous cell metaplasia is caused by directly blocking the effects of TGFβ on the epithelium, or is secondary to changes in the underlying fibroblasts and smooth muscle cells. This otherwise useful study does not allow one to distinguish these possibilities.

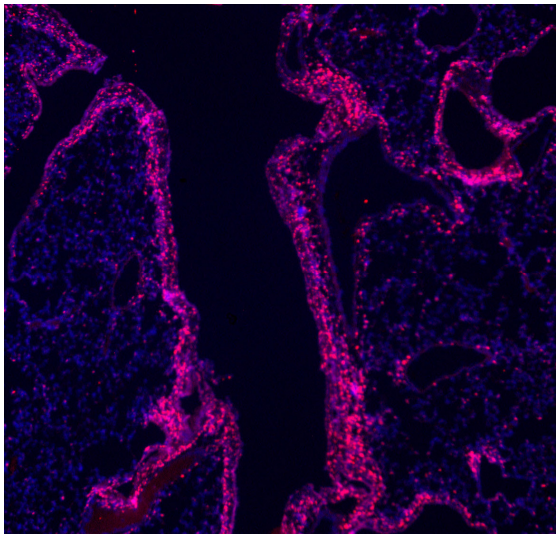

Figure 2: Mesenchymal Proliferation After Epithelial Injury

A mouse was labeled with BrdU for seven days following naphthalene exposure. Abundant BrdU incorporation is seen (magenta) in cells surrounding the airway. In this particular animal, there was almost no epithelial BrdU incorporation at this time point. DAPI nuclear counterstain.

While the EMTU is a very useful conceptual paradigm in wound repair, there are more review articles on the subject than primary data papers. There are two main approaches to determining the relative contributions of various compartments in the EMTU: co-culture systems and cell type specific genetic ablation models. An example of the co-culture approach is found in

a recent paper from Nishimura's group. In this paper, the relative effects of TGFβ and HGF on lung fibroblasts and epithelial cells were determined [63]. A co-culture system was used in which fetal fibroblasts were grown on the bottom of a Trans-well insert, and fetal tracheal epithelial cells were grown on the top. In tracheal epithelial monoculture, treatment with TGFβ or HGF blocking antibodies had no effect on proliferation. However, in fibroblast co-culture, blocking antibodies to TGFβ and HGF increased epithelial proliferation. From this and other data, they proposed a model in which the epithelial growth suppressive effects of TGFβ are actually secondary to a TGFβ induced decrease in fibroblast HGF production. From this study, one might predict that blocking TGFβ signaling within the epithelium (as is done in this dissertation) would have no effect, while blocking HGF signaling would decrease epithelial proliferation. The primary limitation of co-culture approaches is the inability to maintain distal airway epithelial differentiation in culture. The second approach of using cell type specific deletion of a gene in a mouse model is much more common. This is the approach we used in Chapters 2 and 3.

1.3.3 TGFβ/BMP signaling in airway epithelial repair

TGFβ addition increases the rate of wound healing, while blocking the activity of TGFβ also increases the rate of wound healing in a variety of systems [64, 65]. TGFβ has different effects on almost every cell type that responds to an injury, which accounts for this paradoxical effect. In the airway, TGFβ is produced and released from the epithelium following injury [63, 66, 67]. It is also likely that TGFβ is released from lung macrophages, neutrophils, and platelets, depending on the magnitude of the inflammatory response [68]. TGFβ is secreted in a latent form, where it is activated through an integrin following airway injury. However, there are

likely other mechanisms for activation of TGFβ, including the actions of proteases, thrombospondin, and reactive oxygen species [63, 66-68].

Once activated, TGFβ has differing effects on the epithelium, fibroblasts, and leukocytes. Within the mesenchyme, TGFβ signaling causes increased ECM formation by inducing the transcription of extracellular matrix genes, suppressing metalloproteinase activity, and increasing fibroblast proliferation [69]. Additionally, TGFβ can stimulate the transcription of smooth muscle actin in lung myofibroblasts [70]. In airway injuries accompanied by fibrosis or airway wall remodeling, TGFβ plays a key role. Smad3 (a key regulator of TGFβ signaling) null mice are resistant to bleomycin induced lung fibrosis [71]. Blocking TGFβ signaling also decreases airway wall remodeling in mouse models of asthma and obliterative bronchiolitis [62, 72, 73].

Inflammation occurs following tissue injury and can inhibit wound repair. As discussed below, inflammation is also a cause of airway epithelial injury in asthma and bronchiolitis obliterans. TGFβ modulates the immune response to injury [74-76]. Skin wounds heal more quickly and with less inflammation and scarring in Smad3 null mice. The increased rate of wound healing in some systems may be due to decreased inflammation, rather than direct effects on the epithelium or fibroblasts [65].

Within the airway epithelium, TGFβ has a strong antiproliferative effect while increasing epithelial migration *in vitro* [66, 67, 77]. This combination can result in rapid epithelial restitution in gaps that can be covered by cell spreading, but slower recovery of normal cell density following an *in vitro* wound. The effects of TGFβ on airway epithelial cells are discussed in greater detail in chapter 3.

1.3.4 Wnt/β-catenin in airway epithelial repair

There is very little evidence that Wnt/β-catenin regulates airway repair, *per se*. There is one report of increased nuclear β-catenin staining following alveolar damage by hyperoxia or the butylated hydroxyltolulene [78]. However, this study was not mechanistic, the injury model is principally alveolar, and the meaning of nuclear β-catenin in this context is unclear. A second report showed regulation of TOPFLASH (a β-catenin reporter plasmid) activity by cell density in human bronchial epithelial cells [79]. These results remain to be verified *in vivo*. Finally, it is proposed that many signaling pathways involved in repair are aberrantly activated in carcinogenesis. Identifying pathways important in cancer would give insight into pathways important in wound repair (and *vice versa)* [80-82]. There is also very little evidence linking Wnt/β-catenin to lung cancer, although relatively less focus has been placed on this pathway in investigations, so it is premature to conclude that Wnt/β-catenin is not involved in lung cancer [83].

The more compelling reason to study Wnt/β-catenin in an airway repair model is that β-catenin signaling regulates stem cell behavior in multiple other organ systems. If the airway repair model used requires airway stem cell activation, then the requirement of β-catenin in regulating the airway stem cell could be determined. Most information regarding the role of β-catenin in stem cell maintenance comes from the small intestine.

The small intestinal epithelium is maintained by a stem cell located near the crypt [47]. This stem cell proliferates and the daughter cells progressively differentiate as they migrate towards the villus tip. Loss of the intestinal stem cells causes the villus to be composed entirely of post-mitotic differentiated cells which is lethal, given the 3-4 day epithelial turnover rate of the mouse gut. Stem cell dysregulation is thought to cause adenoma formation [84]. The

association of Wnt/β-catenin with epithelial homeostasis came through the association of mutations in the APC gene with familial adenomatous polyposis (FAP), an inherited colon cancer syndrome. In FAP the Wnt/β-catenin pathway is hyperactive, and the gastrointestinal epithelium develops hundreds to thousands of polyps [84]. Ectopic activation of Wnt/β-catenin signaling in mice, also causes intestinal polyp formation [85]. Loss of β-catenin signaling, either through inducible recombination of a null allele or Tcf4 deletion, results in crypt loss due to defective crypt stem cell maintenance [86]. Similar research in the skin bulge and epidermis suggests that Wnt/β-catenin regulates stem cell behavior in these stem cell niches as well (reviewed recently by Fuchs) [47]. Because of the prominent role of β-catenin in regulating stem cell fate, we pursued this pathway in studying a stem cell mediated epithelial repair process.

1.4 ROLE OF AIRWAY REPAIR IN HUMAN LUNG DISEASE

Defective airway repair may influence the pathogenesis of cystic fibrosis, asthma, and bronchiolitis obliterans.

1.4.1 Cystic fibrosis

Cystic fibrosis is a chronic lung disease caused by mutations in the chloride channel CFTR. This mutation disrupts the secretion/absorption balance of the airway surface lining fluid, causing it to become more viscous. Mucociliary clearance is decreased, and patients' lungs become colonized with a variety of bacteria, including *Staphylococcus sp* and *Pseudomonas sp.* Death results from chronic respiratory insufficiency.

Chronic infections cause repeated damage to the airway epithelium. A variety of pathological changes are seen including squamous metaplasia, goblet cell hyperplasia, and increased epithelial height [87]. In response to the chronic injury, the epithelial proliferation rate is increased [87, 88]. While it is clear that chronic lung infections in cystic fibrosis damage the airway epithelium, cystic fibrosis patients may have an inherently impaired epithelial repair capacity in the absence of infection [89]. Augmenting epithelial repair capacity might also delay the onset of end-stage lung disease.

1.4.2 Asthma

Asthma is a chronic inflammatory disease characterized by periods of pharmacologically reversible airway obstruction. Chronic inflammation damages the airway epithelium. Airway changes in asthma include goblet cell metaplasia, subepithelial fibrosis, smooth muscle hypertrophy and hyperplasia, and increased vascularity [1]. The extent of airway injury in asthma is controversial. Clumps of desquamated epithelial cells in bronchoalveolar lavage fluid known as creola bodies are a pathologic finding specific to asthma. Many studies have reported increased epithelial desquamation in biopsy samples from asthmatics. However, a number of other studies have failed to find this effect [90, 91]. One popular model of asthma pathogenesis proposes that the epithelium has a decreased proliferative response to injury. The decreased response to airway injury causes incomplete or aberrant repair and leads to airway remodeling [68, 74-76]. The proliferative state of the epithelium in asthma is another controversial subject, but recent evidence suggests that there is actually increased proliferation in severe asthma and in atopic asthmatics following allergen exposure [91, 92]. Despite debate over the extent of epithelial damage in asthma, the increased epithelial proliferation is indicative of some chronic

mitotic stimulus. Understanding the molecular mechanisms controlling airway epithelial proliferation may give insight into the pathogenesis of asthma.

1.4.3 Bronchiolitis Obliterans

Constrictive bronchiolitis obliterans occurs in 50-70% of patients following lung transplant, and carries a grim prognosis. Current 5-year survival following lung transplant is only 50% largely because of progressive bronchiolitis obliterans [93]. Histologically, constrictive bronchiolitis obliterans is marked by purely bronchiolar airway wall fibrosis with an intact epithelium. As the disease progresses, bronchioles are eventually narrowed to the point of disappearance [94, 95]. The epithelium typically remains grossly intact. This disease process is likely immune regulated, as a constrictive bronchiolitis obliterans also develops following hematopoietic stem cell or bone marrow transplantation. The immune target is unknown, although some suggest that airway epithelial cells are the primary immune-mediated target [96, 97]. While the histological changes in constrictive bronchiolitis obliterans are mainly in the airway wall, this is still compatible with a model of chronic epithelial injury. As seen in Figure 2, focused airway injury can cause widespread proliferation in subepithelial compartments.

Bronchiolitis obliterans can also follow severe injury to the airway epithelium by inhaled gases, toxins or pathogens [98]. In this case, the airway lumen is initially occluded by damaged epithelial cells and a fibrinous exudate. If the basement membrane is intact, epithelial repair ensues. However, in more severe injuries where the basement membrane is damaged, the underlying fibroblasts proliferate and a mix of fibroblasts, capillaries, and new collagen obstructs the airway lumen [94]. In both cases, chronic or severe injury to the terminal bronchiolar

epithelium that can not be repaired may be an underlying pathophysiologic process in bronchiolitis obliterans.

1.5 TGF-BETA/BMP SIGANLING

The Transforming Growth Factor β (TGF-β) and Bone Morphogenic Protein (BMP) families of signaling molecules controls cell proliferation, apoptosis, differentiation, and migration, as well as other cellular functions. There are at least 42 TGFβ/BMP ligands in the human genome, including three TGFβ, eight BMPs, five activins, nodals, myostatin and anti-Muellerian hormone [99].

1.5.1 Canonical TGFβ/BMP Signaling

Signaling begins when a ligand binds to cell surface serine/threonine kinase receptors. The receptor complex is a heterotetramer made of two type-I receptors and two type-II receptors. Ligand binding activates the type-II receptor which then phosphorylates the type-I receptor. The phosphorylated type-I receptor can interact with downstream Smads [100]. Smad proteins (excluding Smad6 and Smad7 discussed below) are transcription factors central to TGFβ/BMP signaling. The receptor-interacting Smads (R-Smads) are phosphorylated during active signaling. Smads 2 and 3 transduce TGFβ and activin signals, while Smads 1, 5 and 8 are involved in BMP signaling. Smads consist of two highly conserved domains: the MH1 domain which binds DNA and the MH2 domain that is phosphorylated during signaling. The domains

are connected by a flexible linker region that can be phosphorylated by other kinase signaling pathways [101]. Phosphorylated R-Smads form homo- or hetero-trimers and partition to the nucleus. They associate with the common Smad4 (Co-Smad) to form a transcription complex. Association with Smad4 can probably occur either in the nucleus or cytoplasm, and nuclear import of the R-Smads is not Smad4 dependent [102, 103]. Interestingly, deletion of the Smad4 nuclear export signal (resulting in exclusively nuclear Smad4 localization) has no gross phenotype in the mouse [104]. Smad transcriptional complexes recognize a four base-pair sequence 5'-AGAC-3' [100, 105]. Because this DNA sequence is very frequent, other mechanisms are needed to select target genes. Smads partner with many families of DNA binding proteins, including E2F, forkhead, homeobox, E-box, and Jun/Fox [100]. Smads may also directly associate with the transcriptional machinery. For more information, the reader is referred to reviews by Massagué and Wotton [100, 101].

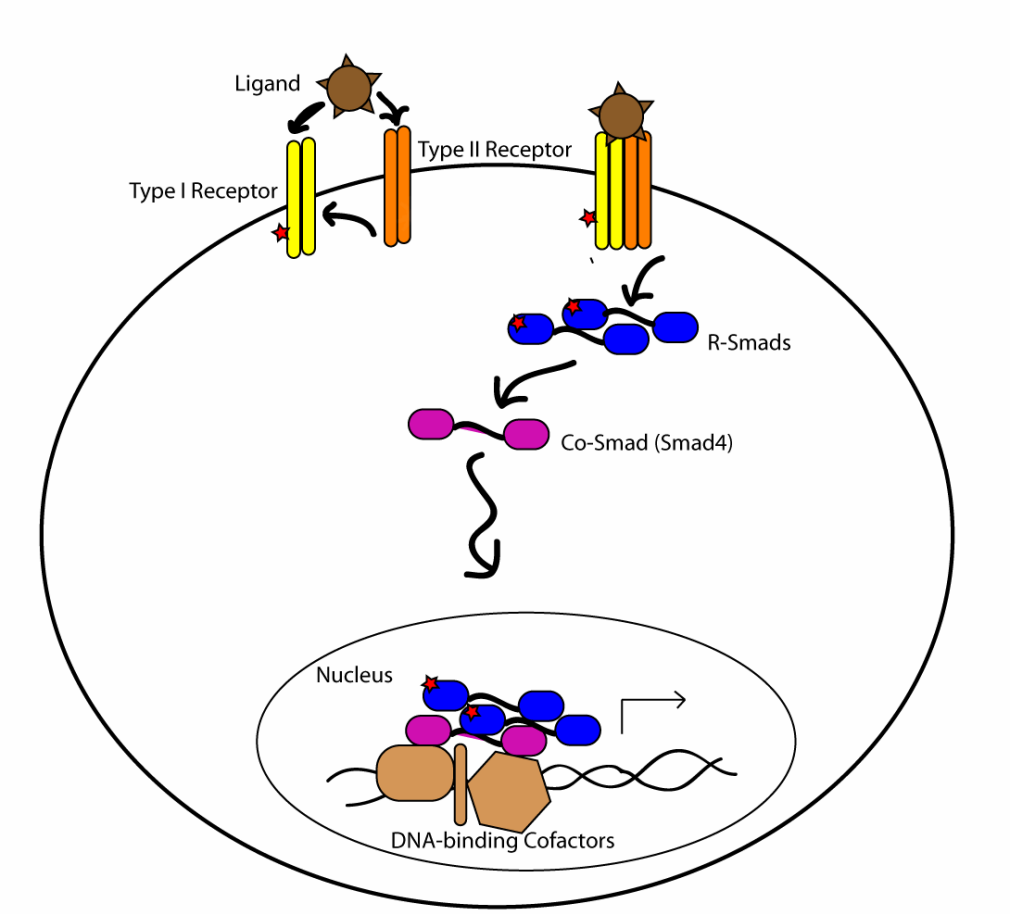

Figure 3: Canonical TGFβ/BMP Signaling

Diagram depicting Smad dependent signaling. A ligand (brown) binds to cell surface receptors (yellow and orange). The receptors are phosphorylated (red star) and phosphorylate R-Smads (blue). The R-Smads complex with the Co-Smad (purple), translocate to the nucleus and cause changes in gene transcription.

1.5.2 Non-Canonical TGFβ/BMP Signaling

While most research has focused on Smad-dependent signaling, there are at least three non-canonical signaling mechanisms. First, several other families of signaling molecules are rapidly activated following TGFβ receptor phosphorylation, including JNK, p38, Erk, Ras, Rho,

PI3K.[106-108] For example, JNK activity is bimodal, with an initial peak 10 minutes following TGFβ signaling, and a second peak 12-24 hours following ligand stimulation. The initial peak is TGFβ-dependent, but Smad-independent [108]. Another example of Smad-independent signaling is found in TGFβ induced cell motility. TGFβ activates Cdc42 and RhoA which cause membrane ruffling in a Smad-independent mechanism, while long term stress fiber formation is Smad-dependent [109].

Second, R-Smads 2/3 can form complexes with other transcription factors instead of Smad4. A recent report shows that Smad2/3 can complex with either Smad4 or TIF1γ during hematopoiesis. The Smad4 complex causes growth arrest while the TIF1γ regulates differentiation. Both complexes are TGFβR-dependent [102]. It is likely that other transcription factors can form complexes with R-Smads in the absence of Smad4.

Finally, the R-Smads can be phosphorylated in the absence of TGFβR activation. Nocodazole treatment causes Smad2 phosphorylation by Mps1 (a protein kinase involved in the spindle checkpoint during mitosis) [107]. The overall role that non-canonical signaling plays in developmental processes and wound repair is unclear.

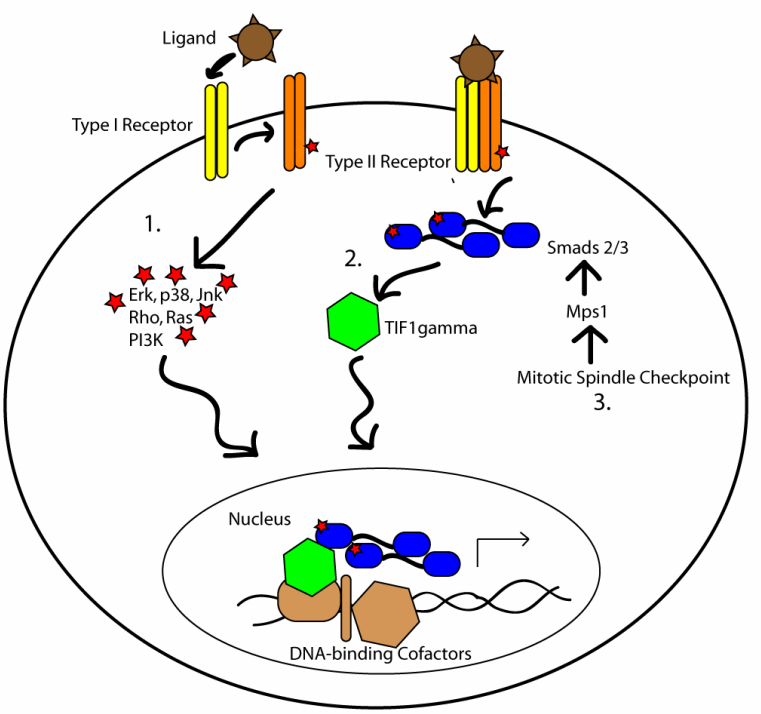

Figure 4: Non-canonical TGFβ Signaling

Three of the known pathways for non-canonical TGFβ signaling. 1. Activated TGFβ receptors can activate a variety of other signaling kinases and small GTP-ases. 2. Smad2/3 but Smad 4 independent signaling through TIF1γ. 3. TGFβ receptor independent signaling following nocodazole administration.

1.5.3 Negative Regulation of TGFβ/BMP Signaling

There are several mechanisms for negatively regulating TGFβ/BMP signaling. These include: dephosphorylation of activated Smads, ubiquitination of Smads and cell surface receptors, and the actions of inhibitory Smads 6 and 7. Recently, the phosphatase PPM1A was identified as the phosphatase for Smad2/3 [110]. A number of phosphatases have been identified for Smad1 including pyruvate dehydrogenase phosphatase and SCP nuclear phosphatases [111, 112]. These phosphatases dephosphorylate activated Smads terminating signaling. The

inhibitory Smad6 and 7 (I-Smads) modulate activated Smad activity at nearly every step from type-I receptor binding to transcriptional complex regulation [113]. An excellent review of negative regulators of the Smad pathway was recently published by Itoh and ten Dijke [113].

1.6 WNT/BETA-CATENIN SIGNALING

The Wnt/β-catenin pathway is best know for orchestrating events during embryogenesis and regulating behavior of stem cells, both during development and in adulthood. The Wnt signaling pathway is highly conserved, and culminates with nuclear translocation of β-catenin [114].

1.6.1 Canonical Wnt/β-catenin signaling

Beta-catenin is a transcription factor that regulates gene expression in response to Wnt signaling. In the absence of Wnt signaling, β-catenin is phosphorylated at the N-terminus by a complex containing Axin, APC, CK1, and GSK3β. Phosphorylated β-catenin is recognized by the E3 ligase βTrCP, ubiquitinated, and degraded by the proteasome [115]. In addition to the cytoplasmic pool, β-catenin is found in the adherens junction along the basolateral cell membrane. In *C. elegans,* the signaling functions and adhesion junction binding functions of mammalian β-catenin are separated into separate molecules, which suggests that these functions may be physiologically distinct [116]. Notably, cells form normal adherens junctions in the absence of β-catenin [117].

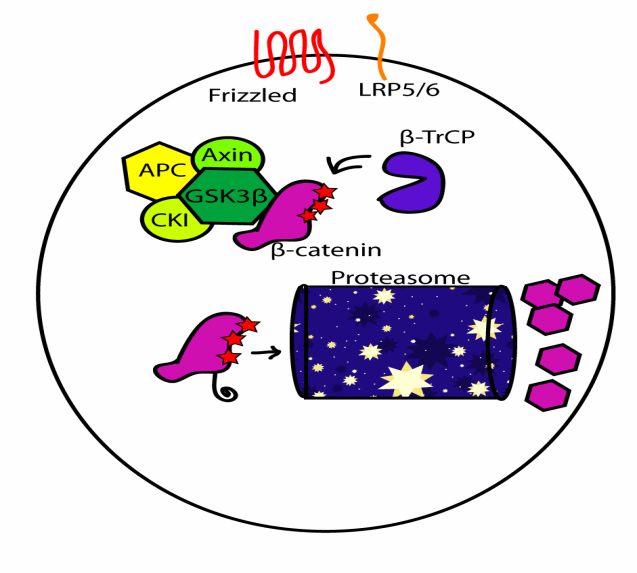

Figure 5: No Wnt Signaling Present

In the absence of Wnt signaling, β-catenin (purple) is phosphorylated (red stars) by the Axin/APC/GSK3β/CKI complex. Phosphorylated β-catenin is recognized by an E3 ligase (blue), ubiquitinated, and targeted to the proteasome for destruction.

Signaling begins when a Wnt binds to the seven-transmembrane domain receptor Frizzled. Wnts are cysteine-rich, secreted proteins that act as morphogens. There are at least 20 mammalians Wnt family members. Although Wnts are secreted ligands, they are palmitoylated, which greatly decreases their solubility. How Wnt signaling gradients are established is unknown, because the low solubility of Wnts limits their diffusion [115]. Frizzled associates with the co-receptor LRP5 or -6. The Wnt/Frizzled/LRP complex then interacts with Dishevelled (Dsh). While genetic studies place Dsh between Wnt/Frizzled/LRP and β-catenin, the actual function of Dsh is not known. Axin translocates to the cell membrane, and the β-catenin destruction complex dissociates. Hypophosphorylated β-catenin is released into the

cytoplasm where it translocates to the nucleus and changes gene transcription [118]. In the nucleus, β-catenin complexes with the Lef/Tcf family of transcription factors. In the absence of Wnt signaling, Lef/Tcf act as transcriptional repressors. Binding of β-catenin transiently turns Lef/Tcf into transcriptional activators [114]. Frizzled/Wnt signaling also controls planar cell polarity and signals through a calcium dependent pathway.

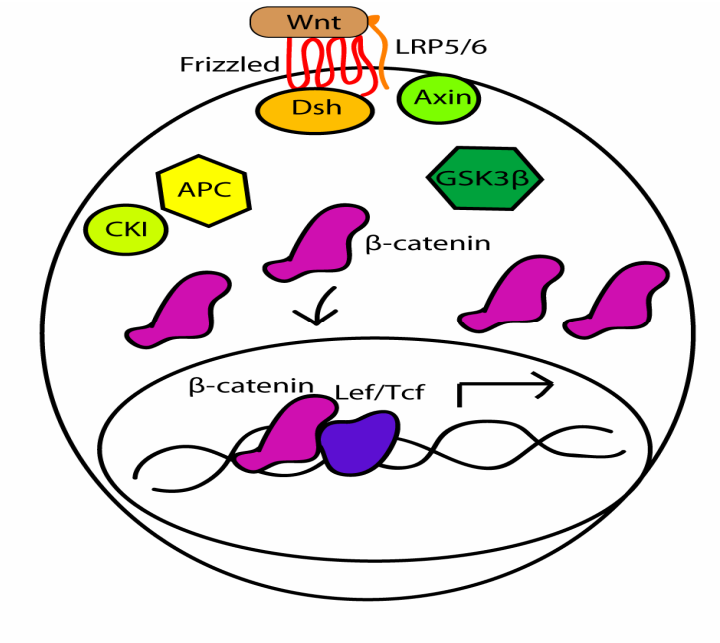

Figure 6: Canonical Wnt Signaling

Wnt binds to Frizzled and LRP5/6. This causes the β-catenin phosphorylation complex to dissociate. Hypophosphorylated β-catenin translocates to the nucleus to change gene transcription.

1.6.2 Negative Regulation of Wnt/β-catenin signaling

Wnt signaling is negatively regulated by Dickkopf (Dkk), a secreted protein that directly binds to LRP5/6. LRP5/6 bound to Dkk is internalized and no longer available for signaling [115]. Soluble Frizzled-Related Proteins (SFRP) and Wnt Inhibitory Factor (WIF) are two secreted molecules that can act as extracellular Wnt inhibitors [119]. It is not clear how active signaling is terminated. There are at least three active mechanisms: nuclear export of β-catenin, disassembly of the β-catenin nuclear complex, and reversing the changes in histone acetylation that are a result of β-catenin signaling [114]. The relative contributions of these mechanisms in specific physiologic situations is an area of active research, but beyond the scope of this discussion.

1.6.3 Cross talk between β-catenin and TGFβ/BMP Signaling

Synergistic signaling can occur between the β-catenin and TGFβ/BMP pathways. Several genes have been reported, including gastrin, *Myc*, *Msx1,* and *Xenopus* twin genes, whose transcription is synergistically increased by the presence of both β-catenin/Lef binding and Smad binding to their respective DNA binding elements within the promoter [120-123]. In these studies, a model is proposed where the cooperative binding of β-catenin, Lef, and Smads recruits co-activator p300/CBP. Interestingly, the control experiments in these studies revealed a role for Smad4 in β-catenin/Lef signaling apart from its role during active TGFβ/BMP signaling. In addition, TGFβ signaling induces mRNA transcription of *Lef1* and increases protein expression of β-catenin, which may sensitize cells to respond to Wnt signaling [124, 125].

Signaling crosstalk is also possible between downstream targets of the Wnt and TGFβ/BMP signaling. The clearest example of this crosstalk is found in the activities of the TGFβ-activated kinase 1 (TAK1) [126]. TAK1 is activated in response to a wide variety of stimuli including inflammation and TGFβ [127]. TAK1 phosphorylates a variety of downstream targets including JNK, IKKβ (eventually leading to NFκB activation), and Nemo like kinase (NLK). NLK in turn, can phosphorylate Lef, which prevents association with β-catenin [128]. Thus the TGFβ-TAK1-NLK pathway can negatively regulate β-catenin signaling. In summary, crosstalk between Wnt/β-catenin and TGFβ/BMP signaling can occur on multiple levels. Situations are found where the crosstalk is both synergistic and antagonistic. The effects of activation of both pathways in any particular cell is likely context specific.

1.7 LUNG DEVELOPMENT

The adult lung is a branching structure with right/left asymmetry and a distinct proximal-distal axis. The asymmetrical branching pattern and proximal-distal cell gradient are both established during lung development and influenced by many signaling pathways, including both TGFβ/BMP and Wnt/β-catenin.

1.7.1 Stages of Mouse Lung Development

Mouse lung development is divided into five stages: embryonic (E9.0-11.5), pseudoglandular (E11.5 to E16.5), canalicular (E16.5 to E17.5), terminal sac (E17.5 to P5) and alveolar (P5-P28) [129]. Lung development begins at E9.0-9.5 dpc as two epithelial tubes invaginate from the

ventral foregut endoderm into the splanchnic mesoderm. During the pseudoglandular phase, these epithelial tubes branch in an stereotyped fashion to produce an airway system that looks like a tree [2]. This process, called branching morphogenesis, continues until after birth in the alveolar space. Branching morphogenesis is accompanied by the development of the vasculature and innervation. The pseudoglandular phase is also marked by the first appearance of ciliated cells around E15.5 [10, 11].

During the cannalicular phase, the distal epithelial tubules change shape to form duct or sac-like structures that will eventually become alveoli. At this point, the developing bronchial system is clearly separated from the future alveoli. More proximally, the first secretory cells are seen. Finally, in the days prior to birth distal air sacs dilate and surfactant production begins. Lung development continues postnatally for at least a 28 days in the mouse. Alveoli continue form during the first month, and the metabolic capacity of the airway epithelium take at least 4 weeks to reach adult levels (see chapter 4.1 for a full discussion of this process) [44].

The fundamental technique used in many lung development studies is the explant culture. Lungs dissected from E11.5 mouse embryos are grown in culture medium or on Matrigel. The lungs will continue to branch in a highly stereotyped fashion for 3-4 days. While in culture the explants can be manipulated by growing them with beads impregnated with a signaling molecule of interest, antisense oligonucleotides can be added to the culture, and signaling molecules can be microinjected into the airway lumen. It is also possible to remove the mesenchyme from the epithelial tube to study epithelial-mesenchymal interactions. The endpoint of these experiments is generally a count of the absolute number of terminal airway buds. While I do not use explant cultures in the research described in this dissertation, it is used in most of the background data discussed below.

Signaling between the developing epithelium and mesenchyme coordinates branching morphogenesis. In the rat, distal lung mesenchyme will induce lung type branching when grafted onto the tracheal epithelium. There is a short time window when the epithelium is sensitive to these inductive effects [130]. The diffusible signals involved in this process were recently reviewed Maeda and Shannon [129, 131]. Sonic hedgehog, fibroblast growth factor 10, Wnts and BMPs play a prominent role in this process.

1.7.2 TGFβ/BMP Signaling in Lung Development

Signaling from both TGFβ and BMP family ligands regulates lung development in the rodent. TGFβ signaling negatively regulates branching morphogenesis *ex vivo*. The use of antisense oligonucleotides to knockdown Smads 2, 3, and 4 causes a 1.5-fold increase in mouse explant branching [132]. Similarly, addition of TGFβ1 to explant cultures decreases branching in a dose dependent manner, while knockdown of TGFbRII increases explant branching [133, 134]. In mice, expression of TGFβ1 under the Sftpc promoter decreased branching and epithelial maturation [135]. The effects of TGFβ on branching are probably mediated through the epithelium, because exposure of the airway lumens in culture to TGFβ decreases branching [136].

BMP signaling regulates both branching morphogenesis and the establishment of the proximal-distal axis. Of the BMP receptors, Bmpr1a is expressed in both the epithelium and mesenchyme, while Bmpr1b is found only in the epithelium [137]. BMP4 is the principal BMP ligand controlling lung morphogenesis. Very strong expression of BMP4 is seen at the tips of lung buds, both in the epithelium and underlying mesenchyme [137-139]. This localized expression pattern suggested that BMP4 might regulate branching. The addition of BMP4

impregnated beads to lung explant cultures causes an exuberant increase in explant branching [136]. The effects of BMPs are probably dose dependent, because expanding the expression zone of BMP4 by expressing it under control of the *Sftpc* promoter caused the development of dilated, cystic airspaces rather than increased branching. Airway cell differentiation appeared normal, but alveolar development was stunted [137]. Additionally, adding BMP to isolated endoderm (epithelial) cultures decreased budding, rather than increasing it as is seen in whole explant culture [139].

When BMP signaling is inhibited, either through expression of the soluble BMP inhibitor XNoggin, expression of dominant negative Bmpr2 in the epithelium, or Cre-mediated deletion of Bmpr1a in the epithelium, a proximalized lung phenotype results [50, 138]. These mice have expanded airway representation at the expense of alveolar development. Autocrine signaling within the epithelium through Bmpr1a is required for normal alveolar proliferation and cell survival [50]. Gremlin (a secreted BMP antagonist) and Smurf1 (an E3 ubiquitin ligase that recognizes Smad1) may negatively regulate BMP4 signaling in the lung [138, 140, 141].

An unresolved issue regarding TGFβ/BMP signaling in lung development that relates to the work in this dissertation is the role of Smad4. In theory both TGFβ and BMP signaling involve Smad4, but the two pathways appear to have opposing effect on branching. It is possible that both pathways are signaling through Smad4 but in spatially or temporally distinct regions. Alternatively, Smad4-independent signaling may be involved. Only one study has explored the involvement of Smad-dependent BMP signaling in lung development. Decreased Smad1 expression in explants decreased branching, however the magnitude of the effect was not large [142].

TGFβ signaling also regulates alveolar development and homeostasis postnatally. In wild-type mice, alveolar size decreases more than 2-fold during the first 28 days of life, reflecting the growth of alveolar septa. This normal decrease in alveolar size does not occur in Smad3 null mice or mice deficient in latent TGFβ binding protein 3 (Ltbp-3) [143, 144]. In the adult, loss of TGFβ signaling in the lung causes emphysema through increased metalloproteinase activity [143, 145, 146]. In these model systems, TGFβ signaling is lost or reduced in all lung cells, including neutrophils and macrophages that might serve as a source of MMPs. It is difficult to determine the contribution of decreased primary alveolarization from the effects of chronic exposure to increased metalloproteinase activity.

1.7.3 Wnt/β-catenin in Lung Development

Wnt/β-catenin signaling regulates lung development. Beta-catenin and its transcriptional partners of the Lef/Tcf family are widely expressed during lung development in both the epithelium and mesenchyme [147]. TOPGAL reporter mice were used to establish β-catenin signaling activity during lung development. In this mouse line, LacZ expression is driven by three Lef/Tcf binding sites connected to a minimal *c-fos* promoter. LacZ activity is seen in cells with active β-catenin signaling. In these mice, LacZ expression is found throughout the developing airway epithelium, with especially strong staining seen in the distal endoderm, which strongly suggests that β-catenin signaling regulates lung development [148, 149].

Several different approaches have been used to disrupt Wnt/β-catenin signaling during lung development including generation of knockout mice, over-expression of Wnt inhibitors, conditional deletion of pathway molecules, and expression of constitutively active pathway components. Wnt 7b signals through the canonical, β-catenin dependent pathway in the lung

[150]. Wnt 7b null mice have decreased branching, but normal proximal-distal epithelial differentiation is maintained. These mice die shortly after birth from respiratory insufficiency. The pulmonary vasculature is abnormal, and lung hemorrhage occurs at birth [151]. This provided the first functional evidence that Wnt/β-catenin signaling is required for lung development.

Loss of β-catenin expression early in lung development through the use of a floxed *Catnb* allele and a doxycycline inducible SPC-Cre line markedly disrupted lung development. These mice developed dilated conducting airways that expressed CCSP and very limited distal airways/alveoli. Mice were not viable [152]. Similarly, when β-catenin signaling is blocked by overexpression of a soluble inhibitor Dkk1, expansion of proximal airway (as defined by CCSP expression) was found at the expense of distal (SPC expressing) airway [149]. Addition of fibronectin to lung explants from mice over expressing of Dkk restored normal development, leading to the conclusion that fibronectin is the downstream target of Wnt/β-catenin signaling responsible for the distal lung phenotype. However, the mechanism by which fibronectin restored normal development has not been determined [153].

While blocking β-catenin signaling during morphogenesis prevents distal lung formation, potentiation of β-catenin signaling does not increase distal lung formation. Rather, over-expression of an activate β-catenin/Lef fusion protein under the *Sftpc* promoter caused the distal lung epithelium to assume an intestinal phenotype [148]. Potentiation of β-catenin through the use of a constitutively active (floxed exon 3) *Catnb* allele just prior to birth arrests epithelial maturation. In these mice, there is an expanded population of airway cells that share the characteristics of an airway stem cell at the expense of generating a metabolically mature epithelium. (Reynolds, unpublished data*)* These studies show that the lung epithelium is

sensitive to both dose and timing of Wnt/β-catenin signaling. Markedly increased signaling early in development can cause a change in cell fate commitment.

Non-canonical Wnt signaling may also regulate lung development. Wnt5a can signal through the receptor tyrosine kinase Ror2 to inhibit canonical Wnt signaling, as well as stabilizing β-catenin through the Fizzled receptors [115]. Wnt5a knockout mice have a shortened proximal-distal axis, with increased distal branching. These mice are not viable, because the perinatal maturation process is slowed. Notably, specification and differentiation of airway cell types is normal [154]. Expression of Wnt5a under the control of the Sftpc promoter decreases branching [155].

Table 1: Development phenotypes associated with abnormal Wnt/β-catenin signaling

Perturbation	Anatomic Compartment	Phenotype
Wnt 5a $^{-/-}$	Both epithelium and Mesenchyme	Shortened Proximal/Distal axis, increased distal branching , blocked perinatal maturation
SPC-Wnt5a	Both	Decreased Branching
Wnt 7b $^{-/-}$	Both	Lung hypoplasia, weak vascular walls
SPC/rtTA:tetO-Cre, fl Catnb	Epithelium	Very limited alveolar lung formation
Sftpc-B-catenin/ Lef fusion	Epithelium	Disrupted branching, switch in lineage commitment to intestine
CCSP-Cre, *Catnb*$^{\Delta E3}$	Epithelium	Altered epithelial differentiation

In summary, β-catenin signaling is required for lung development. Signaling regulates the formation of the distal airways and alveoli, but is not required for normal airway cell differentiation. The lung is sensitive to β-catenin signaling dose, because increased signaling results in a lineage commitment change early in development and altered epithelial differentiation late in development.

1.8 ORIGIN OF LUNG CARCINOMA

Lung carcinomas are classed into two clinical subgroups: small cell or non-small cell according to histology [1]. Small cell lung cancers express neuroendocrine markers and are likely derived

from neuroendocrine cells [18]. Non small cell lung carcinomas (NSCLC) are generally classed as squamous, adenocarcinoma, and large cell. Squamous carcinomas are usually found within the first three bronchial division, and progress from squamous metaplasia to carcinoma *in situ*. Large cell carcinomas consist of undifferentiated malignant cells that can not be classed as squamous or adenocarcinoma [1].

The origin of adenocarcinomas has greater bearing on this dissertation because a subset of these tumors may be derived from either Clara cells or Type II pneumocytes. A pathological finding known as atypical adenomatous hyperplasia is thought to be a precursor lesion for a subset of adenocarcinomas [156]. In this lesion, alveoli are lined by plump cells that morphologically resemble type-II pneumocytes or Clara cells, rather than the usually type-I cells that compose alveolar walls. These lesions are similar to very small bronchoalveolar type adenocarcinomas, and are thought to be the precursor lesion to this tumor [156, 157]. Of interest is whether these lesions are derived from Clara cells or Type-II pneumocytes. Subpopulations of both cell types can act as stem cells for the airways and alveoli, respectively, making them attractive targets for malignant transformation. This is a technically difficult question to conclusively answer. These cell types are typically identified by expression of protein markers or morphology. In a sample of >500 tumors, 10% of tumors were immunoreactive for CCSP in at least 10% of tumor cells [158]. This suggests that most NSCLC are not derived from Clara cells. However as cells "dedifferentiate" during the progression to cancer, expression of CCSP could be lost, thus underestimating the contribution of Clara cells to the development of NSCLC [158]. Extrapolation of animal studies to human NSCLC is difficult, because the representation of different histologic lung cancer subtypes is very different in rodents [159]. It is likely that both Type II pneumocytes and Clara cells can serve as the cell of origin in NSCLC. The relative

frequency of malignant transformation of these cell types may vary. It would be useful to determine if differences in biological behavior between various adenocarcinomas is influenced by the cell of origin.

1.9 GOALS OF THIS DISSERTATION

The conducting airways provide a necessary barrier between the air we breathe and our internal environment. Infections, inflammation, and bioactivated toxins can all damage the airway epithelial lining. A subsequent repair process ensues that depends on the activation of an airway stem cell. When this repair process is incomplete or aberrant, permanent airway remodeling may result. This airway remodeling contributes to the morbidity and mortality seen in diseases such as asthma, cystic fibrosis, and chronic bronchitis. Currently, we only have therapies that decrease the inflammation associated with airway injury. There are no therapies that directly augment epithelial repair. Understanding the signaling pathways governing the epithelial response to injury may provide new ways of treating chronic lung disease.

This dissertation contains three projects relating to airway epithelial repair. In the first project, the role of Wnt/β-catenin in airway repair is studied. Wnt/β-catenin signaling regulates stem cell behavior in the gut and skin. Because both of these organs contain a barrier epithelium, we tested the hypothesis that **β-catenin is necessary for airway epithelial homeostasis and repair.** To test this hypothesis, we used tissue specific deletion of β-catenin in the naphthalene injury model.

The second project contains two parts. TGFβ/BMP signaling regulates wound repair in a variety of systems, lung branching morphogensis and epithelial homeostasis *in vivo.* Smad4 is

the common signal transducer for TGFβ/BMP signaling, although there is evidence for Smad-independent signaling. We hypothesized that **loss of TGFβ/BMP signaling would disrupt airway epithelial homeostasis, repair, and lung branching morphogenesis.** To test the various parts of this hypothesis, we first compared the phenotypes of mice with tissue specific Smad4 deletion early in lung development with mice that did not lose Smad4 signaling until just prior to birth. Next, the naphthalene injury model was used to determine whether loss of Smad-dependent signaling disrupted the epithelial repair process.

The third part of this dissertation is a technical advance. Currently, we are able to follow epithelial morphology, cell kinetics, the generation of mucus, and a limited range of molecular markers. The molecular markers available do not represent the full range of functional differences seen among the secretory cell populations. In this project, a combination of cell ablation models was used to deplete lungs of secretory cells. This was followed by microarray analysis, to determine which genes were no longer expressed following secretory cell ablation. A number of novel secretory cell markers were identified that allow more precise mapping of molecular events associated with epithelial differentiation in development and repair. While these three projects are distinct, they share the common purpose of furthering our understanding of epithelial behavior during development and disease.

2.0 BETA-CATENIN DEFICIENCY DOES NOT IMPACT THE REPARATIVE POTENTIAL OF THE BRONCHIOLAR EPITHELIUM

2.1 INTRODUCTION

The conducting airway is lined by an epithelium that is maintained through the concerted action of cells belonging to a stem cell hierarchy. Following injury the contribution of stem cells or their more differentiated progenitor/transit-amplifying (TA) progeny to the regenerative pool depends upon factors including their relative abundance and the extent of epithelial cell depletion [14]. Injury that is targeted towards terminally differentiated epithelial cells of small (bronchiolar) airways is repaired through proliferation of a widely distributed progenitor cell, the Clara cell, which has the capacity for both self-renewal and differentiation into ciliated cells [160]. In contrast, airway injury resulting from chemical ablation of Clara cells is repaired through the proliferation of sparsely distributed cells that exhibit functional characteristics of tissue-specific stem cells [21, 49, 56]. Accordingly, bronchiolar stem cells have been defined by pollutant resistance, localization to discrete microenvironments, capacity for bipotential differentiation, and infrequent proliferation [21, 51, 56, 161]. In this regard, airway stem cells share properties of tissue-specific stem cells within other organs such as skin, intestine, liver and cornea [162-166]. Even though stem cells of the bronchiolar epithelium have been spatially localized and some insight gained regarding their molecular phenotype [21, 51, 167, 168], little

is known of mechanisms regulating their activation, maintenance, and differentiation in either homeostasis or following injury.

Phenotypic analysis of transgenic and knockout mouse models have revealed a central role for β-catenin signaling in the regulation of tissue regeneration and stem cell fate within numerous organs [85, 86, 169-174]. Nuclear translocation of β-catenin and downstream target gene activation enhances hematopoietic stem cell growth and survival [172]. Furthermore, lymphoid enhancing factor 1 (LEF1) and T-cell factor 4 (TCF4), heterodimerization partners for β-catenin, play central roles in regulating stem and transit-amplifying cell populations within the intestinal crypt [85, 86, 171]. Similar observations have been made within the epidermal stem cell niche, where Wnt/β-catenin signaling regulates follicle-associated proliferation and TA cell migration [169, 175-178]. In addition to roles for β-catenin signaling in normal tissue maintenance, dysregulation of β-catenin signaling through mutation of pathway components has been demonstrated in cancers, including epidermal carcinomas and the majority of colon cancers [85, 177, 179-182]. Taken together, these data highlight the widespread involvement of β-catenin signaling in regulating aspects of stem cell-associated proliferation, differentiation, and migration in tissue maintenance and repair.

Activation of downstream target genes by functional β-catenin/TCF heterodimeric transcription factor complexes has been visualized *in vivo* using transgenic reporter lines. In these lines, reporter genes have been placed downstream from promoter elements harboring canonical TCF cis elements. The TOPGal reporter transgenic line, in which expression of β-galactosidase is restricted to cells undergoing active β-catenin signaling, has been best characterized. Numerous *in vitro* reporter assays have used this TCF-optimized promoter (TOP) construct to confirm that expression of genes by the TOP promoter specifically and exclusively

reflect β-catenin signaling induction [85, 176, 177, 183-186]. *In vivo*, the specificity of TOPGal transgene reporter activation was determined by crossing TOPGal mice with transgenic mice expressing a constitutively active form of β-catenin in epidermal basal cells (K14-ΔNβ-catenin) [175, 176]. Results of these studies demonstrated increases in TOPGal activity that localized to regions of β-catenin transgene expression. TOPGal reporter mice have also been bred with transgenic mice expressing a dominant negative form of β-catenin (K14-ΔNΔCβ-catenin) [187]. In these experiments, TOPGal activation was inhibited within cells specifically expressing the dominant negative β-catenin protein construct. Based on these *in vitro* and *in vivo* studies, it is highly likely that LacZ expression in TOPGal mice is due to β-catenin dependent promoter activation.

The purpose of this study was to characterize the temporal and spatial pattern of β-catenin signaling in normal and progenitor cell depleted airways, and to determine whether β-catenin signaling was necessary for maintenance or repair of the naphthalene-injured epithelium. Our results indicate that β-catenin is an active but variable contributor to the signals that regulate the unperturbed and repairing bronchiolar epithelium. However, β-catenin is not necessary for either of these processes. Overall our data support the conclusion that proliferation and differentiation of bronchiolar stem and TA cells is regulated by a β-catenin independent signaling mechanism.

2.2 MATERIALS AND METHODS

Animal Husbandry: Colonies of either wild-type or genetically modified mice were maintained as in house breeding colonies under specific pathogen free conditions in an ALAC accredited Facility at the University of Pittsburgh. All experimental and breeding animals were maintained on a twelve hour light / dark cycle and given access to food and water *ad libitum*. TOPGal(B6) congenic mice were generated by back-crossing transgene positive mice to C57Bl/6 wild type mice through 10 generations. Mice used in naphthalene experiments were between eight and twelve weeks of age. All procedures involving animal models were approved by the Institutional Animal Care and use Committee of the University of Pittsburgh.

Genotyping: Genotype was determined by PCR amplification of genomic DNA prepared from tail biopsy. TOPGal was detected using primers specific for the *E. coli LacZ* coding sequence: forward primer, 5'- GTGGCAGCATCAGGGGAAAACCTT-3' and reverse primer, 5'- GAATTCCGCCGATACTGACGGGCT-3' and resulted in an amplicon of 476 bp. CCSP-Cre mice were identified as previously described (Reynolds, unpublished data). Homozygous $Catnb^{flox(E2-6)}$ were identified by PCR amplification of the wild type and the floxed exon 2-6 alleles using primer pairs that detected the loxP modification as previously desccribed[188]. Mice heterozygous and homozygous $Catnb^{flox(E3)}$ were distinguished by PCR amplification of the wild type and modified alleles as previously described (Reynolds, unpublished data).

Naphthalene Administration: Naphthalene administration was carried out as previously described [49]. Naphthalene doses for wild type littermates and genetically modified mice were: TOPGal(B6) congenic, 275 mg/kg body weight; and CCSP-Cre/$Catnb^{flox(E2-6)}$ (referred to as DE2-6 mice) 250 mg/kg body weight.

Bromodeoxyurindine Administration: Proliferating cells were continuously labeled with bromodeoxyuridine (BrdU, Sigma St. Louis, MO) using a 14-day mini-osmotic pump and a delivery rate of 0.5 μl/hour (Alzet 2002, Durect). Pumps were charged with sterile 20 mg/ml BrdU in normal saline and primed for 2 hours at 37 °C in sterile 1X PBS. Pumps were implanted 24 hours after naphthalene exposure. Pumps were implanted as previously described [7]. In some experiments, proliferating cells were continuously labeled by repeated administration of 50 mg BrdU/kg body weight at 24 hour intervals starting immediately after naphthalene treatment and continuing through the 10 day recovery time point. The method of BrdU delivery did not result in appreciable differences in labeling index.

Tissue Recovery*:* Animals were sacrificed by injection of 2.5% avertin and exsanguinated. The tracheas was canulated, and left lobes were removed for RNA extraction. For standard light microscopy, right lung lobes were inflation fixed in situ for 10 minutes with 10% neutral buffered formalin (NBF) at 10 cm water pressure, removed, and immersion fixed in 10% NBF for an additional 20 minutes (for detection of βgal activity) or 2 hours (for immunostaining).

β-gal Histochemical Detection*:* Accessory lobes were equilibrated to βgal staining solution: 5 mM $K_3Fe(CN)_3$, 5 mM $K_4Fe(CN)_6$, 2mM $MgCl_2$, 0.02% Nonidet P-40, 0.01% sodium deoxycholate, 1X PBS, and 1 mg / ml X-gal. β–gal detection was performed in the dark at 37°C for 6 hours. Following β-gal detection, tissues were washed in PBS to remove residual X-gal staining solution and post-fixed for 16 hours in 10% NBF at 4°C. X-gal stained accessory lobes were microdissected to expose the lumen of intrapulmonary conducting airways and minor daughters. The surface of the airway epithelium was examined for the presence of X-gal stained (blue) cells using a dissecting microscope and representative images were obtained. X-gal

stained cardiac lobes were cryoprotected and embedded in paraffin and sectioned at 5 μm to reveal the major axial pathway as well as numerous airway terminal bronchioles.

Immunohistochemistry: Paraffin embedded, adjacent serial sections were rapidly cleared with 3 changes xylenes, hydrated through graded ethanol solutions (100% to 70%), equilibrated to water, and quenched with 3% peroxide for 20 minutes. Sections were blocked with PBS/0.5% BSA (Blocking solution) for 20 minutes and incubated with rabbit-anti-CCSP (1:32,000), mouse IgG2b-anti-acetylated tubulin (1:10,000), or blocking solution overnight at 4°C. Sections were washed extensively in 1X PBS and incubated with biotinylated goat-anti-rabbit Ig (1:6000 in blocking solution) or goat-anti-mouse IgG2b in blocking buffer for one hour at room temperature. Sections were washed and further incubated with streptavidin-horseradish peroxidase (1:4000) in PBS. Antigen-antibody complexes were detected using a diaminobenzidine substrate detection kit (DAB, Vector Laboratories). Images were obtained using an Olympus Provis AX70 microscope equipped with a Spot RT digital camera and processed using Image-Pro Plus and Adobe Photoshop.

Table 2: Antibodies Used in Chapter 2

Antigen	Supplier	Titer
Rabbit α CCSP	In house	1:10,000 IF, 1:32,000 IHC
Mouse IgG_1 α FoxJ1	Gift from Steven Brody (Washington Univ).	1:1500
Mouse IgG_1 α β-catenin	BD Transduction	1:500
Rat α BrdU	Accurate Chemical Inc	1:500
Mouse IgG_{2b} α	Sigma	1:8000

acetylated tubulin		

Immunofluorescence: Sections were prepared as indicated above. Antigens retrieval was done by microwaving sections in 10mM citrate buffer (pH 6.0) for 20 minutes. Sections were blocked with 5% BSA/PBS prior to application of primary antibodies. Primary antibodies were diluted in 5%BSA/PBS and used at the concentrations listed in Table 2. Slides were incubated overnight at 4°C, washed, and secondary antibodies applied for 0.5 hours at room temperature. FoxJ1 signal was enhanced by application of 0.5% Sudan Black in 70% ethanol (Spectrum, SU121) for 5 minutes followed by extensive washing in PBS. Coverslips were mounted using Fluoromount-G containing 2μg/mL 4, 6, diamidino-2-phenylindole (DAPI, Sigma, St. Louis MO). Antigen-antibody complexes were visualized as single optical planes using an Olympus Images were obtained as indicated above.

Morphometric Analysis*:* Repair index: Epithelial repair was quantified at the 45 day recovery time point by determining the length of basement membrane underlying CCSP-immunoreactive regions of the epithelium and dividing this value by the total length of the basement membrane. Repairing regions were defined as those bounded by 2 adjacent CCSP positive cells. Lengths were determined using the measurement function of Image-Pro Plus (Media Cybernetics, Silver Spring, MD). Values are presented as the average ± SEM for 4-5 mice per genotype. Cumulative mitotic index: The cumulative mitotic index was defined as the number of BrdU-labeled nuclei divided by the total number of nuclei and was presented as a percentage. FoxJ1 index: Ciliated cells were identified by immunofluorescence staining for FoxJ1. Ciliated cell differentiation was assessed by determining the number of FoxJ1 positive nuclei within nascent regions of epithelium and expressing this value as a percent of the total

number of nuclei. Data are displayed as average percent FoxJ1 positive nuclei within nascent epithelium ± SEM. Three mice were analyzed per genotype..

RNA abundance: Quantitative RT-PCR (Q-PCR) was used to assess mRNA abundance. Total RNA from the left lung lobe [189] [49, 51]. Complementary CDNA was prepared as previously described. [190]. Differential gene expression was determined using an ABI PRISM 7000 Sequence Detection System and values calculated by the ΔΔCT method described by Heid [191]. At least 3 RNA samples from each tissue or cell population were assayed. Assays-on-Demand gene expression probes (Applied Biosystems, Foster City, CA) included: secretoglobin (Scgb1a1/CCSP, Mm00442046_m1); cytochrome P450-2F2 (CyP450-2F2, Mm00484087_m1); surfactant associated protein (Sftpc, Mm00488144_m1); forkhead box J1 (Foxj1, Mm00807215_m1); and beta glucuronidase (Gusβ, Mm00446953_m1).

Airway Cell Isolation: Airway cells were prepared by the method of Chichester and colleagues with the following minor modifications [43]. Lungs were perfused via the vasculature with 1X phosphate buffered saline (PBS), lavaged with 1X PBS/0.2 mM EGTA, digested with 4.0 units/ml (Worthington #2279) in Ham's F12 (Mediatech, Inc. #10-080-CV), and erythrocytes lysed with Red Blood Cell Lysis Solution (eBiosciences #00-4333-57). Fibroblasts were depleted by panning for 1.5 hours on tissue culture grade petri plates in DMEM/10% fetal bovine serum. Cell recoveries after the panning step were 2-3 X 10^6 cells/lung and cell viability was >95%. CD45 positive cells were depleted using Dynabeads (Dynal #M-280) and biotinylated anti-CD45 according to the manufacturer's directions. Approximately 50% of cells were recovered after CD45 depletion and cell viability was ~85%.

Clonogenic Frequency Analysis: Clonogenic frequency within CD45(-) airway cell preparations was determined by plating 2 X 10^4, 1 X 10^4, 5 X 10^3, 2.5 X 10^3, 1.25 X 10^3, 6.25 X

10^2, or 3.13 X 10^2 cells into collagen 1-coated wells of a 96-well tissue culture plate [192]. Twenty-four wells were seeded for each cell dilution. Cells were cultured in mouse tracheal epithelial medium (MTEC, [10] at 5% CO_2, 37 ºC for 1 week. Wells were washed 3 times with saline, fixed with 10% neutral buffered formalin (Fisher Scientific, Pittsburgh, PA) for 30 minutes, stained with 1X Giemsa (Sigma #GS-500, St. Louis, MO) for 30 minutes, washed 3X with water, and dried. Colonies were counted and categorized at 12X using a dissecting microscope Clonogenic frequency was calculated according to the linear regression analysis method [192]. Briefly, the number of wells containing clusters of 5 or more cells was scored. The percent of wells that were negative for growth was calculated and the natural log of this value plotted verses the number of input cells. The equation representing the Ln(% negative) vs. cell input line was solved for X= Ln(37%). Clonogenic frequency was calculated as 1/N and was reported as the number of clonogenic cells/1000 cells. Studies with R^2 values from 0.99 to 0.89 were accepted for further analysis. Clonogenicity assays were carried out at least twice for each genotype (n=4 individuals/genotype/experiment) and condition tested.

2.3 RESULTS

2.3.1 Sporadic activation of TOPGal transgene activity in the unperturbed adult airway.

To determine if β-catenin mediated signaling contributed to airway homeostasis, lung tissue from wild type and TOPGal(B6) congenic mice was analyzed by whole mount β-gal staining and microdissection to reveal the major axial pathway and minor daughters to terminal bronchioles. Endogenous (eukaryotic) β-gal activity was not detected at pH 7.0 in transgene-negative tissues

(data not shown). TOPGal transgene activity was weak relative to levels observed in the developing lung (Reynolds, unpublished data and data not shown) and no clear association between transgene activity and anatomical features of the airway could be discerned (Figure 7A-C). The β-gal reporter was co-expressed with the secretory cell marker CCSP (Figure 7G). However, only a subset of CCSP were β-gal positive. In contrast, the majority of cells expressing the ciliated cell marker acetylated tubulin were β-gal positive. The TOPGal transgene was silent in the unperturbed adult alveolar epithelium. These data suggest that β-catenin mediated signaling contributes to airway homeostasis at the level of individual cells or small cell clusters and that it is not operative in the adjacent alveolar compartment.

2.3.2 TOPGal transgene activity in the repairing airway epithelium

To determine whether signaling via β-catenin was modulated in the context of progenitor (Clara) cell-specific lung injury, wild type and TOPGal(B6) congenic mice were exposed to naphthalene and recovered 2, 3, 5, or 10 days. Analysis of Clara cell gene expression demonstrated a 80% depletion of CCSP on day 3 (Figure 7M). These data mimicked the kinetics of epithelial marker gene expression reported previously for naphthalene-exposed FVB/n mice [49] and indicated that the injury and repair process was similar in TOPGal(B6) congenic mice. Endogenous β-gal activity was not detected in transgene-negative tissue at any recovery time point (data not shown). Limited or no transgene activation was observed in individuals exposed to naphthalene and recovered 2 (data not shown) or 3 days (Figure 7B, E, H, K). Transgene activation, if detected at these time points, tended to be observed within terminal bronchioles. This period of relative transgene inactivity correlated with the period of Clara cell necrosis and initiation of the proliferative phase of the repair response. β-Gal reactivity indicative of TOPGal transgene

activation was noted on recovery day 5 (data not shown) and was maintained at this level through recovery day 10 (Figure 7C, F, I, and L). At these time points β-Gal-positive cells were detected throughout the main axial pathway. As observed for the unperturbed lung, transgene-expressing cells tended to be present as isolated cells or as small clusters within the epithelium (Figure 7N). Within repairing regions, β-gal positive/CCSP-expressing cells were identified. However, the majority of acetylated tubulin-expressing cells within repairing regions were β-gal negative. β-gal positive cells were also identified within non-repairing epithelial zones. Although the pattern of TOPGal transgene activity during epithelial injury and repair further supported a role for β-catenin in airway homeostasis, the absence of transgene expression during the period of peak proliferation on day 3, expression in terminally differentiated ciliated cells, and the lack of restriction to regenerative zones suggested that this pathway was not a proximal regulator of the repair response.

We next asked if signaling through β-catenin was present following progenitor (Clara) cell-specific injury to the conducting airway epithelium. To address this question, C57Bl/6 congenic mice carrying the TOPGal transgene were exposed to naphthalene and recovered 2, 3, 5, or 10 days. Naphthalene exposure caused 80% depletion of the Clara cell specific CCSP mRNA in this strain as assayed by RT-PCR (Fig 7M). Abundance of CCSP did not rebound during the period studied. No significant change in SPC message was seen by one way ANOVA analysis. By 2 (data not shown) and 3 days following naphthalene exposure, expression of β-galactosidase was uniformly lost as seen in Figure 6B. On section, almost no X-gal staining was seen in any animal analyzed (Figure 7E, H, K). The rare X-gal staining seen was found at terminal bronchioles. There was a rare population of CCSP immunoreactive cells, (Figure 7H) and the airway was primarily lined by acetylated tubulin reactive cells (Figure 7K). This period

of TOPGAL gene suppression coincides with Clara cell necrosis and the earliest proliferative response following naphthalene exposure. At day 5 (data not shown) and day 10 following progenitor cell depletion, the pattern of TOPGal transgene activation resembles that seen in control mice (compare Figure 7A and C). Small patches of cells with TOPGal transgene activity were seen along the airway (Figure 7C and F), however 1/3 animals had no detectable TOPGal activity. TOPGal activity was seen both within the repairing zones expressing CCSP (Figure 7I) and within acetylated tubulin immunoreactive regions (Figure 7L). Regions of X-gal staining did not correspond to areas of epithelial repair as described by CCSP immunoreactivity during this period (Figure 7N). CCSP immunoreactive units were seen that did and did not stain for X-gal. Additionally, X-gal staining was seen within some CCSP negative regions. Additionally, TOPGal transgene activity was detected in spatially- distinct, peribronchial mesenchymal cells. Endogenous and bacterial β-galactosidase activity were not detected in lung tissue from any time period or treatment group. The very consistent finding of this study was that early after progenitor cell depletion, TOPGal activity is lost both due to cell death within the CCSP expressing cell population, and due to gene down regulation within the ciliated cell population. The dynamic expression of TOPGal transgene expression during airway repair suggests that β-catenin dependent signaling is actively regulated during the repair process.

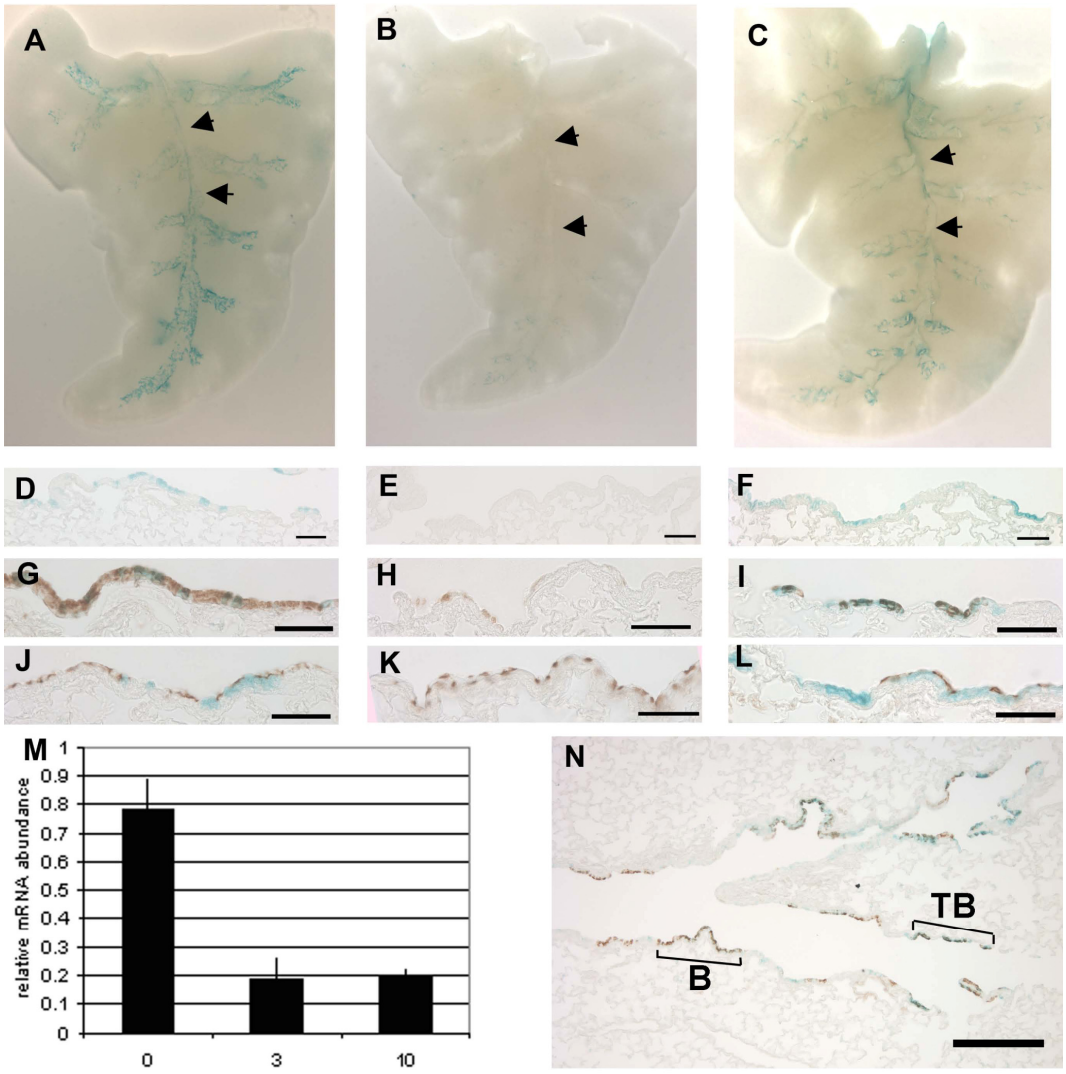

Figure 7: TOPGal transgene activity in the unperturbed and repairing airway

Panels A-C: The spatial context of cells expressing the β-galactosidase reporter (blue) was determined in accessory lobes of untreated control mice (A) and those treated with naphthalene and recovered 3 (B) or 10 (C) days. The proximal end of the main axial pathway (arrows) is located at the top of each panel. Original magnifications 12.5X. Panels D-L: The identity of cells expressing the β-galactosidase reporter was determined by immunohistochemical detection (brown) of the Clara cell marker, CCSP (G-I) and the ciliated cell marker, acetylated tubulin (J-L). No primary antibody controls (D-F). Representative lung tissue sections from

control mice (D, G, J) and those treated with naphthalene and recovered 3 (E, H, K) or 10 days (F, I, L) are shown. Scale bars 50 μm.

Panel M: Abundance of CCSP mRNA was determined by quantitative reverse transcription PCR in control mice (0) or those treated with naphthalene and recovered for 3 or 10 days. Data are presented as average ΔΔCT ± SEM (n=3). A statistically significant drop in CCSP mRNA occurred at day 3 (ANOVA, followed by Tukey test). Panel N: The relative distribution of β-galactosidase and CCSP positive cells was determined in lungs of animals treated with naphthalene and recovered 10 days. Examples of reparative units in bronchiolar (B) and terminal bronchiolar (TB) regions are indicated by brackets. Measure bar = 100 μm

2.3.3 Cell type specific modification of Clara cell gene expression.

In order to probe the relationship between β-catenin regulated gene expression and Clara cell differentiation, the β-catenin locus was modified specifically in CCSP-expressing cells. This approach made use of a transgene in which Cre recombinase was expressed under regulation of the rat CCSP promoter [193, 194]. Cellular specificity and kinetics of Cre recombinase activity were determined through analysis of mice hemizygous for the CCSP-Cre transgene and heterozygous for the ROSA-RS [195] (Reynolds, unpublished data). Importantly, in adult tissue, both CCSP positive cells and ciliated cells expressed β-gal (Reynolds, unpublished data) a finding consistent with previous reports of a precursor-progeny relationship between airway CCSP-expressing cells and ciliated cells [160]. Rare β-gal positive alveolar duct or alveolar saccule cells were detected, but these cells did not form contiguous clones. This analysis demonstrated that the CCSP-Cre transgene was activated specifically in airway CCSP-expressing cells during the pseudoglandular to cannalicular transition, that transgene activity paralleled that

of the endogenous CCSP gene, that genetic modifications could be introduced with high efficiency into embryonic CCSP-expressing cells, and that this modification could be followed into adult secretory and ciliated cells.

2.3.4 Recombination of the Catnb$^{flox(E2-6)}$ allele.

In order to assess the necessity of β-catenin for appropriate epithelial regeneration, β-catenin null CCSP-expressing cells were generated through Cre-mediated deletion of *Catnb* exons 2-6 [188]. Necessity of β-catenin for airway epithelial maturation and regeneration was assessed in mice that were hemizygous for the CCSP-Cre transgene and homozygous for the Catnb$^{flox(E2-6)}$ allele (DE2-6 mice). Recombination efficiency was determined by immunofluorescence analysis of β-catenin using the C-terminal-specific β-catenin antibody (Figure 8A, B). Analysis of the adult wild type lung detected lateral plasma membrane β-catenin staining in all airway epithelial cells (Figure 8A). Similar analysis of DE2-6 demonstrated extensive recombination with an overall recombination varying from a minimum of 90% (Figure 8B) to a maximum of 95%. Secretory and ciliated cells were identified within the recombined cell population (data not shown) and suggested that β-catenin deficiency did not impact the differentiation potential of CCSP-expressing cells. Cells containing at least one wild type *Catnb* allele were usually found as isolated cells within a field of recombined cells although small tracts (average of 4 cells) of β-catenin positive cells were observed. Non-recombined cells were randomly distributed and were not associated with any specific anatomic feature of the airway. The non-recombined fraction of epithelial cells included pulmonary neuroendocrine cells, within which no recombination was observed (data not shown), and rare Clara and ciliated cells. These data indicated that the CCSP-

Cre transgene mediated efficient generation of homozygous β-catenin null airway epithelial secretory and ciliated cells.

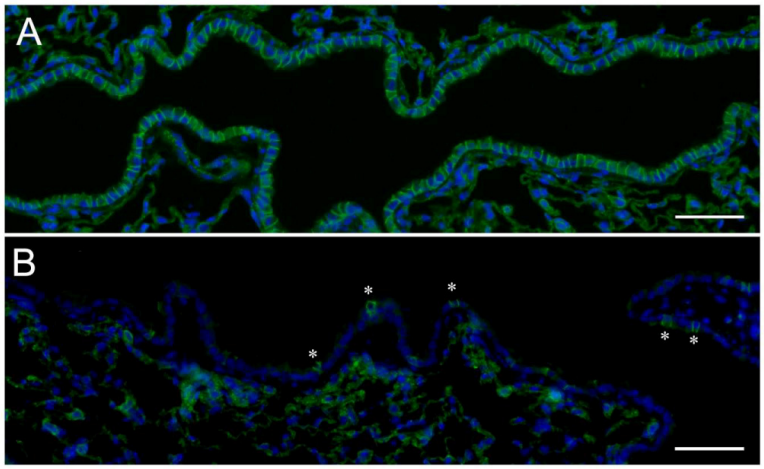

Figure 8: Cell type-specific deletion of Catnb

Efficiency of Cre recombinase-mediated modification of the Catnb$^{floxE2-6}$ allele was determined by immunostaining lung tissue from wild type (A) and CCSP-Cre/Catnb$^{floxE2-6/floxE2-6}$ (B) mice for β-catenin (green). Nuclei were counterstained with DAPI (blue). Asterisks mark unrecombined cells. Scale bar = 50 μm.

2.3.4.1 Phenotype of the β-catenin null airway epithelium

Previous studies demonstrated a critical role for β-catenin in proximal-distal lineage specification but suggested that β-catenin was not necessary for airway maturation once the lung had been patterned [196]. This conclusion was verified through quantitative RT-PCR analysis of CCSP gene expression in total lung RNA which demonstrated that CCSP mRNA abundance did not vary according to genotype (Figure 9A). No phenotypic distinctions were observed between CCSP-expressing cells of the two genotypes. Similar numbers of ciliated cells were detected in wild type and Catnb$^{\Delta E2-6}$ airways (data not shown) and suggested that ciliated cell differentiation was unaffected by β-catenin deletion. Analysis of aged wild type and Catnb$^{\Delta E2-6}$ mice (6-12 months, n>60) did not detect genotype-associated alterations in any of the above parameters or in

the development of lung tumors (data not shown). These results indicated that the airway and alveolar secretory cell lineages were correctly specified and differentiated in the absence of β-catenin. In addition, β-catenin was not necessary for CCSP-expressing cell maturation in the post-natal airway or for maintenance of the airway secretory lineage in adult animals.

While early deletion of β-catenin in the lung causes a severe developmental phenotype with disrupted proximal-distal lineage specification [152], we saw no gross developmental phenotype when β-catenin was deleted within the secretory cell populations starting at embryonic day 16.5. The allele was transmitted to live offspring in a Mendelian fashion and mice displayed normal longevity (data not shown). Expression of CCSP mRNA and protein was normal (Fig 9E). Similar numbers of ciliated and CCSP expressing cells were seen (data not shown). No tumors or other histological abnormalities were seen in mice aged 6-12 months (n>60). These data show that the airway and alveolar secretory lineages were correctly specified in the absence of β-catenin. The loss of β-catenin dependent signaling does not appear to impair CCSP-expressing cell maturation or lead to tumorigenesis.

2.3.4.2 β-catenin is dispensable for repair of the airway epithelium

A critical role for β-catenin in proliferation, migration, and differentiation of continuously renewing epithelia has been documented through use of genetic modifications that result in loss- and gain-of-function alterations in Wnt/β-catenin signaling [118]. Necessity of β-catenin for regeneration of the conducting airway epithelium was assessed through exposure of wild type and $Catnb^{\Delta E2\text{-}6}$ mice to naphthalene and recovery for 3-45 days. Quantitative RT-PCR analysis of CCSP mRNA abundance demonstrated similar depletion of CCSP-expressing cells in wild type and $Catnb^{\Delta E2\text{-}6}$ mice at the 3 day time point and normal regeneration of the epithelium by day 45 (Figure 9A). The extent of epithelial regeneration was assessed through immunofluorescence

analysis of CCSP immunoreactive cells in the bronchiolar and terminal bronchiolar epithelium on recovery day 10. No genotype dependent differences were detected (Figure 9B). The nascent epithelium was 5-10 cell diameters in length and cells within the regenerating epithelium expressed CCSP (Figure 9C-F) or the ciliated cell marker acetylated tubulin (data not shown). The genotype of nascent cells was determined by dual immunofluorescence analysis of CCSP and β-catenin on sections adjacent to those used for identification of regenerative units (Figure 9D-F). In the wild type airway, all cells within the regenerating epithelium were β-catenin positive and no evidence of nuclear β-catenin was detected. In contrast, regenerative units within the $Catnb^{\Delta E2-6}$ bronchiolar and terminal bronchiolar epithelium were composed primarily of β-catenin negative cells (≥95%) with a small number of isolated β-catenin positive cells.

Continuous BrdU labeling and histomorphometric methods were used to compare the mitotic index for naphthalene exposed wild type and $Catnb^{\Delta E2-6}$ mice. Dual immunofluorescence analysis of BrdU and CCSP detected similarly sized reparative units located at branch points and in terminal bronchioles of wild type and $Catnb^{\Delta E2-6}$ airways (Figure 9C-F). No genotype-dependent differences in the cumulative mitotic index of wild type and $Catnb^{\Delta E2-6}$ tissues were detected (Figure 10A).

Analysis of injury and repair in mice expressing a stabilized form of β-catenin (Reynolds, unpublished data) suggested that β-catenin truncation resulted in amplification of bronchiolar stem cells and distribution of these cells throughout the bronchiolar epithelium. This observation suggested that stabilization of β-catenin either replaced niche-derived signals that regulate stem cell maintenance and participation in epithelial repair. In order to determine whether deletion of β-catenin in bronchiolar stem or transit amplifying cells has a subtle effect of the number of clonogenic cells, we compared the clonogenic frequency of wild type and $Catnb^{\Delta E2-6}$ epithelial

cells in vitro. As previously reported, this analysis detected an increase in the number of colongenic cells in airways of Catnb$^{\Delta E3}$ mice (Figure 10B). However, no genotype-dependent differences in clonogenic frequency were detected in Catnb$^{\Delta E2\text{-}6}$ airway cells and colony size and morphology did not vary by genotype (data not shown). These results indicated that deletion of β-catenin in CCSP-expressing cells does not impact the number of colony forming cells in vitro. Overall, these results demonstrated that a β-catenin null progenitor cell pool could reconstitute the conducting airway epithelium and suggested that β-catenin was not necessary for repair of the conducting airway epithelium.

2.3.5 Differentiation of β-catenin null progenitor cells

The ability of β-catenin null progenitor cells to regenerate the ciliated cell population was assessed in wild type and Catnb$^{\Delta E2\text{-}6}$ animals at the 45 day recovery point. As ciliated cell representation varies by anatomical location this analysis was limited to the last 200 μm basement membrane ending in a well-defined bronchoalveolar duct junction [3]. In both wild type and Catnb$^{\Delta E2\text{-}6}$ tissue, dual immunofluorescent analysis of CCSP and FoxJ1 detected zones of columnar epithelium (Figure 11B, C) were separated by regions that were deficient in CCSP-expressing cells. Quantitative analysis demonstrated that representation of FoxJ1 immunopositive cells in repairing regions did not vary by genotype (Figure 11A). These data indicate that β-catenin deficiency did not impact the differentiation potential of the bronchiolar progenitor cell pool.

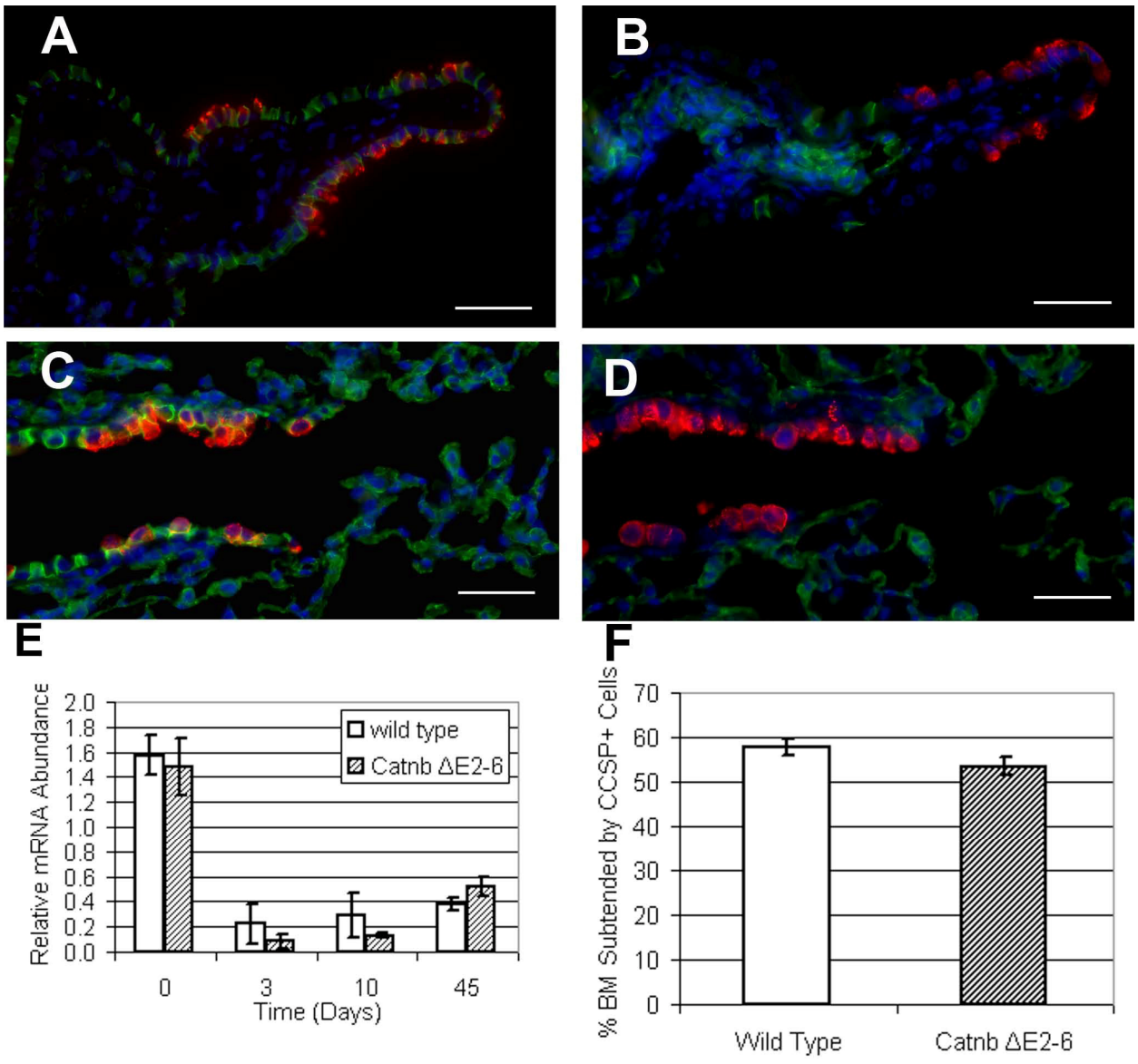

Figure 9: Normal naphthalene-susceptibility and repair of the β-catenin null epithelium

Panels A-D: Dual immunofluorescence detection of CCSP (red) and β-catenin (green) in wild type (A, C) and or Catnb$^{\Delta E2\text{-}6}$ (B, D) mice exposed to naphthalene and recovered 10 days. DAPI counterstain (blue). Representative images of CCSP immunoreactive regions at branch points and terminal bronchioles are presented. Scale bar = 50 μm. Panel E: The impact of genotype on naphthalene-mediated epithelial injury was determined by quantitative reverse transcription PCR analysis of CCSP mRNA abundance in control mice (0) or those treated with naphthalene and

recovered for 3, 10, or 45 days. Black bars: wild type mice; hatched bars, Catnb$^{\Delta E2\text{-}6}$ mice. Data are presented as average ΔΔCT ± SEM (n=3). No genotype-dependent differences were detected. Panel F: The impact of genotype on epithelial repair was determined 45 days post-naphthalene exposure. Histomorphometric methods were used to determine the length basement membrane subtended by CCSP immunoreactive epithelium in wild type (solid bar) or Catnb$^{\Delta E2\text{-}6}$ mice (hatched bar) mice. Results are presented as average percent ± SEM (n=3). Genotype-dependent differences were not detected.

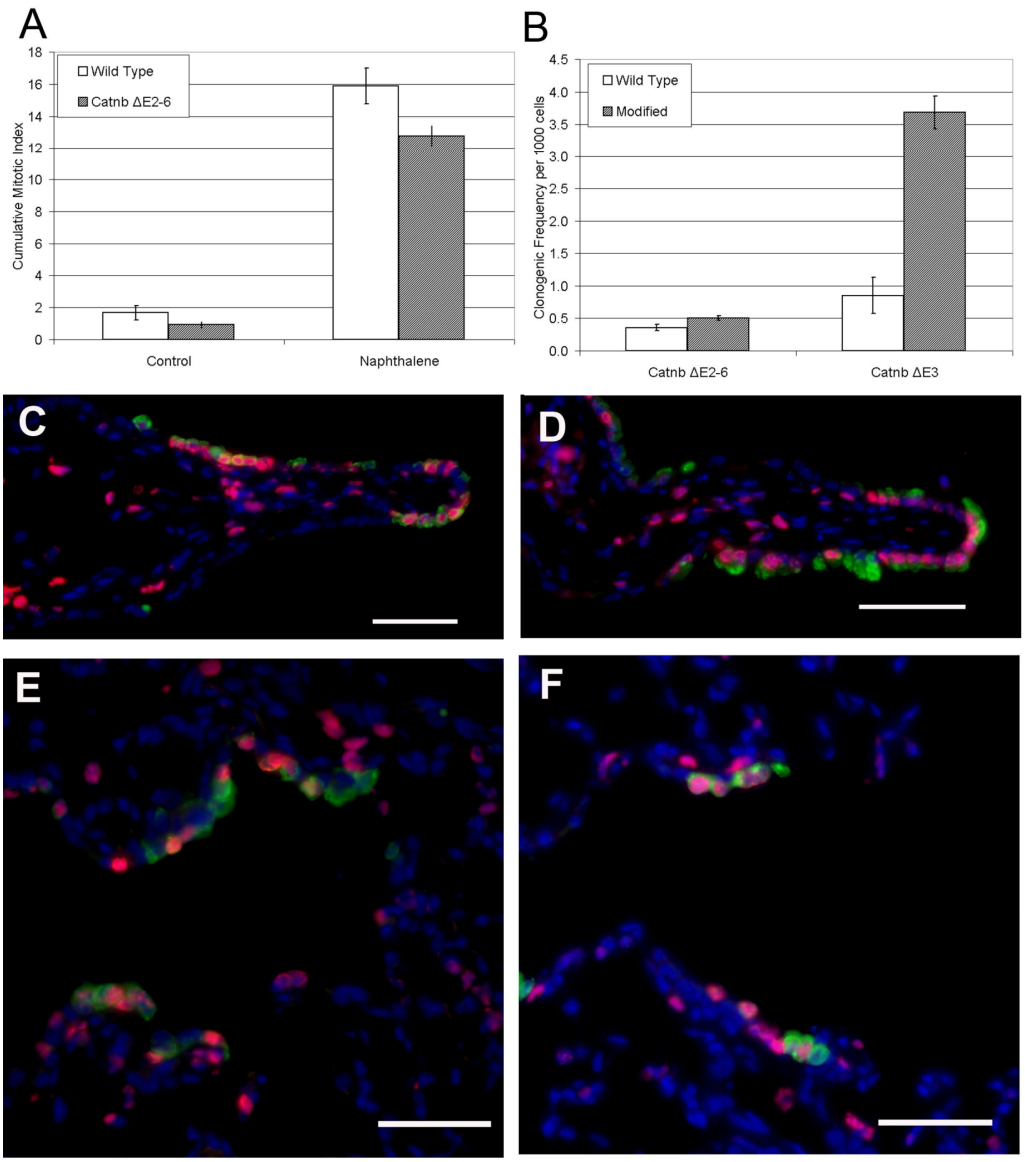

Figure 10: Normal proliferation in a β-catenin null epithelium

Panel A: The impact of β-catenin deficiency on proliferation of control and naphthalene-treated wild type (solid bars) and CatnbΔE2-6 mice (hatched bars) was determined in mice that were injected with BrdU on recovery days 1-10. Results are reported as the average mitotic index ± SEM (n=3). Mitotic index did not vary significantly by genotype at baseline or during recovery from naphthalene. Panel B: The frequency of clonogenic cells in airway epithelial cell preparations from wild type and CatnbΔE2-6 littermates (left bars) was determined. Cells from

wild type and CatnbΔ3 littermates served as positive controls (right bars). Data are presented as the mean ± SEM (n=4). The difference between wild type and CatnbΔE3 mice was statistically significant. Panels C-F: Tissue from mice that were continuously labeled with BrdU was dual immunostained for CCSP (green) and BrdU (red) and counterstained with DAPI (blue). Representative images of regenerating areas are shown for wild type (Panels C and E) and CatnbΔE2-6 (Panels D and F) mice. Regenerating zones located at branch points (Panels C and D) and terminal bronchioles (Panels E and F) are presented. Scale bar = 50μm.

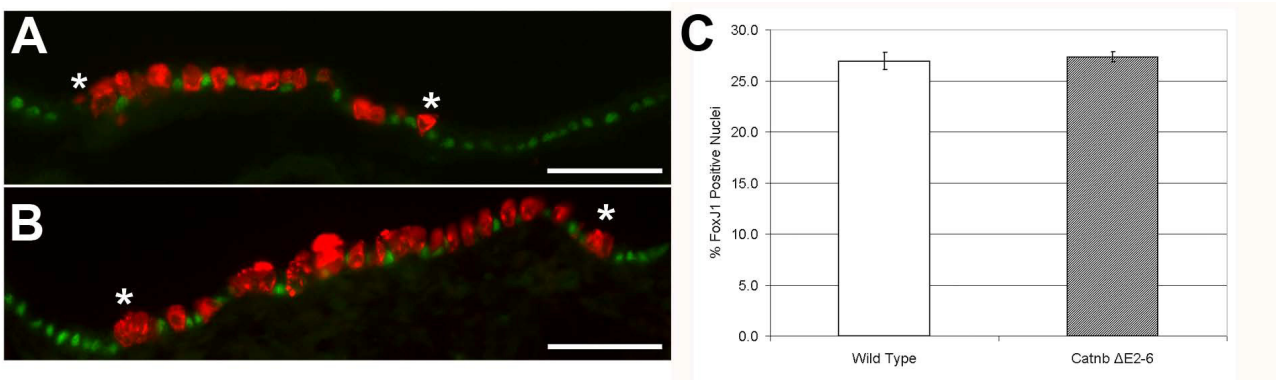

Figure 11: Normal regeneration of ciliated cells within the β-catenin null epithelium

Panel A: the impact of β-catenin on ciliated cell differentiation was determined in wild type (solid bar) and Catnb$^{\Delta E2-6}$ mice (hatched bar) that had been exposed to naphthalene and recovered 45 days. The FoxJ1 index was determined for repairing regions of the epithelium. Data are presented as average percent FoxJ positive nuclei within nascent epithelium ± SEM (n=3). Panels B-C: Wild type (B) and Catnb$^{\Delta E2-6}$ (C) mice were treated with naphthalene and recovered for 45 days. Tissue was dual immunostained for CCSP and FoxJ1. Asterisks mark the extent of the nascent epithelium. Scale bars = 50 μm.

2.4 DISCUSSION

We have used transgenic and cell type specific knockout strategies to determine roles for β-catenin regulated gene expression in maintenance and repair of the bronchiolar epithelium. Analysis of TOPGal transgene activity detected β-catenin dependent signaling in the unperturbed and repairing bronchiolar epithelium. However, the broad distribution and phenotype of signaling cells precluded establishment of a clear role for β-catenin in maintenance or repair of the bronchiolar epithelium. Therefore, we tested the necessity of β-catenin signaling through Cre-mediated deletion of *CATNB* exons 2-6 in Clara cells. Functional knockout of β-catenin had no impact on expression of Clara cell differentiation markers, mitotic index, or sensitivity of these cells to the Clara cell-specific toxicant naphthalene. Repair of the naphthalene-injured airway proceeded with establishment of focal regions of β-catenin null epithelium. The size of the regenerative units, epithelial mitotic index, and restoration of the ciliated cell population did not vary between wild type and genetically modified mice. Thus, β-catenin signaling was not necessary for maintenance or efficient repair of the bronchiolar and terminal bronchiolar epithelium. In contrast with the gut where β-catenin plays a dominant role in regulation of proliferation and differentiation[84, 86, 115, 197, 198], our data support the conclusion that these aspects of bronchiolar repair are regulated by other as yet unidentified signaling pathways.

2.4.1 Roles for β-catenin signaling in bronchiolar cell proliferation

We have used TOPGal transgenic mice to demonstrate that naphthalene-induced progenitor cell depletion results in changes in the cellular context of β-catenin mediated signaling. At baseline, subsets of Clara cells and ciliated cells express the TCF promoter-regulated β-gal reporter. Following injury, transgene activity was decreased due to depletion of Clara cells and down-regulation of the transgene in naphthalene-resistant ciliated cells. As epithelial repair progressed, the transgene was re-expressed primarily in Clara cell comprising repairing regions with minimal participation of ciliated cells (Figure 7). Because β-catenin is a proximal regulator of proliferation in some systems, finding TOPGal transgene activity in post-mitotic ciliated cells and on recovery days 5-10 when the epithelium has returned to the quiescent state was unexpected [11]. The disassociation of β-catenin signaling and proliferation was further supported by the finding that the TOPGal transgene was nearly silent during the period of peak epithelial proliferation on recovery day 3. These results suggested that β-catenin dependent gene expression in the bronchiolar epithelium was not linked with proliferation. This notion was supported by the finding that β-catenin null airways exhibited a similar mitotic index to wild type at baseline and after injury (Figure 10A). Likewise, β-catenin status did not impact the colony formation in vitro (Figure 10B). The finding of TOPGal activation in post-mitotic cells is not without precedent. In the hair follicle, nuclear Lef1 and TOPGal transgene activity were detected in the non-mitotic compartment at the follicle base and co-localization with hair keratins suggested that these cells had committed to the differentiation pathway [175]. In aggregate, this analysis supports the conclusion that β-catenin is not necessary for regulation of cell cycle entry or exit by bronchiolar epithelial cells.

Roles for the Wnt/β-catenin signaling pathway in regulation of cell proliferation were initially revealed through analysis of tumor cells of the mammary gland and colon, for which pathway components such as Wnt, β-catenin and adenomatous polyposis coli (APC) were identified as proto-oncogenes [199]. Even though mutations involving genes whose products constitute elements of the Wnt/β-catenin signaling pathway are frequently found in colorectal tumors, the frequency with which these mutations are found in association with lung cancer is very low; approximately 5% [200]. There are fundamental differences in the proliferative state of the gut and the lung epithelia. The intestinal epithelium turns over every 3-5 days, which requires continuous proliferation of intestinal TA cells and the support of the intestinal stem cell. Consequently, proliferation in the gut epithelium does not appreciably increase in the setting of injury. In contrast, the half-life of bronchiolar epithelial cells is on the order of months, and injury can increase proliferation both within airway TA cells and airway stem cells [184, 201]. The differences in baseline proliferation and the capacity to respond to injury by proliferating may provide a biological basis for the apparent differences in signaling mechanisms regulating proliferation. Collectively these data suggest fundamental differences between these organs in signaling pathways contributing to regulation of cell proliferation and growth control.

2.4.2 Roles for β-catenin in regulation of bronchiolar differentiation

Numerous studies have linked β-catenin signaling with regulation of cell fate determination in the skin follicular bulge stem cell and intestine [169, 175-177, 187, 202]. In skin, TOPGal reporter studies confirm activation of β-catenin signaling in stem cell microenvironments at discrete times during epidermal development and follicular growth [176, 187, 203]. Skin-

specific alterations to β-catenin regulatory domains results in altered epidermal daughter cell phenotypes causing *de novo* follicular growth within the interfollicular epidermis and eventual tumorigenesis [176, 177, 181, 187]. Disruption of both N- and C-terminal domains of β-catenin protein induces a fate choice reversal between follicular and interfollicular stem cell [187]. The importance of β-catenin signaling in the regulation of intestinal stem cell fate was first highlighted by prominent defects in crypt-villus architecture that were observed in Tcf4 knockout mice [86, 204, 205]. Intestinal Wnt/β-catenin signaling influences EphB / ephrin-B levels resulting in differential segregation between stem and daughter cells [85, 198]. These studies suggest a regulatory role for Wnt-β-catenin signaling in cell fate determination in classical stem cell hierarchies.

In the lung, gene deletion and misexpression studies demonstrated a critical role for Wnt/β-catenin signaling in the specification of lung endoderm [148, 151, 196, 206-208] and attenuation of β-catenin signaling in the late prenatal-early postnatal period [148, 208]. A reciprocal relationship between TOPGal transgene expression and airway epithelial differentiation suggested that β-catenin dependent gene expression in airways was down-regulated as the secretory cell differentiation program was activated (Reynolds, unpublished data). These data suggested that β-catenin signaling maintained presumptive airway cells in a relatively undifferentiated state and that attenuation of this pathway was necessary for expression of differentiated secretory cell characteristics. This role for β-catenin was supported by the finding that stabilization of β-catenin in Clara cells blocked post-natal secretory cell maturation and secretory to ciliated cell differentiation (Reynolds, unpublished data). The present data showing that β-catenin deficiency has no detectable consequence for regulation of cellular

differentiation in the adult bronchiolar epithelium further supports the idea that low levels of β-catenin signaling are conducive to bronchiolar epithelial cell differentiation.

Overall, our studies suggest that levels of β-catenin are closely regulated in the adult lung, with low cytoplasmic/nuclear β-catenin being the norm. Maintenance of embryonic levels of stable (unphosphorylated) β-catenin has a profound impact of cell differentiation but no impact on proliferation (this manuscript and Reynolds, unpublished data) while deletion of β-catenin phenocopies the normal state and has no detectable phenotypic consequence.

2.4.3 What process does TOPGal activity in the bronchiolar epithelium report?

Activation of a β-catenin responsive gene requires the positive effect of transcriptional activator (β-catenin/TA-Lef1 or β-catenin/TA-TCF) interaction with Lef1 or TEF consensus sites and in some cases displacement of DN-Lef1 or DN-TCF from negative regulatory elements such as the WRE of the Lef1 gene [114]. Thus, stabilization of β-catenin via Wnt signaling or by genetic manipulation of pathway components induces gene transcription only if TA-forms of Lef1 or TCFs are present within the target cell and if the signal tips the balance between negative and positive regulatory mechanisms. In addition, Lef1 and TCFs are self-regulatory and cross-regulatory resulting in a situation in which gene activation can be amplified or attenuated depending on the form of transcription factor that is produced. Activation of a Wnt responsive gene involves a complex web of interactions that may be transient.

In the lung the situation that is permissive for TOPGal transgene expression is found in subsets of unperturbed ciliated cells, Clara cells, and nascent Clara cells after injury. Activation of the TOPGal transgene in all of these cell types may be indicative of previously unidentified and potentially transient process that “fine-tunes” a common function within these cell types.

Based on the finding that β-catenin is unnecessary for post-natal establishment of differentiated secretory or ciliated cell phenotypes, proliferation of bronchiolar reparative cells, expression of mature Clara cell characteristics, or Clara to ciliated cell differentiation, we suggest that TOPGal transgene expression senses a homeostatic mechanism that is common to cells of the bronchiolar secretory/ciliated lineage.

2.5 ACKNOWLDEGMENTS

Drs. Susan Reynolds, Adam Giangreco, Roxana Teisanu, and I collaborated on the production of Figure 7. Dr. Susan Reynolds performed the clonogenic frequency assay in Figure 10B.

Dr. E. Fuchs (Rockefeller University) kindly provided the TOPGal/Cd1 mice. Christine Burton provided assistance with mouse husbandry and genotyping.

2.6 FUTURE DIRECTIONS

The results of this study were largely negative. While evidence of active β-catenin signaling was seen in the epithelium at homeostasis, no role for β-catenin signaling was found in maintenance or repair of the adult bronchiolar epithelium. There are two lingering questions. First, what is the meaning of the sporadic TOPGal transgene activation seen in homeostasis? To confirm that TOPGal activation in this context is truly β-catenin dependent, mice carry both TOPGal and

conditional deletion of β-catenin could be produced. No TOPGal transgene activity should be within the β-catenin null epithelial cells of these mice. This approach is similar to that taken in the skin by Dr. Fuchs and colleagues [175]. Second, loss of TOPGal signaling following naphthalene exposure was quite uniform. Stabilization of β-catenin alters the differentiation program of airway epithelial cells leading to an expansion of immature, stem-like cells. This suggests that down regulation of β-catenin signaling is important for normal differentiation of the airway epithelium (Reynolds, unpublished data). Preliminary data from another member of the laboratory suggests that sFRP, a soluble Wnt pathway antagonist, increases following naphthalene exposure. The functional significance of this increase in sFRP could be explored. The initial experiment would involve localization of sFRP expression, to insure that it is being expressed in an anatomic compartment consistent with a role in suppressing epithelial β-catenin signaling.

3.0 SMAD4 REGULATES LUNG BRANCHING MORPHOGENSIS AND TUMOR FORMATION BUT NOT EPITHELIAL REPAIR

3.1 INTRODUCTION

The airways form a branching, tree-like structure that acts as a conduit to move air from the mouth to the lung periphery. Because the airway epithelium is constantly exposed to pathogens and chemical irritants that can cause damage, it must be able to repair injuries. The TGFβ/BMP family has been implicated both in embryogenesis of the airways and airway epithelial repair following injury.

TGFβ/BMP signaling regulates many biologic processes including cell proliferation, apoptosis, migration, and differentiation (reviewed by Massagué) [100]. TGFβ/BMP ligands bind to a heteromeric complex of Type I and Type II cell surface receptors, and activate the Type II receptor. The Type II receptor then phosphorylates the Type I receptor, which phosphorylates the C-terminus of the receptor Smads. TGFβ signaling causes phosphorylation of Smad2 and Smad3, while BMP signaling phosphorylates Smads 1, 5, and 8. Smad phosphorylation state regulates nuclear accumulation of the RSmads. RSmads associate with the Smad4 to form an active transcription complex. Once in the nucleus, Smad complexes activate or suppress gene transcription in a cell type specific fashion [101]. The phosphatase PPM1A terminates TGFβ signaling by dephosphorylating Smads 2 and 3 [110]. Smad4 is partitioned equally between the

cytoplasm and nucleus independently of signaling activity. In addition to canonical Smad signaling, TGFβ/BMP can signal through a variety of other pathways including TAK1, Erk, JNK, p38, and Rho [209]. Additionally, Smads 2 and 3 can complex with TIF1γ instead of Smad4 [102]. The relative contributions of Smad-dependent and Smad-independent signaling in the lung are unknown.

Both TGFβ and BMP signaling regulate lung development. During branching morphogenesis, simple epithelial tubes branch in a stereotypic fashion to generate the respiratory tree. Loss of Smad2/3 or Smad4 signaling increases lung explant branching *ex vivo,* suggesting that TGFβ is a negative regulator of branching morphogenesis [132]. However, the function of the Smads or Tgfbr1 in lung development has not been tested *in vivo*. Disruption of epithelial BMP signaling through Cre mediated deletion of Bmpr1a markedly stunts distal lung development, leading to a "cystic" phenotype [50]. Distal epithelial proliferation and survival are both decreased. Bmpr1a can signal through Smad4, but the dependency of branching morphogenesis on Smad4 *in vivo* is not known.

Inhibition of TGFβ signaling increases the rate of wound repair in a variety of models. Smad3 knockout mice re-epithelialize skin wounds more rapidly than wild type mice [65]. However, these mice also have much less inflammation associated with the wound which may account for the increased rate of healing. Inhibition of TGFβ signaling also speeds corneal epithelial wound healing [210]. In culture, TGFβ decreases lung epithelial proliferation, while enhancing cell migration [63, 66, 67, 77]. It is thought that TGFβ released during airway injury may have a growth suppressive effect on the epithelium, and thus slow the repair process [68].

In this chapter, we used CCSP-Cre and SPC-Cre to cause recombination of a floxed *Smad4* allele. In contrast to the severe phenotype seen with loss of Bmpr1a, loss of Smad4

dependent signaling during early lung embryogenesis through recombination by SPC-Cre, caused a relatively benign increase in airway branching. Epithelial differentiation and proliferation were normal in the absence of Smad4. Next, the CCSP-Cre line was used to cause conditional loss of Smad4 within the conducting airways. In the naphthalene injury model, loss of Smad4 did not increase proliferation or change the repair response. However, loss of Smad4 signaling throughout the entire airway epithelium caused tumor formation.

3.2 MATERIALS AND METHODS

Animal Husbandry: Colonies of genetically modified mice were bred and maintained under specific pathogen free conditions in an AAALAC accredited facility. Mice were given access to food and water *ad libitum* and housed with a 12-hour light/dark cycle. All procedures involving animals were approved by the Institutional Animal Care and Use Committee.

Mouse Lines Used*:* Mice homozygous for the *Smad4* floxed exon 10 and hemizygous for a CCSP-Cre or SPC-Cre allele were used. The floxed exon 10 *Smad4* allele was originally described by Yang *et al* as exon 8 [211]. Briefly, exon 10 is deleted resulting in mRNA instability and a functionally null allele. The generation and specificity of the CCSP-Cre transgene was described by Hoyle [212]. Mice carrying the SPC-Cre transgene were kindly donated by Brigid Hogan and previously described [50]. Cre-negative littermate controls were used for all experiments. All mice used in this study were on a mixed background. For generation of timed embryos, female mice were co-housed with males for one night. DPC 0.5 was based on noon of the morning males were removed.

G**enotyping:** Mice were genotyped by PCR amplification of genomic DNA extracted from a tail biopsy. Both Cre lines were detected with primers 5' GGA CAT GTT CAG GGA TCG CCA GGC G 3' and 5' GCA TAA CCA GTG AAA CAG CAT TGC TG 3' (amplicon 267 bp). The floxed *Smad4* allele was detected with primers 5'-GGG CAG CGT AGC ATA TAA GA-3' 5'-GGG CAG CGT AGC ATA TAA GA-3'. The predicted wild type amplicon is 385 bp.

Naphthalene Exposure: Male mice, 8-10 weeks of age were given naphthalene (Sigma, St. Louis, MO) dissolved in Mazola brand corn oil at a dose of 275 mg/kg. Intraperitoneal injections were given prior to 10 a.m. Tissue was collected at 3, 10 and 42 days following naphthalene exposure.

Bromodeoxyuridine administration: To determine instantaneous proliferation, a 1.5 mg pulse of BrdU (Sigma, St. Louis MO) was given 2 hours prior to tissue collections. For cumulative proliferative index, mice received 1.5 mg of BrdU every morning for 7 days.

Tissue Collection: Mice were anesthetized with 2.5% Avertin (50% *tert*-amyl-alcohol/50% tribromoethanol), exsanguinated, and the trachea was cannulated. The left lobe was ligated and homogenized for RNA isolation.[189] Lungs for morphometry were inflation-fixed with neutral buffered formalin at 15 cm pressure for 10 minutes with the chest cavity open. Tissue was then immersion fixed in formalin for 6-8 hours and paraffin embedded.

Immunostaining: *Immunofluorescence:* Sections were cleared with xylene, hydrated in graded ethanol solutions, and rinsed with phosphate buffered saline. Slides were microwaved for 20 minutes in 10 mM citrate buffer (pH 6). Sections were blocked with 5% bovine serum albumin/PBS for 30 minutes. Primary antibodies were diluted in blocking solution in incubated for 2 hours at room temperature (see table 1). All secondary antibodies were purchased from Molecular Probes and used a 1:400 with a 2 hour incubation at room temperature. FoxJ1 signal

was enhanced by application of 0.5% Sudan Black in 70% ethanol (SU121, Spectrum Chemical, Gardena, CA) for 2 minutes followed by extensive washing in PBS. Slides were coverslipped using Fluoromount–G (Southern Biotech, Birmingham, AL) and 2 μg/ml 4, 6, diamino-2-phenylindole (DAPI, Sigma, St. Louis, MO). Images were captured as described [51].

Immunohistochemistry for phospho-SMAD2: Slides were deparaffinized, rinsed in PBS, boiled in citrate buffer as above, and blocked in peroxidase blocking solution. Sections were rinsed in PBS, and incubated in primary antibody for 1 hour at room temperature. The Dako EnVision+ Kit (Dako #4011, Carpinteria CA) was then used according to the manufacture's instructions. Slides were counterstained with hematoxylin.

Whole mount immunostaining: The accessory lobe was microdissected along the main axial pathway. Following dissection, lobes were blocked and permeabilized in 5% bovine serum albumin, 1% Triton X-100 in PBS for one hour. Lobes were incubated in rabbit α CCSP antibody diluted 1:2000 in blocking solution overnight. Lobes were rinsed in PBS for at least two hours, and incubated in biotinylated anti-rabbit secondary antibody (1:3000) for at least 12 hours. Lungs were rinsed in PBS for 2 hours and incubated in streptavadin conjugated to horseradish peroxidase for at least 2 hours. Antigen-antibody complexes were detected with a DAB kit (SK 4100, Vector Labs, Burlingame, CA). Stained lobes were photographed using a dissecting microscope.

Table 3: Antibodies Used in Chapter 3

Antigen	Supplier	Titer
Rabbit α CCSP	In house	1:10,000 IF, 1:32,000 IHC
Mouse IgG_1 α FoxJ1	Gift from Steven Brody	1:1500
Mouse IgG_1 α Smad4	Sigma	1:1000
Rat α BrdU	Accurate Chemical Inc	1:500
Rabbit α phospho-Smad2	Cell Signaling, #3101	1:1500
Rabbit α Sftpc	Gift from Peter Di	1:1000

Relative mRNA Abundance: Quantitative RT-PCR was done to measure relative mRNA abundance as described by Reynolds et al [190]. Assays-on-Demand gene expression kit was purchased from Applied Biosystems, Foster City, CA. The following assays were used: *Scgb1a1* (Mm00442046_m1), *SftpC* (Mm00488144_m1), and *Gusb* (Mm00446953_m1), *Foxj1* (Mm00807215_m1), *Claudin-10* (Mm00457974_m1), *Cyp2f2* (Mm00484087_m1). mRNA abundance was determined using an ABI PRISM 7000 Sequence Detection System. Differential gene expression values were calculated by the ΔΔCT method using a standard total lung RNA sample as the calibrator [191]. At least 3 RNA samples were used for each analysis.

Morphometry: *Counting Terminal Bronchioles:* Lungs were inflation-fixed at 15 cm of water with 10% buffered formalin for 20 minutes. The lower right lobes were paraffin embedded in the same orientation. Five μm sections were collected every 250 μm through the entire lobe. A similar number of sections were collected for each animal. The sections were

stained with hematoxylin and eosin, and the number of terminal bronchioles per sections was counted. Twelve sections were counted per animal, and at least 5 mice per genotype were analyzed. The mean number of terminal bronchioles per lobe was calculated. Data are displayed as the mean number of terminal bronchioles ± standard error.

Cumulative proliferative index: Mice were given BrdU for seven days as described above. The proliferative index was calculated by dividing the number of BrdU positive nuclei by the total number of DAPI positive nuclei. Five animals per genotype were used for each time point. Analysis was restricted to cells within one, 20X field of a terminal bronchiole.

Instantaneous proliferative index: Mice were given a 1.5 mg pulse of BrdU two hours prior to tissue collection. The proliferative index was calculated as above. Three animals per genotype were used for each time point. Analysis was restricted to cells within one, 20X field of a terminal bronchiole.

Ciliated cell representation: The representation of ciliated cells was calculated by dividing the number of FoxJ1 immunoreactive nuclei by the number of DAPI positive nuclei. In unperturbed mice, analysis was restricted to the terminal bronchiole. In mice following naphthalene exposure, analysis was restricted to repairing zones in the distal 1/3 of the airway. Repairing zones were defined as linear areas of epithelium bounded on both ends by CCSP immunoreactive cells containing at least 2 adjacent CCSP immunoreactive cells. Three mice were analyzed per genotype.

Nuclear Density: Nuclear density was determined using tissue that was inflation-fixed at 15 cm of pressure with 10% formalin for 20 minutes. Only tissue collected and processed in the same batch was analyzed. One 5 μm section was stained with hematoxylin and eosin. All terminal bronchioles per section were included for analysis. The length of basement membrane

was measured using ImagePro software (Media Cybernetics, Silver Spring, MD). We included only regions of terminal bronchiole where a single layer of epithelial cells and a basement membrane were seen. Nuclear density was calculated by dividing the number of nuclei by the length of basement membrane. Five animals per genotype were analyzed.

Statistics: Where two genotypes were compared, a 2-way t-test was done using Excel (Microsoft, Redmond WA). For time course experiments involving multiple genotypes, Minitab Software (State College, PA) was used to generate a general linear model of the one-way ANOVA type with time and genotype as factors. A p-value of <0.05 was considered significant.

3.3 RESULTS

3.3.1 Smad4 regulates branching morphogenesis

To test the hypothesis that the Bmpr1a signaling in lung branching morphogenesis is SMAD4 dependent, we used Cre-mediated deletion of SMAD4 early in lung embryogenesis to generate lung epithelium without SMAD4 expression. The human surfactant protein C promoter was used to drive Cre expression being at E9.5 dpc [50]. A floxed exon 10 (*Smad4*$^{\Delta E10}$) allele was used to produce a functionally null allele following Cre recombination [211]. The recombination efficiency was determined by immunostaining for SMAD4. At E14.5 and E16.5 dpc, abundant SMAD4 staining is seen in the epithelium and mesenchyme of wild type mice (Figure 12A and 12C). In *SPC-Cre, Smad4*$^{\Delta E10}$ mice, efficient recombination can be seen by E14.5 dpc (Figure 12B). Loss of SMAD4 staining clearly distinguishes the developing epithelium at E16.5 dpc

(Figureure 12D). We concluded that *SPC-Cre* causes efficient recombination of the *Smad4*$^{\Delta E10}$ allele during lung development.

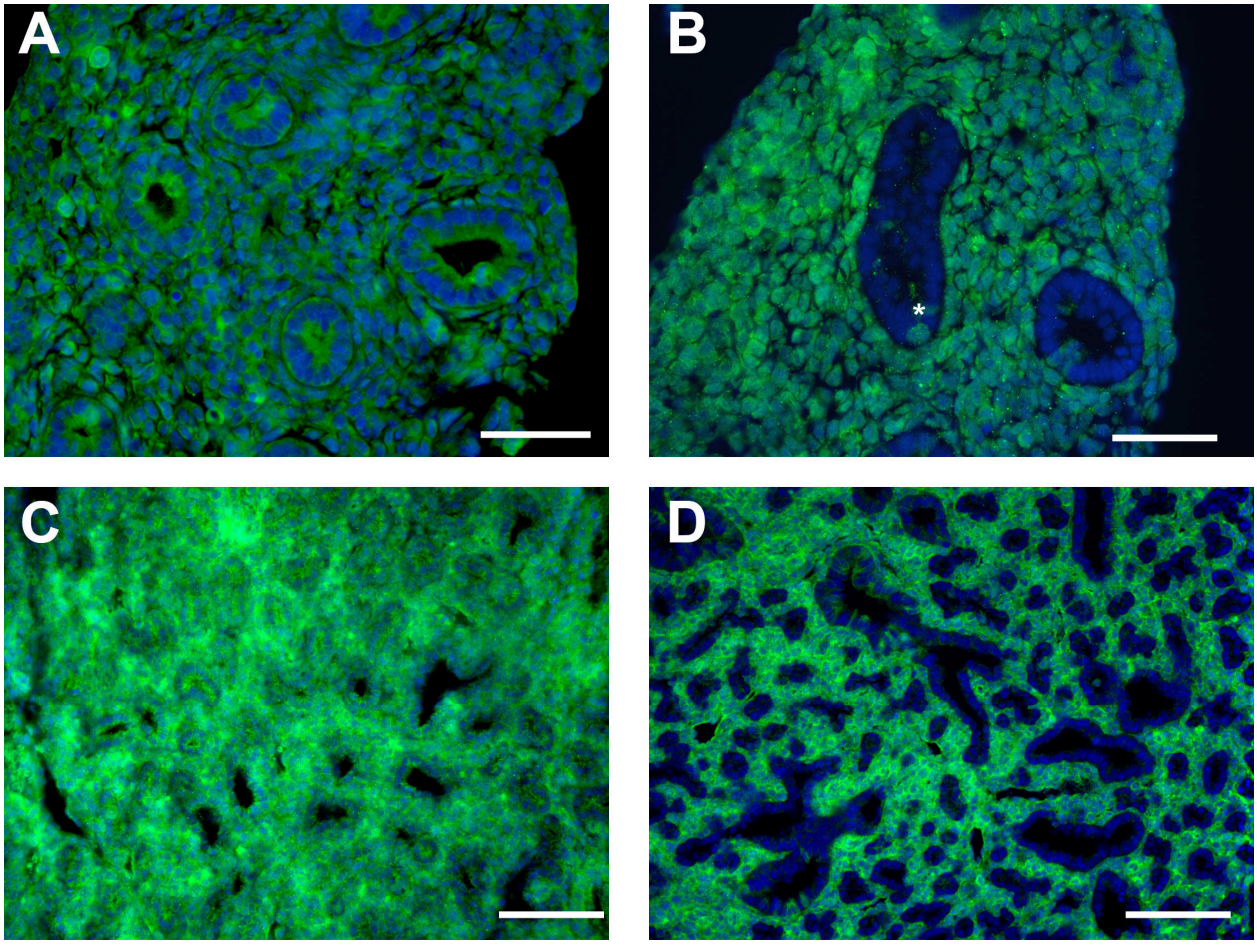

Figure 12: Cell type specific deletion of Smad4

Panel A. Lung tissue from wild-type E14.5 dpc embryos was immunostained for SMAD4 (green). DAPI nuclear counterstain (blue) was also used. Ubiquitous SMAD4 immunostaining is seen in the developing lung epithelium and mesenchyme. B. Lung tissue from an *SPC-Cre, Smad4*$^{\Delta E10}$ E14.5 dpc embryo was stained as above. Smad4 staining is largely absent from the airways. Rare, unrecombined epithelial cells are seen (asterisk). C. At E16.5 dpc, intense SMAD4 staining is seen in both the epithelium and mesenchyme. D. SMAD4 staining is lost in the developing airways of *SPC-Cre, Smad4*$^{\Delta E10}$ E16.5 dpc embryos. Measure bar = 100μm

SPC-Cre, Smad4$^{\Delta E10}$ mice were born live and survived to adulthood in the predicted Mendelian ratio. They exhibited no obvious signs of respiratory distress and gained weight normally (data not shown). On gross dissection, the lungs of *SPC-Cre, Smad4*$^{\Delta E10}$ mice were not remarkable. However, upon tissue section, the lungs of *SPC-Cre, Smad4*$^{\Delta E10}$ mice appeared to have greater airway branching. To confirm that airway branching was abnormal, the accessory lobe was microdissected to reveal the main axial airway. In wild type mice, 2-3 airway branches per daughter from the axial airway could be seen (Figure 13A and C). In *SPC-Cre, Smad4*$^{\Delta E10}$ mice there was increased branching, with minor daughters having 4-5 visible branches (Figure 13B and D). We predicted that if the number of airway branches increased, the number of terminal bronchioles increase. To test this prediction, the number of terminal bronchioles was counted through a systematic sampling of the right lower lobe. Loss of Smad4 signaling caused a 3-fold increase in the number of terminal bronchioles (Figure 13E). We confirmed this finding by measuring the expression of airway specific genes. The expression of surfactant protein C (found in alveolar type II cells), Clara Cell Secretory Protein (*Scgb1a1*), cytochrome P4502f2, claudin-10, and FoxJ1 was measured by quantitative real-time PCR in whole lung homogenate. *Scgb1a1*, *Cyp2f2*, and *Cldn10* are expressed in non-ciliated Clara cells, while *Foxj1* is expressed by ciliated cells [10, 44]. A two-fold increase in airway specific messages (*Scgb1a1, Foxj1, Cyp2f2,* and *Cldn10*) was found in *SPC-Cre, Smad4*$^{\Delta E10}$, while expression of *Sftpc* did not vary by genotype. The comparative mildness of this phenotype supports the conclusion that BMP-dependent branching morphogenesis phenotype is largely Smad4-independent, but reveals Smad4 as a negative regulator of airway branching *in vivo.*

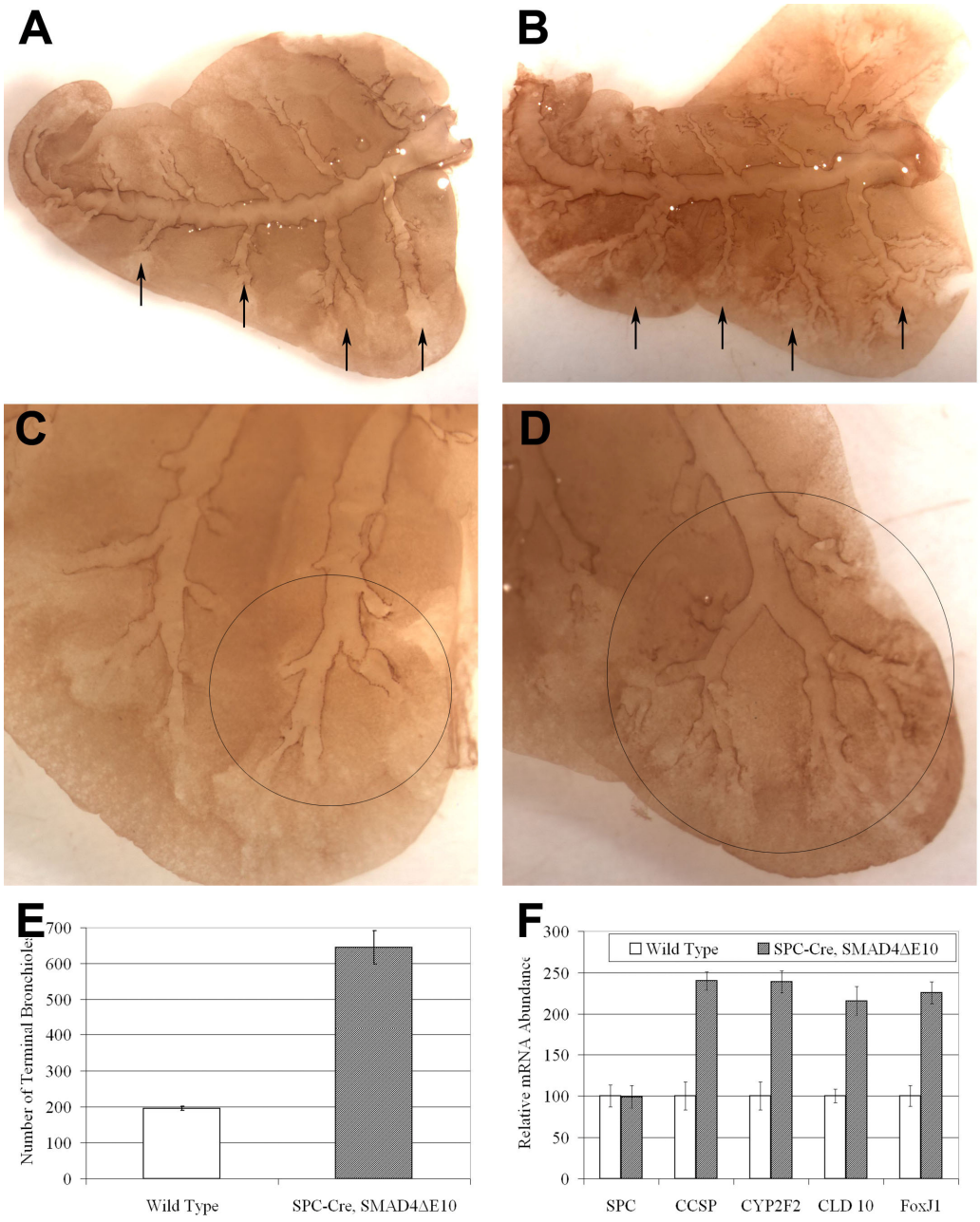

Figure 13: Smad4 regulates branching morphogenesis

Panels A-B. The main axial airway of accessory lobes from wild-type and *SPC-Cre, Smad4*$^{\Delta E10}$ mice was whole mount immunostained for CCSP to increase contrast. DAB staining is seen in brown along cut surfaces of airways. A. The main axial pathway through the accessory lobe of an adult wild-type mouse reveals a stereotypic branching pattern. B. In *SPC-Cre, Smad4*$^{\Delta E10}$ mice, there was a variable increase in the number of airway branches past generation 4. Arrows indicate minor daughters. Original magnification: 12.5X Panels C-D. Higher magnification of

the second airway branch from the main axial pathway of microdissected lung lobes. C. In wild-type mice, one additional generation can be seen branching off of the minor daughter. D. In *SPC-Cre, Smad4$^{\Delta E10}$* mice, 3-4 generations can be seen branching off of the minor daughter.

Panel E: The number of terminal bronchioles was determined using a systematic sampling of the lower right lobe. *SPC-Cre, Smad4$^{\Delta E10}$* mice (hatched bar) have 3-fold more terminal bronchioles than wild-type mice (white bars). Data represented as mean ± SEM. This result is statistically significant by 2-way t-test.

Panel F: Expression of airway and alveolar specific mRNAs. Relative mRNA abundance was determined by real-time PCR on whole lung homogenate for wild-type (white bars) and *SPC-Cre, Smad4$^{\Delta E10}$* mice (hatched bars). *Scgb1a1*, *Cldn 10, FoxJ1,* and *Cyp2f2* expression increased 2-fold in *SPC-Cre, Smad4$^{\Delta E10}$* mice compared to wild-type littermates. The increase was statistically significant by 2-way t-test. *Sftpc* expression did not vary by genotype. Data presented as average ΔΔCT normalized to mean wild-type expression level. Error bars are SEM.

3.3.2 Smad4 is not required for airway cell differentiation

We next determined if Smad4 dependent signaling was required for normal lung epithelial differentiation. At E16.5 dpc, expression of SFTPC protein was seen in small nests of cells regularly scattered throughout the developing wild type lung (Figure 14A). A similar distribution of SFTPC expression was seen in *SPC-Cre, Smad4$^{\Delta E10}$* mice (Figure 14B). By E18.5 dpc, the post-natal distribution of ciliated and secretory cells can be seen in the developing airway. Wild-type mice showed a mix of CCSP and FOXJ1 immunoreactive cells lining the conducting airway (Figure 14C). The airways of *SPC-Cre, Smad4$^{\Delta E10}$* mice were lined by a similar mix of CCSP and FOXJ1 immunoreactive cells at E18.5 dpc (Figure 14D). In adulthood, wild-type (Figure 14E) and *SPC-Cre, Smad4$^{\Delta E10}$* (Figure 14F) had similar distributions of ciliated (FOXJ1 immunoreactive) and non-ciliated (CCSP immunoreactive cells). To more precisely quantitate the ratio of ciliated to non-ciliated cells in the adult, the proportion of FOXJ1

immunoreactive nuclei in terminal bronchioles was determined (Figure 14G). There was no difference in representation of ciliated cell by genotype, and the overall proportion of 30-33% ciliated cells was in agreement with previously reported ratios [3]. Notably, while cell representation in *SPC-Cre, Smad4*$^{\Delta E10}$ mice was normal, the overall architecture of the terminal bronchiole appeared disorganized. In a wild-type terminal bronchiole (Figure 14E), the bronchioalveolar duct junction is abrupt and all airway cells are confined to a simple, columnar epithelium. In *SPC-Cre,Smad4*$^{\Delta E10}$ mice, CCSP immunoreactive cells were seen below the basement membrane of the terminal bronchiole and the bronchoalveolar duct junction was less abrupt. We thought that the bronchiolar epithelium appeared hyperplastic, so we measured the nuclear density. Surprisingly, the nuclear density was slightly lower in *SPC-Cre, Smad4*$^{\Delta E10}$ mice (Figure 14I). Because TGF-β signaling negatively regulates epithelial proliferation *in vitro,* we determined the baseline proliferative index [67]. The proliferative index in the bronchiolar epithelium of *SPC-Cre, Smad4*$^{\Delta E10}$ mice was not statistically different from wild-type mice (Figure 14H). These data support the conclusion that Smad4 dependent signaling is not required for normal differentiation or proliferation in the conducting airway. However, Smad4 may regulate airway morphogenesis in the establishment of the bronchoalveolar duct junction.

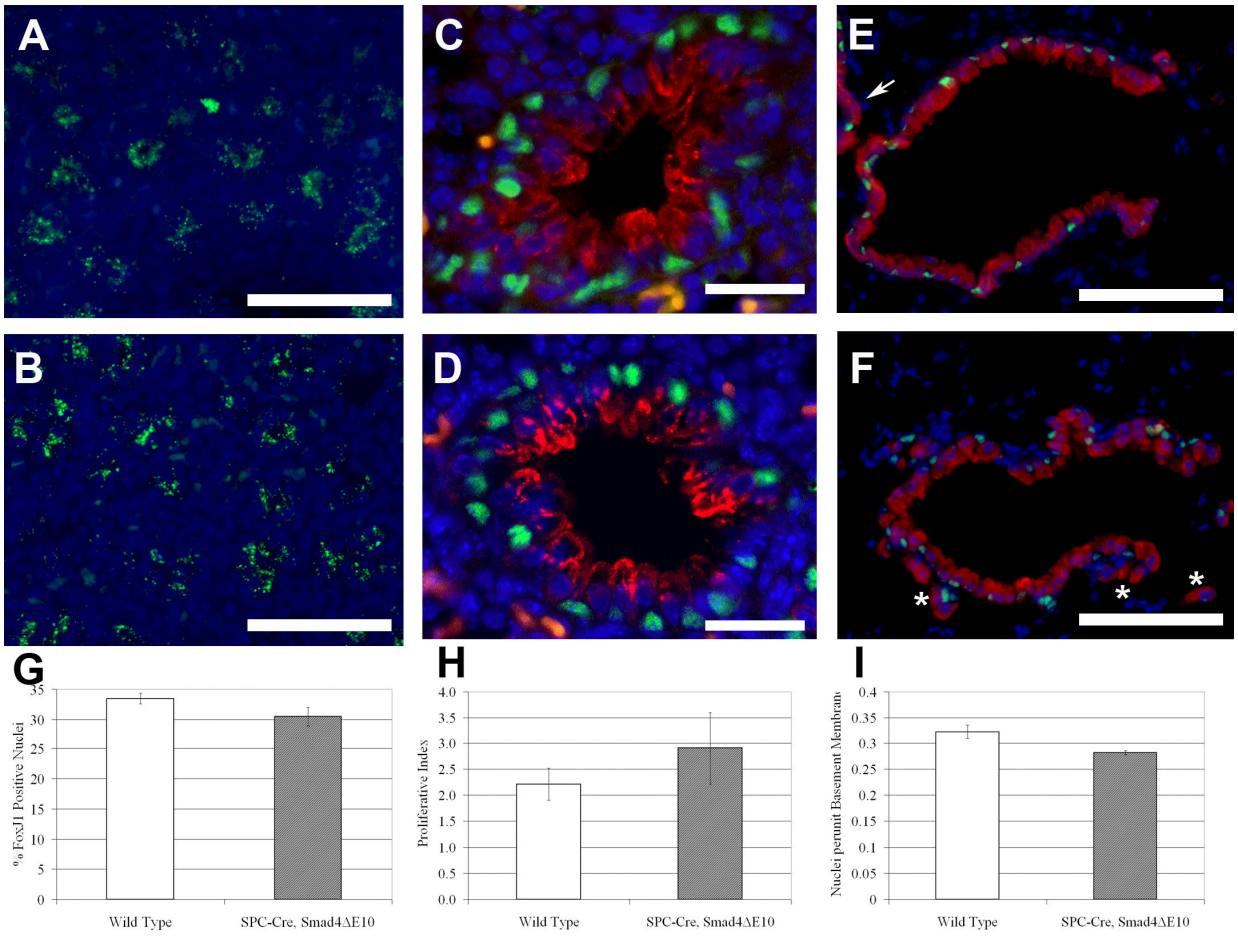

Figure 14: Epithelial Differentiation Proceeds Normally in the Absence of Smad4

Panels A-B: Embryonic lung tissue from E16.5 dpc was immunostained for SPC (green) and counterstained with DAPI (blue). A: SPC immunostaining is seen in the distal developing airways of wild-type mice at E16.5. B: *SPC-Cre, Smad4*$^{\Delta E10}$ mice show a similar pattern of SPC immunoreactivity at E16.5. Measure bar 100 μm.

Panels C-D. Lung tissue from E 18.5 dpc mice was immunostained for CCSP (red) and FOXJ1 (green) to identify developing Clara and ciliated cells respectively. C: In wild type mice, a mixture of CCSP and FOXJ1 reactive cells line the airway. D: *SPC-Cre, Smad4*$^{\Delta E10}$ mice show a similar mixture of CCSP and FOXJ1 reactive cells at E18.5 dpc. Measure bar 30 μm

Panel E-F. Lungs from adult mice were immunostained as above. E. A terminal bronchiole from a wild-type mouse is lined by CCSP (red) and FOXJ1 (green) immunoreactive cells. The arrow marks the wall of another terminal bronchiole. The terminal bronchiolar

epithelium is generally linear, and ends abruptly at the bronchioalveolar duct junction. F. In *SPC-Cre, Smad4*$^{\Delta E10}$ mice, the airway epithelium is made up of a mix of CCSP and FOXJ1 immunoreactive cells. The terminal bronchiole is less organized than those found in wild-type mice (compare to E). Asterisks mark CCSP immunoreactive cells found outside of the terminal bronchiole. Measure bar 100 μm

Panel G: Quantification of the percent FOXJ1 immunoreactive nuclei in the terminal bronchiole for wild-type (white bars) and *SPC-Cre, Smad4*$^{\Delta E10}$ mice (hatched bars). Data presented as average percent FoxJ1 positive nuclei ± SEM. This difference was not statistically significant by 2-way t-test.

Panel H: The cumulative proliferative index following a 7 day labeling period is shown for wild-type (white bars) and *SPC-Cre, Smad4*$^{\Delta E10}$ (hatched bars). Data are shown as an average mitotic index ± SEM. Mitotic index did not vary significantly by genotype at baseline.

Panel I: The number of nuclei per unit basement membrane in terminal bronchioles is shown for wild-type (white bars) and *SPC-Cre, Smad4*$^{\Delta E10}$ mice (hatched bars). Data are displayed as average ± SEM. This result was statistically significant by 2-way t-test.

3.3.3 Deletion of SMAD4 within the conducting airway

TGFβ signaling has been suggested as a negative regulator of epithelial proliferation in response to injury [63, 66, 67]. We wanted to determine if loss of Smad4 signaling would speed the epithelial repair response following naphthalene exposure, an *in vivo* airway injury model [49]. Because of the developmental phenotype found in the *SPC-Cre, Smad4*$^{\Delta E10}$ mice, we used a Cre line with temporally restricted expression. The CCSP-Cre gene is expressed solely within the conducting airway epithelium beginning during the late pre-natal period [212]. To determine if CCSP-Cre caused efficient recombination of the *Smad4*$^{\Delta E10}$ allele, lung tissue was immunostained for SMAD4. Airways showed cytoplasmic and nuclear staining for SMAD4 in

wild type-mice (Figure 15A). Less than 15% of airway cells immunostained for SMAD4 in *CCSP-Cre, Smad4*$^{\Delta E10}$ mice (Figure 15B). *CCSP-Cre, Smad4*$^{\Delta E10}$ mice were born and survived in the expected Mendelian ratio. No increase in branching was seen, as confirmed by identical expression of CCSP by real-time PCR in Figure 17G. Additionally, the terminal bronchioles of *CCSP-Cre, Smad4*$^{\Delta E10}$ mice were indistinguishable from those of wild-type littermates (data not shown).

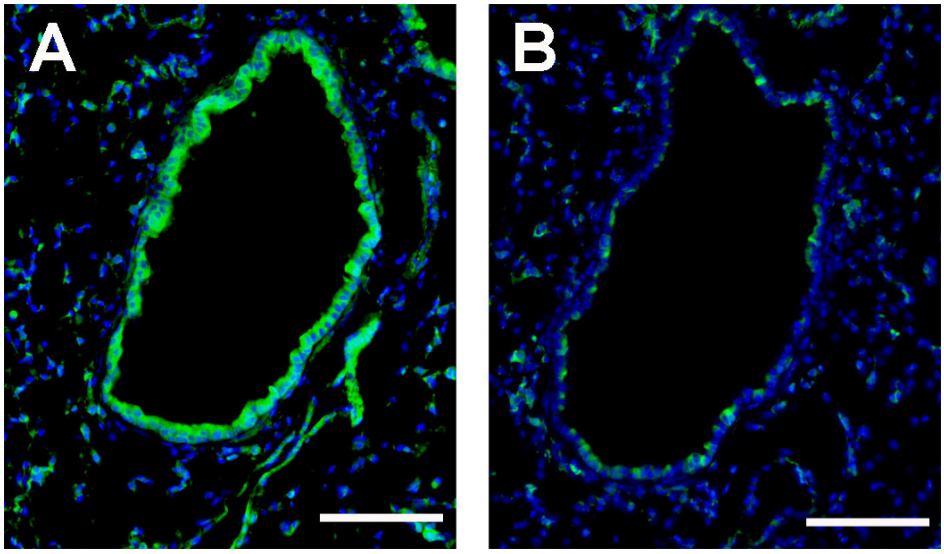

Figure 15: Airway specific deletion of SMAD4

Lungs were immunostained for SMAD4 (green). A: Smad4 staining is seen in the airway epithelium, lung vasculature, and alveoli. B: Smad4 staining is largely lost from *CCSP-Cre, Smad4*$^{\Delta E10}$ airways. The alveolar staining SMAD4 staining is maintained. DAPI nuclear counterstain. Measure bar 100μm.

3.3.4 Evidence of TGFβ signaling during airway repair.

We next determined if there was evidence of TGFβ signaling during the injury and repair response following naphthalene exposure. Lung tissue from mice exposed to naphthalene was immunostained for phosphorylated SMAD2, a downstream signaling molecule from TgfbR2

[100]. There were very rare airway epithelial cells with nuclear pSMAD2 staining in control mice (Figure 16A). Four days following naphthalene exposure, intense pSMAD2 immunostaining was seen throughout the epithelium (Figure 16B). Nuclear pSMAD2 staining persisted until at least 7 days following naphthalene exposure, and was seen in both repaired and unrepaired zones (data not shown). From these data, we concluded that TGFβ signaling is present in the epithelium during repair following naphthalene exposure.

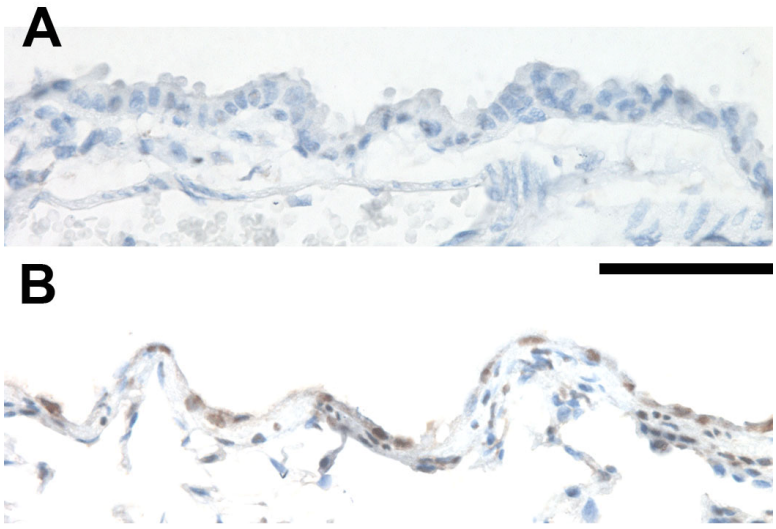

Figure 16:TGFβ signaling following naphthalene exposure

Lungs from mice exposed to naphthalene were immunostained for the presence of phospho-Smad2 (brown) and counterstained with hematoxylin. A: In unperturbed mice, no nuclear pSMAD2 staining is seen within the epithelium. B: Four days following naphthalene exposure most airway epithelial cells show nuclear pSMAD2 staining. Measure bar 100 μm.

3.3.5 Loss of SMAD4 does not speed lung epithelial repair:

To determine if loss of SMAD4 signaling would accelerate airway repair, we exposed wild-type and *CCSP-Cre, Smad4*$^{\Delta E10}$ mice to naphthalene. The airways of both wild-type (Figure 17A) and *CCSP-Cre, Smad4*$^{\Delta E10}$ (Figure 17B) mice were lined with CCSP immunoreactive cells. No

difference in the expression of CCSP (Figure 17G) was seen by quantitative real-time PCR at baseline. Three days following naphthalene exposure, CCSP mRNA abundance dropped to 15% of baseline levels in both wild-type and *CCSP-Cre, Smad4*$^{\Delta E10}$ mice. This drop is accompanied by loss of CCSP immunostaining in both genotypes (Figure 17C-D). At 10 days following naphthalene exposure, repairing foci can be seen at terminal bronchioles and branch points in wild-type (Figure 17E) and *CCSP-Cre, Smad4*$^{\Delta E10}$ mice (Figure 17F). No difference in the number or size of repairing foci was seen by genotype. CCSP mRNA abundance returned to >80% of control levels at day 10 (Figure 17G). No further increase in CCSP mRNA abundance was seen by day 42. There was no statistical difference by genotype in CCSP mRNA abundance at any time point. We concluded that there was no change in the extent of airway repair in the absence of Smad4 dependent signaling.

3.3.5.1 No increase in proliferation with loss of Smad4

Because TGFβ signaling is thought to decrease epithelial proliferation during airway repair, we determined to assess proliferative index in wild-type and *CCSP-Cre, Smad4*$^{\Delta E10}$ mice following naphthalene exposure. No difference in proliferation was seen at baseline, 3 days, or 10 days following naphthalene exposure. As previously described, proliferation was statistically greater at days 3 and 10 following naphthalene exposure [49]. We concluded loss of Smad4 signaling does not increase proliferation in response to naphthalene exposure.

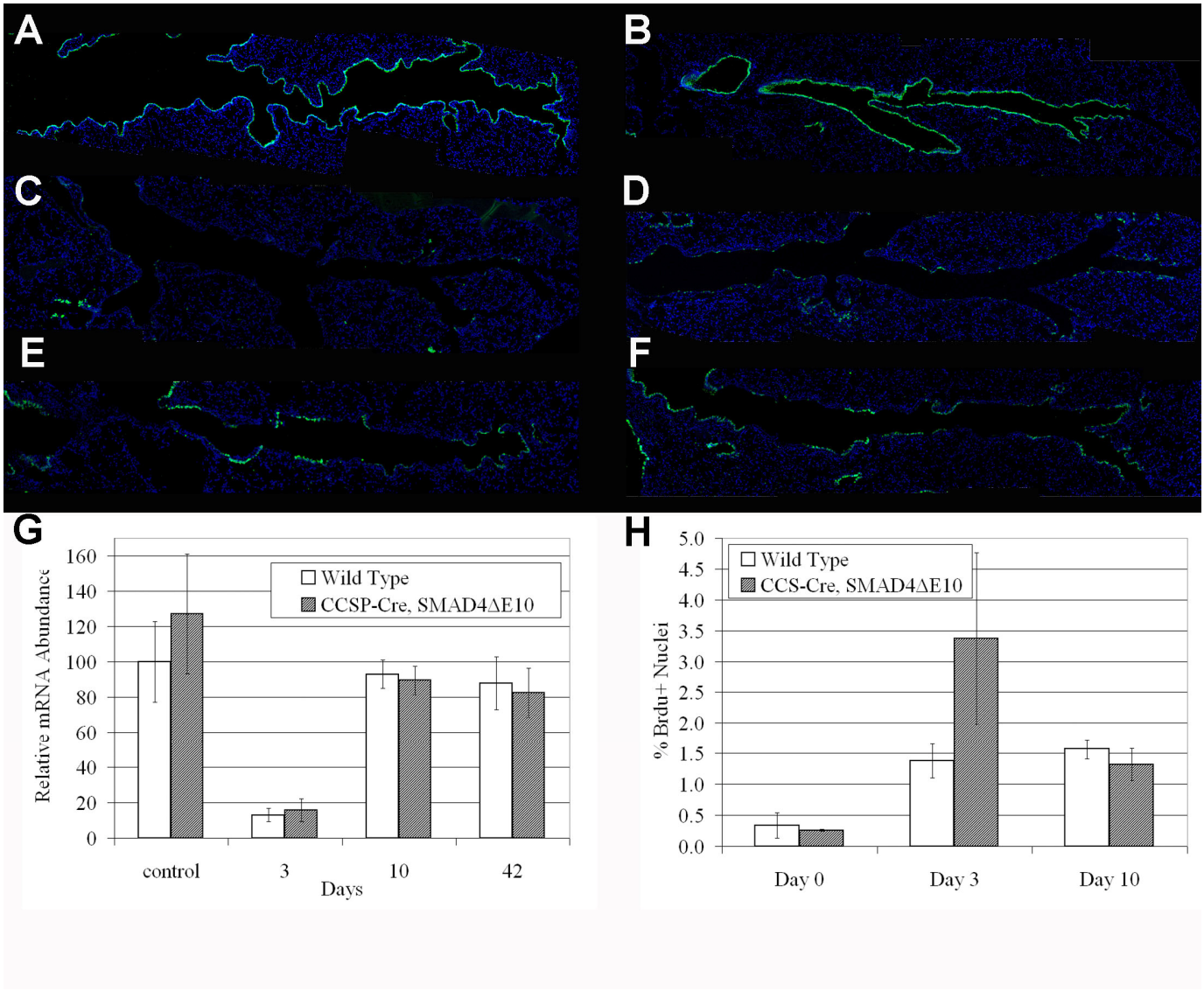

Figure 17: SMAD4 Loss Does Not Effect Epithelial Repair

Panels A-F. Mice were exposed to naphthalene, and the recovered tissue was immunostained for CCSP (green). Airways are oriented proximal (left) to distal (right) in all panels. At baseline, airways of both wild-type (A) and *CCSP-Cre, Smad4*$^{\Delta E10}$ mice (B) are lined with CCSP immunoreactive cells. Three days following naphthalene exposure, CCSP immunoreactivity is lost from both wild-type (C) and *CCSP-Cre, Smad4*$^{\Delta E10}$ mice (D). At day 10, repairing foci, marked by CCSP immunoreactivity, are seen at the terminal bronchioles and at regular intervals along the airway in both wild-type (E) and *CCSP-Cre, Smad4*$^{\Delta E10}$ mice (F). Original magnification 20X

Panel G: Expression of CCSP mRNA in wild-type and *CCSP-Cre, Smad4*$^{\Delta E10}$ mice exposed to naphthalene and recovered for 3, 10, and 42 days. Total lung RNA of untreated control mice (day 0) and treated mice (days 3, 10 and 42) was assayed by quantitative RT-PCR for CCSP mRNA. White bars: wild-type mice. Hatched bars: *CCSP-Cre, Smad4*$^{\Delta E10}$ mice. Data are presented as average ΔΔCT ± SEM.

Panel H: Mice were pulse labeled with BrdU at baseline, 3 days and 10 days following naphthalene exposure. A 5-fold increase in proliferation was seen in the naphthalene treated mice compared to unperturbed mice. No difference was seen by genotype (1-way ANOVA, general linear model).

3.3.5.2 Generation of ciliated cells in the adult

Ciliated cells are formed during embryogenesis prior to secretory cells. In the adult, new ciliated cells differentiate from Clara cells [11, 14]. To determine if loss of Smad4 signaling disrupted the differentiation capacity of Clara cells in adulthood, we counted the number of ciliated cells formed within the nascent epithelium of repaired zones following a 6 week recovery after naphthalene exposure. Tissue was immunostained for CCSP and FOXJ1 to identify Clara and ciliated cells respectively (Figure 18A-B) [10]. Within repairing zones 6 weeks following progenitor depletion, we found 37.8 ± 0.8 of all nuclei were FOXJ1 positive in wild type mice, while 38.3% ± 0.8 of nuclei were FOXJ1 positive in *CCSP-Cre, Smad4*$^{\Delta E10}$ mice (Figure 17C). This difference was not statistically significant, but it was slightly higher than the 30-33% ciliated cells seen in unperturbed terminal bronchioles (Figure 13G). We concluded that loss of Smad4 signaling does not impair differentiation of ciliated cells from Clara cells in the adult epithelium.

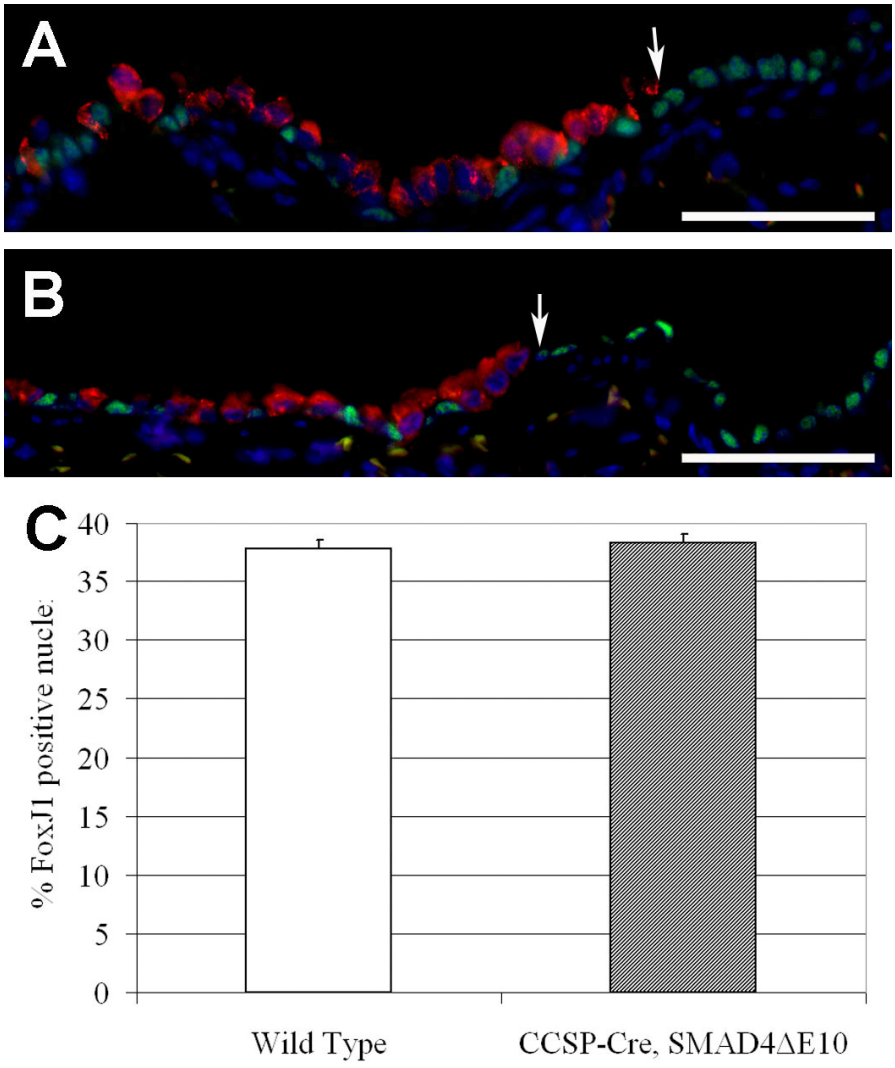

Figure 18: Ciliated cell differentiation is not affected by loss of SMAD4

Panels A-B: Wild-type (Panel A) and *CCSP-Cre, Smad4*$^{\Delta E10}$ mice were exposed to naphthalene and recovered for 6 weeks. Lung tissue was immunostained for CCSP (red) and FOXJ1 (green), secretory and ciliated cell markers respectively. Within the regenerating unit (marked by an arrowhead) approximately 1/3 of all nuclei are FOXJ1 immunoreactive. Measure bar 50 μm. Panel C: The percent of FOXJ1 positive nuclei in regenerating units is shown. White bars: wild-type mice. Hatched bars: *CCSP-Cre, Smad4*$^{\Delta E10}$ mice. Data presented as average percent ± SEM. There was no statistical difference by genotype.

3.3.6 Production of tumors in SPC-Cre, Smad4ΔE10 mice

To further investigate the role of Smad4 in tumorigenesis, a cohort of *SPC-Cre Smad4$^{\Delta E10}$*, *CCSP-Cre Smad4$^{\Delta E10}$*, and wild-type littermates was aged for a minimum of 6 months. We encountered 4 mice with spontaneous adenomas among the *SPC-Cre Smad4ΔE10* group (Table 4).

Table 4: Tumor Incidence in SMAD4 null mice

Age	SPC-Cre	CCSP-Cre	No Cre
<10 weeks	**1/18**	**0/71**	**0/99**
16 weeks	**1/17**	**0/15**	**0/38**
>6 months	**2/13**	**0/14**	**0/15**

No tumors were seen in *CCSP-Cre Smad4$^{\Delta E10}$* or wild-type mice. The tumor incidence increased with age, reaching approximately 1/6 by 6 months of age. One mouse, 8 months of age, had multiple lung adenomas. No increase in mortality was seen within the study period, and tumors remained confined to the lung parenchyma. The tumors were less than 1.5 mm in diameter (Figure 19A), consisted of dense nests of cuboidal cells (Figure 19B), and tended to be found towards the lung periphery. Tumors were immunoreactive for SPC and not CCSP (Figure 19C). The bulk of the tumor did not immunostain for SMAD4, although intense staining was seen in meshlike pattern of spindle shaped cells surrounding the more cuboidal tumor cells.

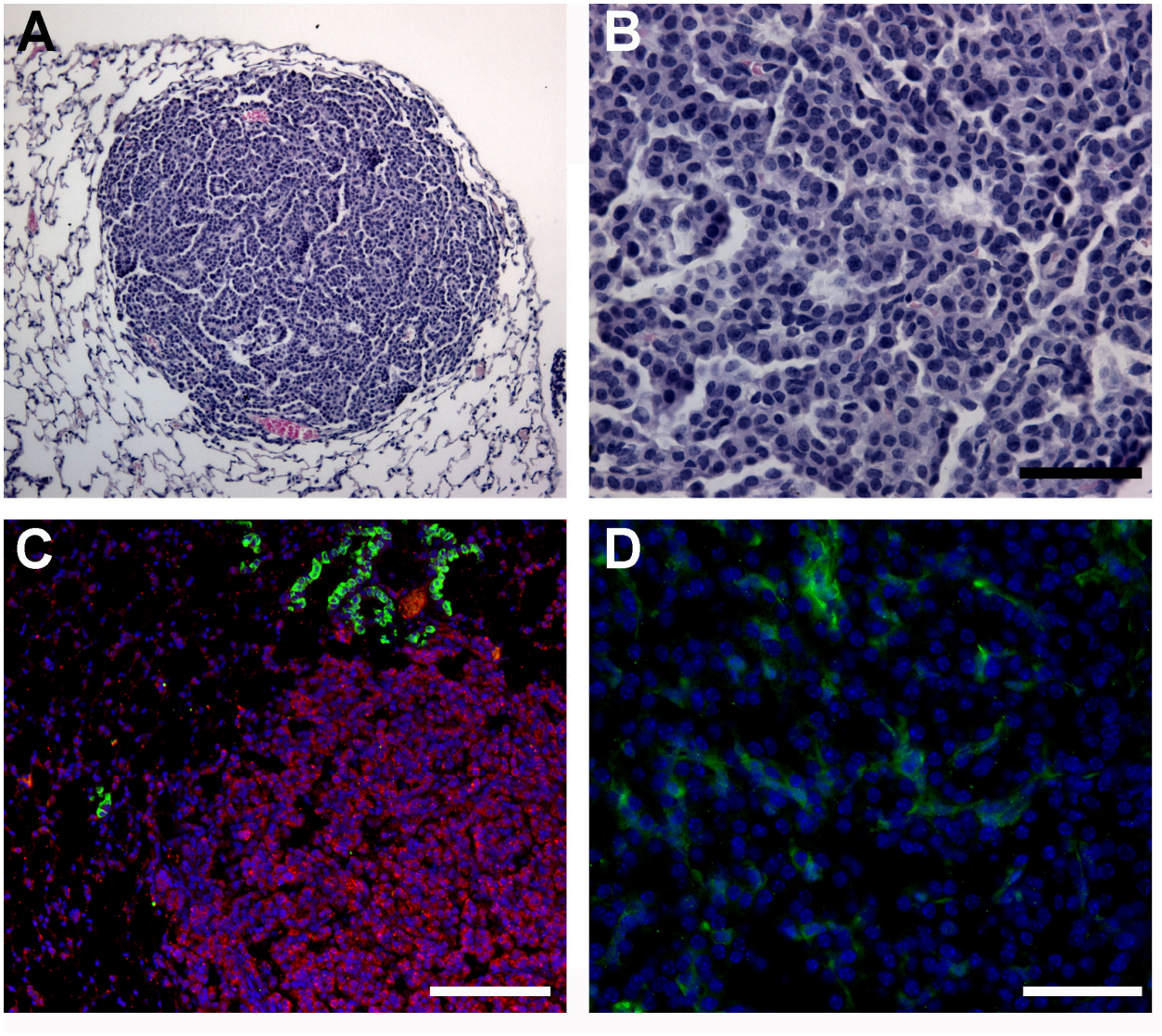

Figure 19: Generation of tumors in SPC-cre, SMAD4 null mice

Panel A: H&E stained section containing a typical tumor. The tumor is approximately 1.2 mm in diameter and located at the lung periphery. Panel B: The tumor is composed of homogenous, cuboidal, nests of cells. Measure bar 50 μm. Panel C: SPC (red) and CCSP (green) immunostaining of an adenoma shows SPC immunoreactivity within the tumor. A CCSP immunoreactive terminal bronchiole is seen at the top of the panel. Measure bar 100 μm. Panel D: Immunostaining for SMAD4 (green) shows that the cuboidal nests of cells within the tumor do not immunostain for SMAD4. Immunoreactivity is seen in spindle shaped cells scattered throughout the tumor. Measure bar 50 μm.

3.4 DISCUSSION

We have used a cell type specific knockout approach to determine the function of Smad4 in lung development, epithelial homeostasis and the repair of epithelial injuries. Loss of Smad4 in the lung endoderm beginning at E9.5 dpc caused increased branching morphogenesis, beginning at the third or fourth airway generation. This increase in branching was a relatively benign phenotype and did not affect the viability of offspring or cause overt physiological problems. Epithelial differentiation was normal in the absence of Smad4, although a 3-fold increase in CCSP and other proteins expressed in the airway was observed. This increase reflected greater representation of airway, rather than disrupted epithelial differentiation. Notably, the terminal bronchiolar epithelium appeared disorganized and possibly hyperplastic. When nuclear density was determined, it was found to be slightly lower than normal, and the mitotic index of terminal bronchiolar epithelial cells was unchanged. Because the appearance of terminal bronchioles did not change appreciably with age, we concluded that this disorganization was a developmental phenotype, rather than a sign of continued epithelial dysregulation in the adult. This finding was reinforced by normal proliferation and differentiation seen in *CCSP-Cre, Smad4*$^{\Delta E10}$ mice. The absence of Smad4-dependent signaling throughout the lung was associated with a greatly increased rate of tumorigenesis. By 6 months of age, 1/6 mice had at least one lung adenoma, with some presenting with multiple tumors.

Next, the function of Smad4-dependent TGFβ signaling was determined in the naphthalene model of airway repair. We observed a large and sustained increase in nuclear

phosphorylated Smad2, and interpreted this as evidence for active TGFβ signaling within the epithelium following naphthalene treatment. Despite clear evidence of TGFβ signaling within the repairing epithelium of wild-type mice, there was no change in the reparative capacity of the Smad4 null epithelium. The size and extent of airway regeneration was unchanged by the absence of Smad4, as was the mitotic index of the repairing epithelium. These conclusions support a role for Smad4 in development and tumor suppression. Regulation of epithelial repair is likely regulated by other, currently unknown, pathways.

3.4.1 Roles for SMAD4 in branching morphogenesis

The relative contributions of TGFβ and BMP signaling to lung development are not fully understood, although it is clear that BMP is a proximal regulator of branching morphogenesis. BMP4 is expressed a branch tips in a dynamic pattern [138, 139]. Perturbation of BMP signaling, either through overexpression of BMP ligands or genetic deletion of BMP receptors, causes a very severe phenotype which culminates in perinatal lethality [50, 138, 139]. Less data exists regarding the role of TGFβ signaling, although it likely is a negative regulator of branching morphogenesis[132]. As both TGFβ and BMP canonical signaling both require through Smad4, despite using distinct RSmads the relative contribution of either pathways is unclear. The observed increase in branching we observed was similar to that seen following disruption of TGFβ signaling as seen in explant studies. It will be important to determine the role of TGFβ receptor dependent signaling *in vivo.* Notably, *SPC-Cre,Smad4*$^{\Delta E10}$ mice develop morphologically normal alveoli. No role for Smad4 in the generation of Type 1 pneumocytes was seen. Bhaskaran and colleagues suggested that autocrine Smad4 signaling is required for the

generation of Type 1 cells from alveolar Type II cells [213]. The difference in results between these two studies is unknown, but may be related to the model systems used.

The relatively mild phenotype we saw on disruption of Smad4-dependent signaling suggests that most BMP signaling within the developing lung is Smad4-independent. Which pathways are involved downstream of Bmpr1a remains to be determined. However, there is ample precedent that Smad-independent signaling is found during embryogenesis. Loss of Bmpr1a or Bmpr2a blocks development prior to gastrulation, as does loss of Smad4. However, Smad4 is required for the formation of extraembryonic lineages, so when embryo aggregation studies were performed, it was found that the phenotype of Smad4 null embryos was much less severe then that of BMP receptor null embryos [214]. Similar results have been obtained in the pancreas, liver, and breast, in which differentiation and organ development proceeded normally in the absence of Smad4-dependent signaling [215-217]. The Smad-independent pathways that are critical during development are largely unknown. These data support a model where Smad4 dependent signaling is required for very early developmental events like pattern development, but has a much less consistent requirement in later developmental events including organogenesis and cellular differentiation.

3.4.2 SMAD4-dependent regulation of proliferation and wound repair

Following naphthalene exposure, we saw increased immunostaining for nuclear phosphorylated Smad2. This suggests that the epithelium was both exposed to active TGFβ or activin receptor ligands, and that the cells are competent to receive such signals. Even so, we saw no change in the extent or kinetics of epithelial repair in the absence of Smad4 when *CCSP-Cre Smad4*$^{\Delta E10}$ and wild type littermates were exposed to naphthalene. This is in contrast to

numerous *in vitro* reports that TGFβ signaling slows bronchial epithelial wound repair, primarily by decreasing epithelial proliferation.[63, 66-68] Additionally, there are multiple *in vivo* studies in the cornea and skin showing increased wound healing with following abrogation of TGFβ signaling [65, 210]. There are several possible reasons for these conflicting results. First, as we saw evidence for Smad4-independent signaling during development, the inhibition of epithelial repair by TGFβ might be Smad4-independent, yet still signaling through the TGFβ receptor. This is comparatively unlikely, as growth arrest is thought to be a Smad- dependent event (evidence reviewed in detail by Massagué)[218]. It is also possible that the epithelium is minimally sensitive to TGFβ in our model system. While we saw evidence of TGFβ signaling through the robust expression of pSmad2, the effects of TGFβ signaling following naphthalene exposure might be masked by the strong mitotic stimuli. Crosstalk exists between TGFβ signaling and a number of other pathways including growth receptor tyrosine kinases. The linker region located between the MH1 and MH2 domains of the R-Smads can be phosphorylated by a number of kinases, including Erk, p38 MAPK, and Jnk. Linker region phosphorylation attenuates Smad-dependent signaling [219, 220]. Thus, it is possible that if a strong enough mitotic stimulus were present in our model, the sum of the signaling inputs might mask any anti-proliferative effects of TGFβ. However, linker region phosphorylation is typically thought to prevent nuclear accumulation of Smads, and we saw evidence of nuclear Smad accumulation. Finally, many wound repair studies involve inhibiting TGFβ signaling within the underlying mesenchyme and inflammatory infiltrate as well as the epithelium [65, 71, 72, 145]. It is difficult to decipher the direct effects of TGFβ on the epithelium from these studies. The decreased severity of epithelial wounding seen in such studies could be secondary to alterations in the inflammatory or mesenchymal response. Further work is necessary to distinguish between

these possibilities, however our data minimally supports the conclusion that loss of Smad4-dependent signaling does not speed epithelial wound repair *in vivo*.

3.4.3 Smad4 in lung tumor suppression

Loss of Smad4 dependent signaling throughout the entire respiratory epithelium early in development caused a markedly increased rate of adenoma formation. These tumors were immunoreactive for SPC, and not CCSP. We saw no tumor formation *CCSP-Cre Smad4*$^{\Delta E10}$ or wild-type mice.

TGFβ and BMP signaling have been associated with tumor suppression in a wide variety of organs. Smad4 is mutated or deleted in more than 50% of all pancreatic ductal carcinomas, and germline mutations in Smad4 or Bmpr1a cause an intestinal juvenile polyposis syndrome [221, 222]. In mouse models, loss of Smad4 causes increased pancreatic, intestinal, and mammary tumor formation [215, 216, 223]. Mice with decreased gene dosage of TGFβ receptor I develop lung adenomas more rapidly following treatment with ethyl carbimate [224]. In humans, disruption of TGFβ signaling is associated with greater adenocarcinoma invasiveness [225]. These studies are in agreement with our data, showing that Smad4 is a crucial tumor suppressor in the lung. It is most likely that TGFβ ligands initiate signaling pathways involved in the lung tumor suppression. In addition to tumor suppression, loss of Smad4 signaling dramatically increases tumor invasion and metastasis in the presence of a constitutively active KRAS, loss of APC, or expression of the polyoma middle T antigen [223, 226], [216, 227]. Whether such an effect is seen in the lung, remains to be determined.

We found a high incidence of tumors in mice carrying the SPC-Cre transgene and no tumors in mice with the CCSP-Cre transgene. The most straightforward interpretation is that

these adenomas rose from an alveolar cell type, probably an SPC expressing Type II , in which recombination does not occur with the CCSP-Cre transgene. This concept is supported by expression of SPC within the developing tumor. However, it is also possible that recombination within an early developmental progenitor, rather than recombination within a specific anatomic compartment, is required for tumor formation.

3.5 ACKNOWLEDGEMENTS

Dr. Roxana Teisanu microdissected the accessory lobes seen in Figure 12. Christine Burton provided valuable assistance with mouse husbandry.

3.6 FUTURE DIRECTIONS

This project has a number of exciting future directions. The finding that loss of Smad4 does not phenocopy loss of Brmpr1a in lung development reveals a role for Smad-independent signaling. This result would be strengthened by determining the developmental phenotype of abrogated TGFβ signaling, as both TGFβ and BMP signaling could be affected by loss of Smad4 and the combined effect of inhibiting both pathways is unknown. A floxed TGFβRII allele exists [228] that could be used in a similar approach to the one used in the current study. If SPC-Cre, floxed TGFβRII mice largely phenocopy the Smad4 null mice, it strengthens the conclusion that Smad4-independent signaling is the critical downstream target of Bmpr1a during lung development. Silencing of Smads 1,5, and 8 could be used in explant cultures as was done by

Zhao and colleagues to determine if Bmpr1a signaling is truly Smad-independent, or just Smad4-independent [132]. This could be technically difficult because, until proven otherwise, all three Smads would need to be simultaneously inhibited. The larger biologic question of interest is what is the identity of the Smad-independent, Bmpr1a dependent pathway that regulates lung development. This is a much more difficult problem to approach. Dr. Krasnow, of Stanford University, has created a detailed map which describes the sequential branching pattern of the mouse airway during early lung development. His group is in the process of high-throughput screening to determine novel regulators of branching events. While extremely laborious, this approach may reveal the downstream target of Bmpr1a.

The negative results in the naphthalene studies are quite surprising. This study is one of the first to directly determine the role of TGFβ/BMP in an epithelium specific manner. It will be useful to confirm these results with signaling blocked at the level of Tgfbr2 using the floxed allele described above. If a Tgfbr2 null airway epithelium repairs indistinguishably from the wild type, then that suggests limited applicability of *in vitro* epithelial wound repair models involving TGFβ to the *in vivo* state. However, the possibility exists that the defects in epithelial repair are due to Smad4-independent signaling, and the proposed experiment would exclude this hypothesis. Also of interest, although beyond the scope of this dissertation, is the role of Smad4 dependent signaling in alveolar epithelial repair. The unexpected viability of SPC-Cre, $Smad4^{\Delta E10}$ mice allows for the design of experiments studying the role of TGFβ signaling in lung fibrosis models.

Finally, the generations of adenomas in the SPC-Cre, Smad4 mice provides a new mouse model for lung carcinogenesis. There is much initial work that must be done to characterize these tumors. Some heterogeneity in tumor morphology was seen, and should be confirmed with

a greater sample size. The onset of tumorigenesis in these mice is comparatively rapid: 1/6 mice had tumors by 6-months of age. However, this is expensive and clumsy from an experimental design approach. There are two general methods for increasing the rate of tumor formation in mice. First, these mice could be exposed to a chemical carcinogen such as the ethyl carbimate (urethane), or the polycyclic aromatics and nitrosylated compounds found in tobacco smoke. There is some strain sensitivity in these models, however with dose adjustment this approach should be effective [159]. The purpose of such exposures would be to demonstrate increased tumor susceptibility with loss of Smad4. The second approach is potentially more powerful, although also more time and resource consuming. NSCLC are frequently associated with alterations in epidermal growth factor receptor (EGFR) signaling or constitutively active KRAS mutations. Genetic mouse models exist that contain constitutively active EGFR alleles as well as activated KRAS alleles [59, 229]. As Smad4-dependent signaling alters the invasiveness of a tumor phenotype in numerous other organ systems, a combination of a promitotic genetic modification and loss of Smad4 could be combined to determine if Smad4-dependent signaling modifies lung tumor invasiveness. Such a model could be also be used to study the effects of various anti-tumor agents in a mouse lung cancer model that more closely approximates the human disease state. Finally, given the role of BMP signaling in intestinal tumorigenesis, it will be interesting to determine if the TGFβ (rather than BMP) signaling pathway activates Smad4-dependent signaling to suppress tumorigenesis. This could be determined using the floxed TGFbRII allele described above.

4.0 GENE EXPRESSION PROFILING IN MOUSE MODELS OF SECRETORY CELL ABLATION DEFINES NOVEL MARKER GENES TO FOLLOW LUNG DEVELOPMENT AND EPITHELIAL REMODELING

4.1 INTRODUCTION

Mammalian conducting airways are lined by a heterogeneous population of non-ciliated secretory cells, including goblet, serous, and Clara cells [3]. In the unperturbed mouse, goblet and serous cells are confined to the trachea, tracheal glands, and most proximal intrapulmonary airways. Clara cells are found along the entire airway, but increase distally to make up more than 60% of all cells in the terminal bronchioles of mice [3]. These cell populations were originally described by their morphological appearance. Clara cells are specifically described as nonciliated, columnar cells with abundant endoplasmic reticulum and dense secretory granules [2]. More recently, Clara cells have been defined by expression of molecular markers, specifically Clara Cell Secretory Protein (CCSP or secretoglobin 1a1). Both approaches have limitations. The use of electron microscopy to classify cells according to their ultrastructural properties is a viable approach for abundant cell types but is cumbersome for the classification of rare cell types. Moreover, use of molecular criteria to describe cell types can lead to confusion since expression of some marker genes such as CCSP, which has long been considered a marker for Clara cells, is broadly expressed by all secretory cell subsets of the murine airway [16, 38].

Clara cells perform multiple physiologic functions in the airway epithelium, including xenobiotic metabolism, eicosanoid production, and the secretion of immunomodulatory proteins. A subset of nonciliated bronchiolar cells acts as the stem cell population for the airway epithelium. Airway stem cells express CCSP, but are distinct from the broader Clara cell population due to their resistance to naphthalene, rarity and localization to discrete airway microenvironments [11, 14, 51, 56].

The airway ciliated and secretory cells are first seen during embryogenesis. Embryonic ciliated cells can first be detected between E14.5 and E16 dpc, depending on the measure used [11, 12]. Currently, the earliest molecular marker of secretory cell specification is CCSP, which is expressed at very low levels beginning at E15.5 dpc and much higher levels prior to birth [44, 230, 231]. Given the earlier appearance of ciliated cells, it is likely that secretory cell differentiation also occurs earlier than we are currently able to detect. The airway epithelium is structurally and functionally immature at birth. Clara cells contain abundant glycogen at birth, which is lost within the first five days of life [230, 232]. The secretory apparatus acquires the adult ultrastructural appearance by 3 weeks of age, and adult xenobiotic metabolizing capacity is not reached until more than 4 weeks of age [44, 230]. The expression of molecular markers also changes during postnatal development. By immunohistochemistry, adult levels of CCSP are found by 2 weeks, while members of the cytochrome P450 family require four weeks to reach adult expression levels [44]. Molecular regulation of post-natal airway epithelial maturation is largely unknown. However, expression of an activated β-catenin allele in the CCSP expressing population arrests postnatal maturation. (Reynolds, unpublished data).

There is functional evidence for multiple CCSP expressing subpopulations. Sensitivity to aromatic hydrocarbons reveals at least two populations of nonciliated bronchiolar cells: toxicant

sensitive and toxicant resistant [49]. In response to allergic inflammation, only secretory cells of the proximal intrapulmonary airways undergo mucus cell metaplasia, while distal airway secretory cells do not [33]. There are limited molecular markers available to distinguish either developmental or spatial subsets of secretory cells. The expression of two secretoglobin family members distinguish very proximal (*Scgb3a1*) from more distal (*Scgb3a2*) secretory cells in the mouse [233]. Acidic mammalian chitinase and Ym1 chitinase distinguish secretory populations that that are respectively resistant and susceptible to mucus cell metaplasia [33]. However, these existing molecular markers only allow for a crude characterization of postnatal airway maturation. In addition to baseline heterogeneity, chronic lung diseases such as asthma, bronchopulmonary dysplasia, and chronic bronchitis cause phenotypic changes within the secretory cell population. These changes include loss of Clara cells, decreased CCSP expression, and increased production of mucus [4, 28, 234]. Given the progenitor role for a subset of secretory cells, the existence of multiple secretory cell subpopulations, and the phenotypic changes seen in human disease states, we sought to further characterize the molecular phenotype of airway secretory cells by expanding the available repertoire of molecular markers that can be used for phenotypic analysis.

In this chapter, we have used two models to specifically ablate mouse Clara cells. In the first model, naphthalene is metabolized to a toxic epoxide by CYP2F2 expressed by mouse Clara cells. Exposure to the aromatic hydrocarbon naphthalene causes Clara cell necrosis in mice [43, 49]. In the second model, the mouse CCSP promoter was used to drive expression of *Herpes simplex* virus thymidine kinase (HSVtk) within the CCSP expressing population. Expression of HSVtk sensitizes cells to the cytotoxic effects of ganciclovir, which CCSP-HSVtk transgenic mice can be used for conditional ablation of CCSP-expressing cells [51, 235]. Microarray

analysis was used to identify genes that significantly decreased in both ablation models. Novel Clara cell-specific genes were identified using this strategy that could be categorized based upon their developmental expression pattern and expression in models of airway injury and epithelial remodeling.

4.2 MATERIALS AND METHODS

Animal Husbandry: Colonies of wild type FVB/n mice, CCSP-HSVtk mice on an FVB/n background, and CCSP-cre, CatnbΔE3 mice on a hybrid 129/B6 background, were maintained as an in-house breeding colony under specific pathogen free conditions in an AAALAC accredited facility. All procedures involving animals were approved by the Institutional Animal Care and Use Committee of the University of Pittsburgh.

Genotyping: CCSP-HSVtk mice were genotyped by polymerase chain reaction (PCR) for the presence of an herpes virus thymidine kinase amplicon as previously described [19]. The CCSP-Cre transgene was similarly detected using the primers 5' GGA CAT GTT CAG GGA TCG CCA GGC G 3' and 5' GCA TAA CCA GTG AAA CAG CAT TGC TG 3' to generate an 267 bp amplicon. Mice carrying the $Catnb^{flox(E3)}$ allele were genotyped using primers 5'- GGT AGG TGA AGC TCA GCG CAG AGC -3' and 5'- ACG TGT GGC AAG TTC CGC GTC ATC C -3'.

Naphthalene Administration: Adult (8-10 week) male mice FVB/n mice were used for all naphthalene exposures. Naphthalene (Sigma, St. Louis MO) was dissolved in Mazola corn oil and injected intraperitoneally at a dose of 275 mg/kg. All injections were performed between 8 and 10 in the morning to normalize injury responses [49].

Ganciclovir Administration: Ganciclovir was administered as previously described [21]. CCSP-HSVtk transgenic mice were exposed to ganciclovir (4.5 mg/day) was administered using 14-day mini-osmotic pumps (ALZET Osmotic Pumps, #2001D; ALZA Corp., Palo Alto, CA). Cytovene-IV (GCV sodium; Hoffmann-La Roche, Inc., Nutley, NJ) was dissolved in sterile normal saline to give a final concentration of 375 mg/ml.

Tissue Recovery for RNA isolation and Histology: Mice were anesthetized using Avertin, exsanguinated, and the trachea was cannulated. Mice were then lavaged extensively with sterile saline, and lung lobes were homogenized. RNA was prepared from whole lung homogenate as described by Chomczynski [189]. For histology, lungs were inflation fixed *in situ* with 10% formalin for 10 minutes and immersion fixed for a minimum of two hours. Tissue was cryoprotected and degassed overnight before being frozen in Tissue-Tek OCT (Pittsburgh, PA) for cryosectioning. Embryonic tissue was immersion fixed with 10% formalin and cryoprotected as above.

Microarray Analysis: Total mouse lung RNA was isolated as described above. Four biologic replicates were used for all time points. RNA samples were cleaned using RNAeasy kits according to the manufacturers instructions (Qiagen, Germantown, MD). Affymetrix Cat# 900493 GeneChip Expression 3'Amplification One-Cycle Target Labeling and Control Reagent kit was used to produce cRNA (Affymetrix, Santa Clara, CA). CodeLink UniSet Mouse 20K I Bioarrays (GE Healthcare Bio-Sciences Corp., Piscataway, NJ) were used for gene expression analysis. Determination of RNA quality, generation of biotin labeled cRNA, hybridization to the Bioarray, scanning and data collection was conducted through the University of Pittsburgh Cancer Institute Clinical Genomics Facility according to the manufacturer's protocol.

Microarray Data Analysis. Genes that did not pass the manufacturer's recommendation for signal quality were excluded from further analysis. After filtering, 18,048 genes were present. Complete data tables were compiled including full annotations using the freeware program *Source* (Stanford University, Stanford, CA) and Microsoft Access (Redmond, WA). Next, data was normalized and statistical analysis performed to determine significant changes in gene expression within each model. Data was imported into *ScoreGenes Software Package* (Jerusalem, Israel) for data normalization and statistical analyses. Significant gene expression changes were defined as fulfilling a Student's t-test p value <0.05 and a threshold number of misclassifications (TNOM) of ≤ 1. Next, genes defined as significant by both criteria at 2 days following naphthalene exposure and either 6 or 9 days following ganciclovir exposure were identified.

RNA Abundance: Quantitative RT-PCR (Q-PCR) was used to assess mRNA abundance. cDNA was prepared and assayed as previously described [190]. Differential gene expression was determined using an ABI PRISM 7000 Sequence Detection System and values calculated by the method described by Heid using a standard total lung RNA preparation as calibrator [191]. Assays-on-Demand gene expression probes were purchased from Applied Biosystems, (Foster City, CA.) We used the following probes: Mm00457974_m1 (*Cldn10)*, Mm00514964_m1 (*Fmo3)*, Mm00508163_m1 (*Aox3)*, Mm00446953_m1 (*Gusb)*, Mm01158777_m1 (*Pon1)*, Mm00484087_m1 (*Cyp2f2),* Mm00488144_m1 (*Sftpc),* and Mm00442026_m1 (*CCSP).*

Immunofluorescence: Immunofluorescence techniques were used to detect Cldn10 (Zymed, 1:1000), β-catenin (BD Transduction Labs, 1:500), CCSP (in house, 1:20,000) and ZO-1 (Zymed, 1:100). Frozen sections were post-fixed in 10% neutral buffered formalin for 10 minutes, rinsed in distilled water, and blocked with 5% BSA/PBS prior to applying primary

antibodies. Primary antibodies were incubated for 2 hours at room temperature, washed, and secondary antibodies were applied for 2 hours at room temperature. All secondary antibodies were purchased from Molecular Probes. Slides were coverslipped using Fluoromount-G (Southern Biotech, Birmingham, AL) containing 2μg/mL 4, 6, diamidino-2-phenylindole (DAPI, Sigma, St. Louis, MO). Antigen-antibody complexes were visualized as single optical planes using an Olympus Fluoview confocal microscope equipped with Nomarski optics for simultaneous brightfield detection. Images were acquired and processed using Metamorph imaging software.

Statistics: ANOVA analysis was done with Minitab software (State College, PA). A p value of ≤ 0.05 was considered significant in these studies. Determination of statistical significance of real-time PCR data involving a time course and two genotypes was done using a general linear model (two-way ANOVA type). Genotype and time were used as factors, with the mRNA abundance as a response factor. In the case of statistical significance, a post-hoc Tukey test was used.

4.3 RESULTS

4.3.1 Models of Clara Cells Depletion.

We used two models of Clara cell depletion to identify genes specifically expressed within Clara cells. The naphthalene and CCSP-HSvTK models were used as previously described [19, 49]. By two days following naphthalene exposure, abundance of the Clara cell specific mRNA *CCSP* decreased to 7.3% ± 2.6, and *Cyp2f2* decreased to 6.9% ± 2.6 of control levels within total lung

RNA ($p<0.05$ for both genes, Figure 20A). The abundance *Cyp2f2* and *CCSP* mRNAs began to increase by day 6, reflecting the previously described repair process [49]. During this period there was no decrease in *Sftpc* mRNA abundance (data not shown). Ganciclovir administration causes selective depletion of *Scg1a1* expressing cells when administered to mice expressing herpes simplex viral thymidine kinase under the Clara cell specific mouse *CCSP* promoter [19]. With 3 days of continuous ganciclovir administration, *CCSP* and *Cyp2f2* mRNa abundances began to decrease. By day 9, *CCSP* mRNA abundance decreased to 6.4% ± 3.5 of control abundance and *Cyp2f2* mRNA abundance decreased to 5.8% ± 3.1 of control abundance ($p<0.05$ for both genes, Figure 19B). Beginning at day 6, a drop in Surfactant Protein C mRNA was seen reflecting the inflammatory response described in this model [235]. However, this drop did not reach statistical significance by 1-way ANOVA (not shown). These data confirmed that the lung tissue used for further microarray analysis showed the previously described pattern of injury and repair.

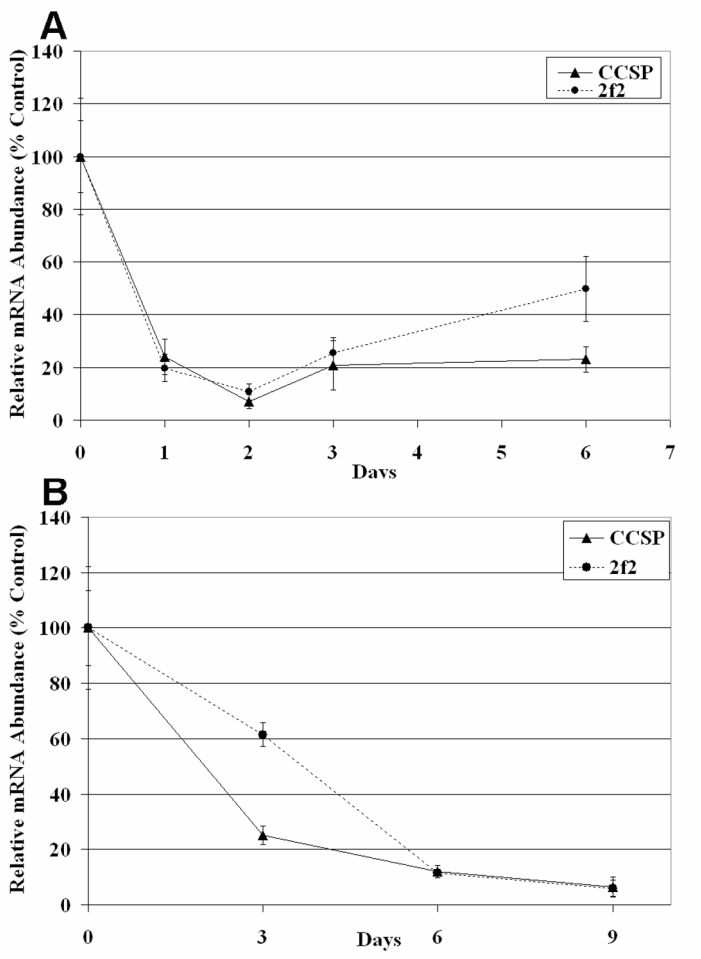

Figure 20: Clara cell depletion in naphthalene and CCSP-HSVtK models

Panel A: Mice were exposed to naphthalene and expression of *Scgb1a1*and *Cyp2f2* was assayed by quantitative real time PCR in total lung RNA. Four mice were used per time point. All RT-PCR data is shown normalized to % mean control mRNA abundance. Naphthalene exposure caused a 90% reduction in both *Scgb1a1* and *Cyp2f2* mRNA abundance by day 2 ($p<0.05$ for both *Scgb1a1* and *Cyp2f2*, control v later time points by 1-way ANOVA). Panel B: Mice carrying the CCSP-HSvTK transgene were exposed to ganciclovir. Four mice were used per time point. *Scgb1a1* and *Cyp2f2* message abundance was assayed as above. Clara cell ablation decreased *Scgb1a1* and *Cyp2f2* mRNA abundance. A minimum mRNA abundance of less than 10% control was seen at day 9 ($p<0.05$ for both *Scgb1a1* and *Cyp2f2*, control versus later time points by 1-way ANOVA).

4.3.2 Identification of Putative Clara Cell Markers

Codelink mouse 20K microarrays were used to identify genes that significantly decreased following Clara cell depletion. At two days following naphthalene administration, 742 genes decreased by more than 2-fold when compared to control abundances. In the CCSP-HSVtK model, 35 genes decreased at day 6, and 65 genes decreased by day 9 when compared to control abundances. As show in Table 5, 19 genes were identified that decreased in both models of Clara cell depletion. We included genes for further analysis if they decreased more than two-fold, had $p<0.05$, and a threshold number of misclassifications (TNOM) of 0 at 2 days following naphthalene treatment, and met the same criteria at either day 6 or day 9 of ganciclovir exposure in the CCSP-HSVtK model. Of these genes, *Cyp2f2* (NM_007817), *CCSP* (NM_11681), and Secretoglobin 3A2 (NM_054038) are well described Clara cell genes [43, 233]. We selected the following genes that met these criteria for further analysis: paraoxonase 1 (*Pon1*), flavin containing monooxygenase 3 (*Fmo3*), aldehyde oxidase 3 (*Aox3*), and claudin 10 (*Cldn10*).

Table 5: Genes that decrease following Clara cell ablation

		Naphthalene Day 2		CCSP-HSVtK day 6		CCSP-HSVtK day 9	
Gene	Description	TNOM	Fold Change	TNOM	Fold Change	TNOM	Fold Change
NM_172484	RIKEN cDNA E030049G20 gene	0	-2.0	0	-1.9	0	-2.4
NM_007902	Endothelin 2	0	-2.1	0	-2.3	0	-2.4
AK01708		0	-2.2	1	-2.2	0	-2.4
NM_007817	Cytochrome P450, family 2, subfamily f, polypeptide 2	0	-2.3	0	-1.9	0	-4.1
NM_021386	Claudin 10 (Cldn10), transcript	0	-2.5	0	-2.0	0	=3.5
NM_008286	Strain B10.S/DvTe histamine receptor H2 (Hrh2)	0	-2.7	0	-2.5	0	-3.0
BG795288	Transcribed locus	0	-2.7	0	-2.7	0	-2.7
NM_009381	Thyroid hormone responsive SPOT14 homolog	0	-3.1	0	-2.8	0	-3.1
NM_011681	Secretoglobin, family 1A, member 1 (uteroglobin)	0	-3.1	0	-1.7	0	-3.7
AF306532	Chemokine (C-C motif) receptor-like 1 (Ccrl1)	0	-3.2	0	-3.1	0	-5.4
BC031432	CDNA clone MGC:6757	0	-3.6	0	-3.0	0	-2.9
NM_021456	Carboxylesterase 1	0	-4.8	0	-2.7	0	-2.4
NM_146017	Gamma-aminobutyric acid (GABA-A) receptor, pi	0	-4.8	0	-3.3	0	-7.2
NM_023617	Aldehyde oxidase 3 (*Aox3*)	0	-5.2	0	-3.1	0	-3.0
AW909485	PREDICTED: leucine-rich repeats and calponin homology (CH) domain containing 1	0	-5.4	1	-2.8	0	-2.2
NM_008030	Flavin containing monooxygenase 3 (*Fmo3*)	0	-6.0	0	-3.1	1	-2.2
NM_144930	Expressed sequence AU018778	0	-7.8	0	-3.3	0	-2.8
NM_054038	Secretoglobin, family 3A, member 2 (Scgb3a2)	0	-8.5	0	-3.9	0	-19.1
NM_011134	Paraoxonase 1	0	-12.1	0	-6.1	0	-15.9

4.3.3 Validation of Identified Genes

We used real-time reverse-transcription PCR as a secondary method to validate changes of mRNA abundance observed by microarray analysis. As shown in Figure 21, *Pon1, Fmo3, Aox3,* and *Cldn10* decreased to 2.7% ± 1.2, 8.5% ± 3.7, 2.9% ± 1.3, and 3.5% ± 1.5 respectively following naphthalene treatment ($p<0.05$ by Tukey test for all 4 genes). The general pattern of depletion and recovery was similar to that of *Scgb1a1* (Figure 20A). In the following recovery period, *Cldn10* recovered the most rapidly (approximately 79.5 ± 18.7% control at day 5, and 41.8% ± 0.7 at day 10). *Cldn10* mRNA abundance did increase more rapidly than that of *Pon1* and *Fmo3,* with a statistically significant increase found at day 5. *Pon1* showed the slowest recovery (17.9% ± 5.7 of control at day 10). In the CCSP-HSVtK model, *Pon1, Fmo3, Aox3,* and *Cldn10* decreased to less than 30% of control at day 6 following ganciclovir administration. After 9 days of continuous ganciclovir exposure, the expression of the putative Clara cell markers was as follows: *Pon1* (1.2% ± 0.3), *Fmo3* (8.9% ± 3.3), *Aox3* (11.6% ± 4.4), *Cldn10* (13.2% ± 5.1). This expression pattern following airway injury is consistent with the identified genes being expressed within the Clara cell population.

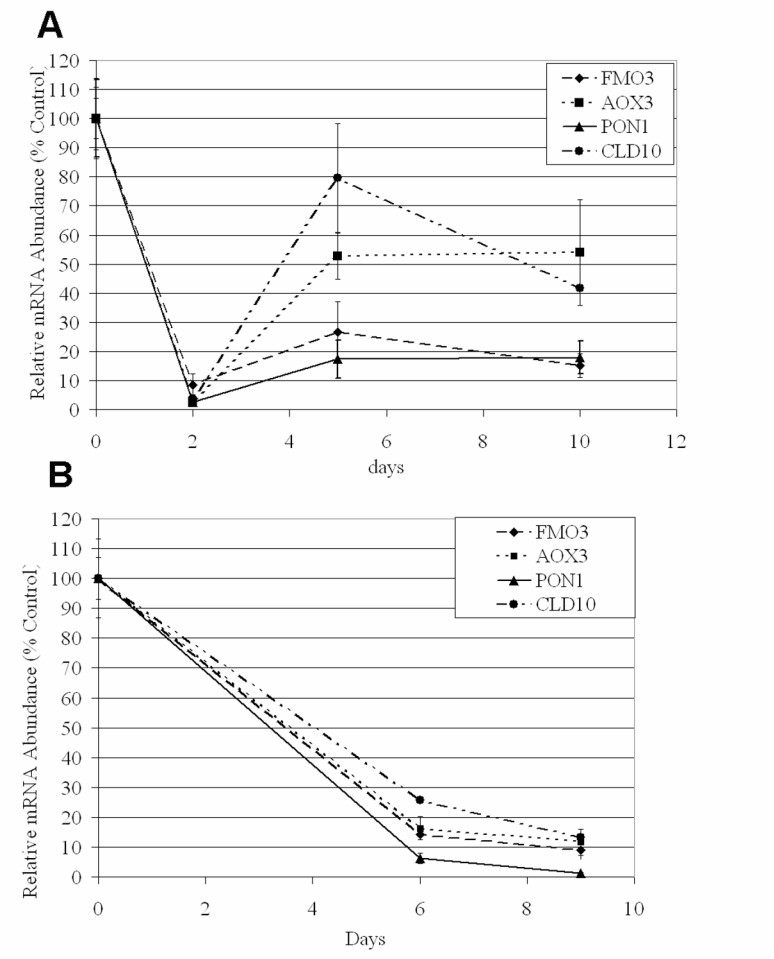

Figure 21: Validation of putative Clara cell markers in naphthalene and CCSP-HSVtK models

Panel A: The expression of the putative marker genes was assayed by real time PCR in total lung mRNA following naphthalene exposure. All markers studied show are expressed at <10% control levels 2 days following naphthalene ($p<0.05$ by 1-way ANOVA, followed by Tukey analysis). Additionally *Cldn10* and *Aox3* showed a statistically significant increase at days 5 and 10 compared to day 2 ($p<0.05$ by 1-way ANOVA, followed by Tukey analysis). Panel B: The expression of putative Clara cell markers was assayed by real time PCR in total lung mRNA from CCSP-HSVtK mice following ganciclovir administration. Decreased expression of all 4 markers was seen with <15% control mRNA abundance seen at day 9 (statistically significant by 1-way ANOVA, followed by Tukey test). Four mice per time point were used in both experiments.

4.3.4 Application of Novel Secretory Cell Markers to Follow Developmental Maturation of the Airway Epithelium

Existing and newly identified markers for secretory cell maturation were applied to the analysis of normal airway maturation in wild-type mice and arrested airway maturation that accompanies potentiation of β-catenin signaling in the late embryonic period. The developmental expression of putative secretory cell markers was determined in total lung mRNA from E17.5 dpc through adulthood. Genes could be classified into two general categories based upon their developmental expression patterns. *Aox3* and *Pon1* showed a large increase in mRNA abundance between day 14 and adulthood (Figure 22A) which mirrored the increase in mRNA abundance seen in *Cyp2f2*. Expression of these three genes (*Aox3, Pon1* and *Cyp2f2)* approximately tripled between birth and adulthood. This increase was statistically significant for all three genes by 1-way ANOVA, followed by Tukey test. *Fmo3* was undetectable prior to day 28, when it was expressed at 28% of adult levels. *Cldn10* showed a different developmental expression pattern, with mRNA abundance at postnatal day 3 only 39.3% ± 9.7 of mRNA abundance at E17.5 dpc (Figure 22A). Only the *Cldn10* mRNA abundance change between embryonic day 17.5 and post-natal day 3 was statistically significant (1-way ANOVA followed by Tukey test).

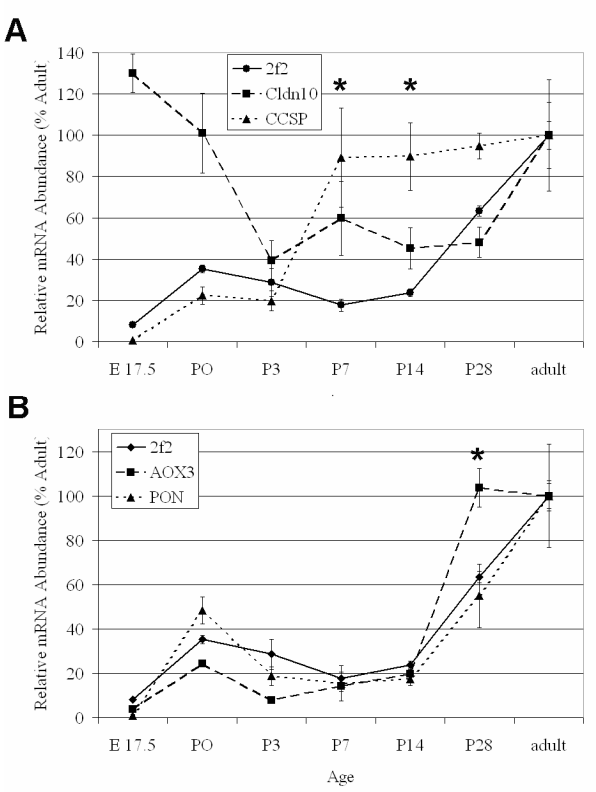

Figure 22: Expression of putative Clara cell markers during development

Expression of *Aox3*, *Cyp2f2*, *Pon1*, *Scgb1a1* and *Cldn10* was assayed by RT-PCR in total lung mRNA from mice of different ages. Three to six mice were used per time point. E17.5 refers to embryonic day 17.5. "P" refers to post-natal day of tissue collection. Expression was normalized to adult expression levels and presented as % adult mouse relative mRNA abundance. A. *Cyp2f2, Scgb1a1,* and *Cldn10* all show different developmental kinetics. *Cyp2f2* increases rapidly between P14 and birth (statistically significant, 1-way ANOVA followed by Tukey analysis). *Scgb1a1* increase earlier, between P3 and P7. The difference kinetics between *Cyp2f2* and *Scgb1a1* is statistically significant at P7 and P14 (general linear model followed by Tukey analysis). *Cldn10* showed yet a third developmental pattern, dropping between E 17.5 and P 3 (the only significant time points by 1-way ANOVA). B. *Cyp2f2*, *Aox3*, and *Pon1* behave similarly. There is a statistically significant increase in expression of all 3 messages across the time course (1-way ANOVA followed by Tukey analysis). *Aox3* mRNA abundance increases more rapidly than *Cyp2f2* or *Pon1* (statistically significant difference at P28 by general linear model followed by Tukey analysis).

4.3.5 Altered Epithelial Maturation Accompanying β-catenin Expansion of Stem-Like Cells.

Expression of a stabilized form of β-catenin within the conducting airway epithelium causes a perinatal developmental arrest (Reynolds, unpublished data). We next used the expression of the putative marker genes to determine at what approximate age the epithelial differentiation was arrested. As previously described, *Cyp2f2* mRNA abundance increases 2.5 fold between 3 weeks and 8 weeks of age. In CatnbΔE3 mice, this increase in expression was not seen (Fig 23A). The expression pattern of *Pon1* (Fig 23B), *Aox3* (Fig 23C), and *Cldn10* (Fig 23D) was similar to that of *Cyp2f2*. This analysis was not done for *Fmo3* because the message was undetectable in wild-type mice prior to day 28. The differences in gene expression become most apparent between 2-3 weeks of age, which suggests that stabilization of β-catenin most alters later post-natal airway maturation. This is in agreement with previously published data showing that glycogen (which disappears within the first 5 days of birth) is not found in Clara cells of CatnbΔE3 mice.

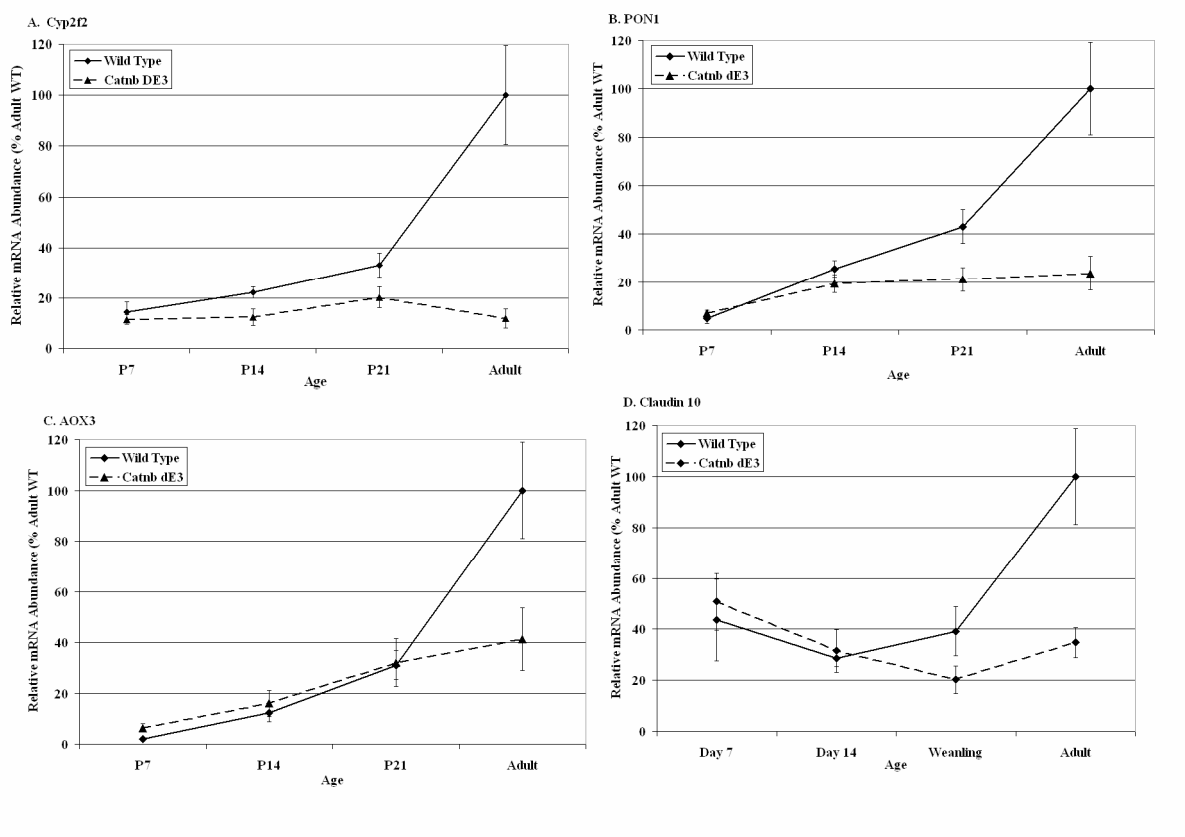

Figure 23: Altered Clara cell marker expression in an epithelium with arrested Clara cell maturation

Lung tissue from CCSP-Cre, CatnbΔE3 mice was collected at various post-natal developmental time points and assayed by real-time PCR for the expression of the identified marker genes. Panel A: As previously described, the post-natal increase in CYP2F2 mRNA does not occur in CCSP-Cre CatnbΔE3 mice. Panels B and C: *PON1* and *AOX3* show a similar pattern to CYP2F2, with a large increase in expression between day 14 and adulthood in wild-type mice. This increase is blunted in CatnbΔE3 mice. Panel D: CLD 10 mRNA increases four-fold between weaning and adulthood in wild type mice, but not in CatnbΔE3 mice. All differences between genotypes are significant at the adult time point by 1-way ANOVA followed by Tukey analysis.

4.3.6 Subcellular Localization of Claudin 10.

Since *Cldn10* shows a Clara cell specific expression pattern in the naphthalene and ganciclovir models, but shows a distinct pattern of developmental regulation to those of phase I metabolizing enzymes, we determined the cellular and subcellular distribution of Cldn10 using confocal immunofluorescence microscopy. As shown in Figure 24A, Cldn10 (red) co-localized with β-catenin (green) along the lateral membrane of conducting airway epithelial cells. It was not located exclusively at the tight junctions. The relationship between the tight junctions and the lateral membrane is seen in Figure 24B. Punctate ZO-1 staining is seen at the apical edge of the lateral membrane, while β-catenin staining is seen along the entire basolateral membrane. Additionally, a small cytoplasmic pool of Cld10 was seen.

4.3.7 Cellular and Developmental Expression Pattern of Claudin 10

To determine the cellular localization of Cldn10, we colocalized Cldn10 with the Clara cell marker CCSP by confocal immunofluorescence microscopy. Cldn10 was located on the membrane of only CCSP immunoreactive cells (Figure 24C-F). Cell junctions between cells that are not immunoreactive for CCSP lack Cldn10 staining (arrows in Figure 24F). No staining was seen in the alveolar space, vasculature, or mesenchyme. Additionally, differences in proximal-distal expression were seen.

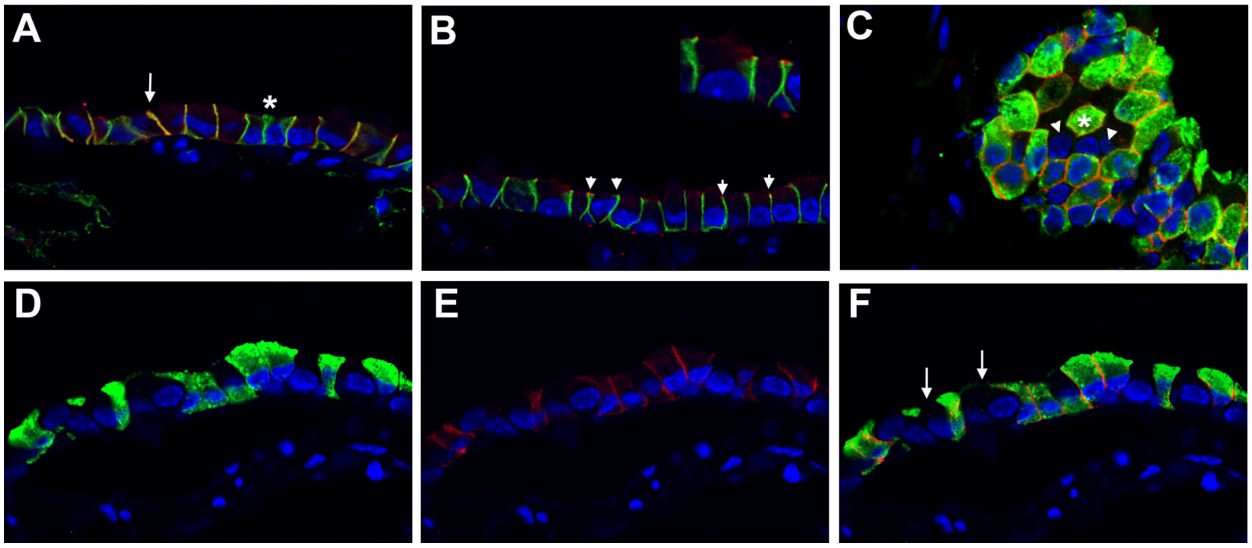

Figure 24: Figure 5: Subcellular localization of Claudin 10

Cellular localization of *Cldn10* was determined on frozen mouse lung sections by immunofluorescence and imaged with confocal microscopy. Panel A: *Cldn10* staining (red) co-localizes along the lateral membrane with β-catenin (green). Arrow shows a cell junction with both *Cldn10* and β-catenin staining along a lateral membrane. Asterisk shows a *Cldn10* negative, β-catenin positive cell junction. Panel B: *Cldn10* is not found exclusively at tight junctions. The tight junction marker ZO-1 (red) is seen as punctate staining along the apical side of lateral membranes. β-catenin is seen in green along the lateral membrane. Inset shows higher magnification regions with punctuate ZO-1 staining. Panel C: CCSP expressing cells (green) are surrounded by lateral *Cldn10* (red) membrane staining. Arrowheads show CCSP negative, *Cldn10* negative cells. The asterisk indicates a CCSP positive cell surrounded by a ring of CCSP negative cells. *Cldn10* staining (red) is only seen around the center cell. Panels D-F: CCSP expressing cells (green in panel D) show lateral membrane staining for *Cldn10* (red in panel E). A small pool of cytoplasmic staining is also seen. Panel F: Co-localization shows that cell borders between CCSP negative cells (arrows) do not have *Cldn10* staining. Nuclear counterstain (DAPI) is seen in blue.

Cldn10 was expressed in the airways quite early in development. At E14.5 dpc, Cldn10 staining was seen throughout the developing airway epithelium (Figure 25A), although staining was relatively weak compared to that seen in the adult. By E18.5 dpc, Cldn10 staining has increased in intensity and is becoming restricted to the differentiating CCSP expressing population (Figures 25B-C). At 5 days following birth, CCSP immunostaining intensity has increased greatly (Figure 25D) while Cldn10 staining has decreased and is entirely restricted to the CCSP immunoreactive population.

We next determined the distribution of Cldn10 following naphthalene exposure. At day 3 following naphthalene, rare Cld10 and CCSP immunoreactive cells could be seen at terminal bronchioles (Figure 26A). At day 7, Cldn10 staining marks the extent of the CCSP immunoreactive regenerating zone (Figure 26B). This pattern persists at day 42 (data not shown). To determine if the cellular specificity of Cldn10 expression was maintained in a genetic model of disrupted epithelial maturation, lung tissue from CatnbΔE3mice was immunostained for Cldn10. As previously described, the epithelium of the CatnbΔE3 mice was more squamous than wild type mice (Figure 26C). Cells in which recombination has not occurred exhibit more classical columnar morphology and express much higher levels of CCSP (Reynolds, unpublished data). While all CCSP expressing cells in the epithelium stained for Cldn1o, only cells with high levels of CCSP exhibited a strong lateral staining pattern (Figure 26C). Together, these data support the conclusion that Cldn10 is a Clara cell specific protein in the adult lung. During development, Cldn10 is expressed through out the developing airway, but expression becomes restricted to Clara cells during late embryogenesis.

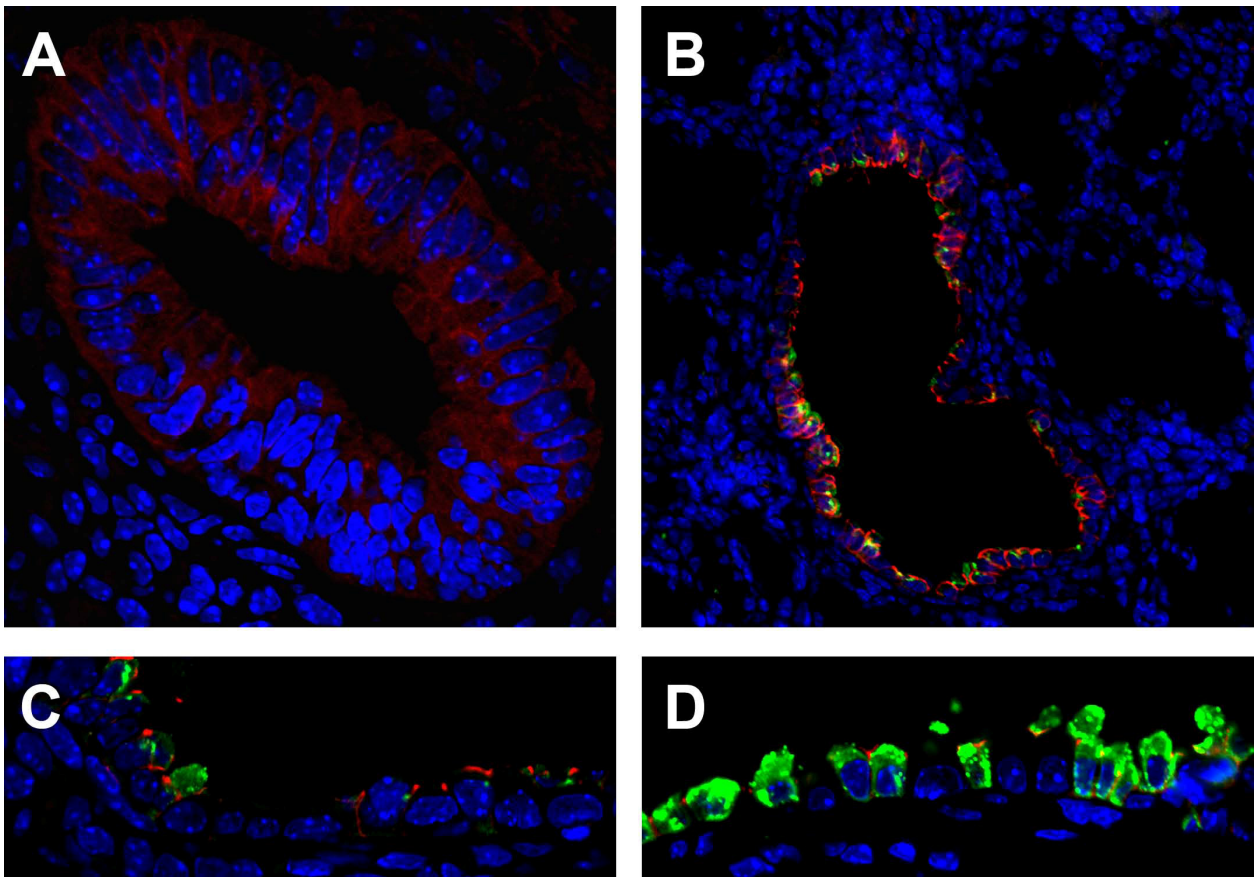

Figure 25: Claudin 10 is expressed early in mouse lung development

Panel A: Mouse lungs from E14.5 dpc embryos were immunostained for *Cldn10* (red) with a DAPI nuclear counterstain (blue). *Cldn10* is expressed through out the developing airway tubules. Panel B: E18.5 dpc embryo lungs were immunostained for *Cldn10* (red) and CCSP (green). Intense *Cldn10* staining is seen along lateral membranes of airway epithelial cells. Faint CCSP immunostaining is seen within the airway as well. Panel C: Tissue from E18.5 dpc embryos was stained as above. A row of 4 CCSP negative, *Cldn10* negative cells is seen surrounded by epithelial cell with strong *Cldn10* lateral membrane staining and weak CCSP staining. Panel D: Lung tissue from a 5 day old mouse was immunostained as above. CCSP expression has greatly increased, and *Cldn10* staining remains restricted to CCSP immunoreactive cells.

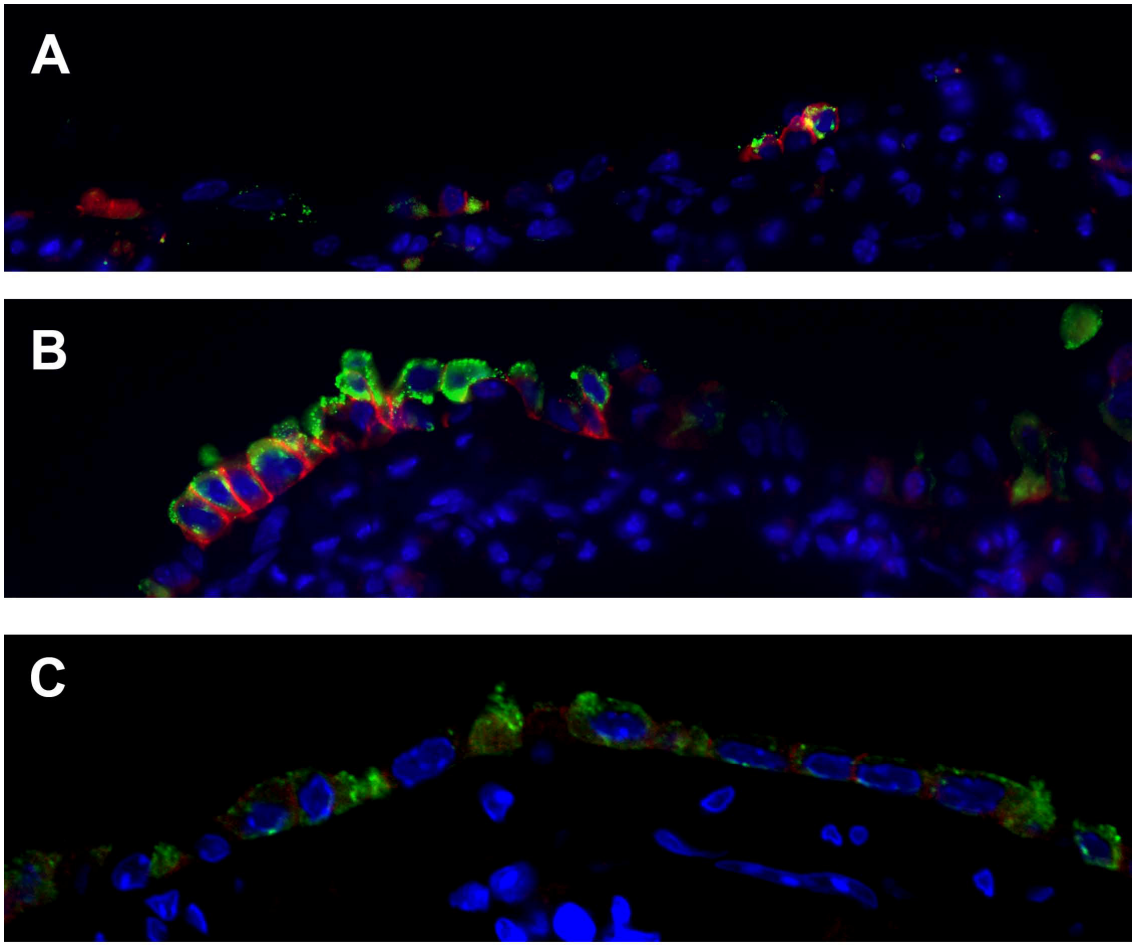

Figure 26:Expression of Cldn10 following Clara cell ablation and in altered epithelial differentiation

Panels A-B: Mice were exposed to naphthalene, and frozen lung sections were prepared. Tissue was immunostained for *Cldn10* (red) and CCSP (green) and imaged by conventional fluorescence microscopy. A: Three days following naphthalene exposure (panel A) rare CCSP positive, *Cldn10* positive cells are seen, but most cells do not immunostain for either protein. B: By 7 days following naphthalene exposure, the repair epithelial area has enlarged and is immunoreactive for both CCSP (green) and *Cldn10* (red). Panel C: Frozen sections were prepared from CCSP-Cre, CatnbΔE3 mice, immunostained as above, and imaged by confocal microscopy. The epithelium appears more cuboidal than in wild-type mice. CCSP (green) and *Cldn10* (red) staining is still seen, however the overall staining intensity is lower.

4.4 DISCUSSION

We have used a combination of cell ablation strategies and microarray screening to identify the novel protein repertoire expressed by mature secretory cells of the conducting airway. These genes can be grouped into three categories by order of maturation and recovery following naphthalene treatment. The first category contains genes with a similar expression pattern to *Cyp2f2,* and include *Pon1, Aox3,* and *Fmo3*. Notably, of these three genes, *Aox3* reaches adult mRNA abundance first. Pon1, Fmo3, and Aox3 are known phase I metabolizing enzymes. Paraoxonase 1 (Pon1) is an esterase capable of hydrolyzing organophosphate compounds. Previously, it has been localized to non-ciliated airway cells in the rat by immunohistochemistry [236]. Flavin monooxygenases oxidizes a wide variety of drugs and xenobiotics. Fmo3 has previously been localized to the mouse terminal bronchiole by *in situ* hybridization [237]. Aldehyde oxidase 3 (also known as AOH1) is a molybdoflavoprotein previously detected in mouse lung by Western blot [238]. In addition to these molecules, carboxylesterase 1 (NM_021456) decreased in both models, as did an unidentified probe that has greater than 90% homology with carboxylesterases in BLAST (NM_144930). The second category of genes contains *CCSP* which reached adult expression levels within 7-14 days. This is in agreement with previous work by Fanucchi *et al*, who found followed appearance of CCSP by immunonhistochemistry [44]. The third category of genes contains *Cldn10*, which was identified as an early airway marker whose expression is subsequently restricted to Clara cells during development. *Cldn10* mRNA abundance was the first to rebound following naphthalene injury was present in adult levels shortly after birth.

These data give a more detailed insight into postnatal airway maturation. Cldn10 is expressed throughout the airway epithelium very early in embryonic development. Prior to birth, expression is restricted to CCSP expressing cells. Maturation of CCSP expression occurs next, and reaches adult levels within the first 1-2 weeks following birth. Next, the xenobiotic metabolizing capacity of the epithelium matures, although not all xenobiotic metabolizing enzymes mature synchronously. AOH1 reached adult expression first. This molecular expression panel was sensitive enough to detect the maturation arrest seen in CCSP-Cre, CatnbΔE3 mice. These molecular markers also revealed the differentiation process of the repair epithelium following naphthalene exposure. Cldn10 and AOH1 expression rebounded much more quickly than CCSP, Cyp2f2, Pon1, or Fmo3. These results suggest that the repairing epithelium is functionally immature immediately following injury, and the nascent secretory cells require an additional day or two to return to physiologic maturity. Immaturity of airway secretory cells immediately following injury may contribute to altered epithelial function seen in chronic lung disease.

Claudin-10 was immunolocalized to the entire lateral surface of CCSP expressing cells in both proximal and distal mouse airways. It was not found on either ciliated cells or other cells within the lung. This cellular localization is in contrast with a previous report using the same antibody for immunolocalization of Cldn 10 in mouse airway [239]. However, the previously published data do not exclude lateral membrane localization of Cldn10 because of the *en face* airway sections used in that report. Claudins are classically thought to be tight junction proteins, but Cldn10 localization along the entire lateral membrane has been previously shown in exocrine glands and scattered epithelial cells of the cecum [239, 240]. Tight junctions form a “fence”

between cells that regulates paracellular traffic, thus claudins found at the tight junction are appropriately localized to regulate paracellular ion movement.

Two splice variants of Cldn10 exist, although only Cldn10b is expressed in the lung [239]. In the kidney, these splice variants form low resistance paracellular pores, with Cldn10b showing greater cation selectivity. In the human, claudins 1, 3, 4, 5, and 7 are highly expressed in airways, and likely regulate paracellular ion permeability [35]. In the study by Coyne *et al*, claudins-3 and 5 were found exclusively at the tight junction. Claudins-1 and 4 were found along the entire lateral membrane, while claudin-7 was located along the lateral membrane and excluded from the tight junction [35]. While the physiologic function of claudins whose expression is not limited to the tight junction is currently unknown, it is likely that Cldn10 regulates paracellular permeability in the airway epithelium. Of interest will be determining possible binding partners for Cldn10 expressed on ciliated cells.

Previously, Clara cells were known to express xenobiotic metabolizing enzymes (notably cytochrome p450 family members) and a variety of immunomodulatory proteins of the secretoglobin and surfactant families. Within the CCSP-HSVtK microarray data set, we found secreteglobins 3A1, 1A1, and 3A2 and PLUNC, which are all previously identified markers of mouse secretory cells [233, 241]. Additionally, there were numerous members of the Cyp450 family present, including 2f2, 2a4, and 1a1. The presence of known secreteglobins and Cyp450 family members indicates that this approach was sufficiently sensitive. This approach combining cell ablation and microarray analysis has several technical limitations. First, because the subpopulation of Clara cells containing the airway stem cells is naphthalene resistant, any molecular marker unique to the stem cell compartment will not be detected by our subtractive approach. Second, comparatively few genes were identified within the CCSP-HSVtK model

compared to the naphthalene model despite the greater severity of injury and inflammation in the CCSP-HSVtK model. This result likely reflected greater variability within the CCSP-HSVtK data set. Finally, because whole lung homogenate was studied, decreases in any messages expressed in both Clara cells and other lung cell types are expected to be masked.

In summary, we have developed a novel technical approach to expand our understanding of the phenotype of mature Clara cells and identified Cldn10 as a Clara cell specific, cell surface marker. The asynchronous appearance of these molecular markers following injury is similar to the postnatal maturational sequence. This suggests that following restitution of airway secretory cells, there is a lag in differentiation. Incomplete secretory cell differentiation may contribute to increased susceptibility to further airway injury.

4.5 FUTURE DIRECTIONS

There are at least three possible continuations of this project. First, while we have used a subtractive approach to identify Clara cell molecular markers, the microarray data set could be exploited to determine differences in signaling or inflammation between the naphthalene and CCSP-HSVtK models. The naphthalene model is accompanied by little inflammation, while the CCSP-HSVtK mice succumb to fatal lung inflammation [235]. Further analysis of the microarray data set could generate hypotheses regarding the role of inflammation in airway repair. Additionally, the naphthalene model involves productive airway repair, while no airway repair is possible in CCSP-HSVtK mice. Comparison of these two data sets might reveal novel pathways important in productive airway repair.

Second, Cldn10 is a cell surface Clara cell molecular marker. The function and binding partners of Cldn10, particularly on the neighboring ciliated cells, are unknown. Also, the existing antibody recognizes the cytoplasmic terminus. Developing an antibody to the extracellular terminus might permit isolation of live Clara cells for other studies. For example, the colony forming assay in Chapter 2 was done with a crude airway cell preparation. A live Clara cell isolation method would allow such assays to be performed starting with a more pure cell population.

Finally there is the broader biological question of claudin function. While claudins located at the tight junction conceivably regulate paracellular ion traffic, the function of claudins with other subcellular localizations is entirely unknown. Presumably, Cldn10 has heteromeric interactions with a claudin found on ciliated cells. It is unknown if there is a ciliated cell-specific claudin counterpart to Cldn10. An initial step in determining the physiologic role of claudins at the adherens junction would be determining the binding partners of Cldn10.

5.0 SUMMARY OF RESULTS

The data presented in this dissertation has furthered our understanding of the molecular mechanisms which regulate airway epithelial homeostasis, development and repair. Specifically, the roles of Smad4 and β-catenin in regulating these processes were determined.

Smad4 was revealed as a critical regulator of branching morphogenesis. Disruption of Smad4-dependent signaling early in lung development caused increased airway branching, which included a corresponding increase in the absolute number of terminal bronchioles and increased expression of airway markers. Notably, airway cell differentiation was maintained, and the mitotic potential of the airway epithelium was unaltered. Mice with alveolar and airway epithelia null for Smad4 developed adenomas with increasing frequency as they aged, indicating the importance of Smad4-dependent signaling in tumor suppression. As these tumors expressed SPC, it is likely that they were derived from an alveolar precursor. Next, the influence of Smad4-dependent signaling during airway epithelial homeostasis and repair was determined. Despite evidence of sustained TGFβ signaling within the epithelium following exposure to the Clara cell toxicant naphthalene, no change in the rate or extent of airway repair was seen in the absence of Smad4. These findings highlight the importance of Smad-independent signaling in development and repair of the conducting airway epithelium.

The role of Wnt/β-catenin in airway homeostasis and repair was determined. We found evidence of sporadic and comparatively rare β-catenin dependent signaling through the use of

mice carrying the TOPGal reporter transgene. To determine the significance of this signaling, we used epithelium specific deletion of β-catenin. Loss of β-catenin did not disrupt epithelial homeostasis by any measure we used. Repair of the bronchiolar epithelium appeared normal in the absence of β-catenin. These data support a model in which the developmental down regulation of β-catenin is an important event for normal differentiation of the airway epithelium.

Finally, we characterized the post-natal differentiation of airway secretory cells. Claudin 10 was identified as an early airway marker, which becomes restricted to the secretory population by birth. During the first week of life CCSP expression matures, followed by the expression of xenobiotic metabolizing enzymes paraoxonase 1, cytochrome P450 2f2, aldehyde oxidase 3, and flavin monooxygenase 3. Identification of these molecular markers also allowed us to more carefully assess secretory cell differentiation during airway repair. This analysis revealed a similar differentiation process during restoration of the secretory population following injury.

5.1 CLINICAL RELEVENCE

The confirmation that Smad4 is an important lung tumor suppressor is the finding of greatest direct clinical relevance in this dissertation. Lung cancer continues to have a dismal prognosis. With the exception of treatments targeted at EGF, other treatments for lung cancer are relatively non-specific. Adding to the complexity of this clinical problem, there are a limited number of molecularly defined mouse models of carcinogenesis [159]. In human samples, TGFβ signaling has been implicated in the suppression of tumor invasiveness in adenocarcinoma [225]. The development of a new mouse model of lung adenoma with signaling similarity to human

adenocarcinoma is exciting because it provides a new tool for dissecting mechanisms of lung tumor growth and invasion, as well as adding insight into the biological processes gone array in lung cancer.

Understanding the mechanisms that regulate airway epithelial repair is relevant to chronic lung disease that cause airway remodeling, including cystic fibrosis, asthma, chronic bronchitis and bronchiolitis obliterans. The lack of epithelial phenotype seen in mice null for epithelial Smad4 is also quite clinically relevant. TGFβ signaling is a key pathway in the development of fibrosis in a variety of organ systems, including lung, liver, kidney, and skin [1]. Additionally, TGFβ signaling is implicated in airway remodeling, particular the development of subepithelial fibrosis and smooth muscle hypertrophy [68]. *In vitro* data suggested that suppression of TGFβ signaling might enhance epithelial proliferation and thus speed wound repairs. The data in this dissertation suggest that blocking TGFβ is unlikely to change the proliferative state of the conducting airway epithelium, but may increase the incidence of lung tumors. This allays concerns that TGFβ targeted therapies would adversely effect epithelial repair, but it also does not encourage the development of such drugs to speed epithelial airway repair. These data also reinforce concerns about the long term carcinogenicity of TGFβ suppressing therapies. Important to remember in this discussion is that more than 50% of all pancreatic cancers have lost Smad4 expression, and abrogation of Smad-dependent signaling is strongly associated with colon cancer [216]. The development of lung tumors at the rate seen in these mice may pale in comparison to the risk of carcinogenicity in other organ systems.

From the data in this dissertation, it seems that loss of β-catenin dependent signaling is unlikely to contribute to chronic airway diseases. Any systemic therapy that blocks β-catenin signaling (for example treatments designed to treat familial colon cancer) is unlikely to harm the

airway epithelium. Finally, the identification of molecular markers that describe secretory cell differentiation contributes to our general understanding on lung biology. Currently, our ability to detect functional changes within the secretory population is limited. These markers will aid in the development of better animal models of airway disease.

BIBLIOGRAPHY

1. Kumar, V., A.K. Abbas, and N. Fausto, *Pathologic Basis of Disease*. 7th ed. 2005.
2. Ten Have-Opbroek, A.A., *Lung development in the mouse embryo.* Exp Lung Res, 1991. **17**(2): p. 111-30.
3. Pack, R.J., L.H. Al-Ugaily, and G. Morris, *The cells of the tracheobronchial epithelium of the mouse: a quantitative light and electron microscope study.* J Anat, 1981. **132**(Pt 1): p. 71-84.
4. Barth, P.J., M. Wolf, and A. Ramaswamy, *Distribution and number of Clara cells in the normal and disturbed development of the human fetal lung.* Pediatr Pathol, 1994. **14**(4): p. 637-51.
5. Evans, M.J., et al., *The attenuated fibroblast sheath of the respiratory tract epithelial-mesenchymal trophic unit.* Am J Respir Cell Mol Biol, 1999. **21**(6): p. 655-7.
6. Adriaensen, D., et al., *Evidence for a role of neuroepithelial bodies as complex airway sensors: comparison with smooth muscle-associated airway receptors.* J Appl Physiol, 2006. **101**(3): p. 960-970.
7. Hong, K.U., et al., *Basal cells are a multipotent progenitor capable of renewing the bronchial epithelium.* Am J Pathol, 2004. **164**(2): p. 577-88.
8. Hong, K.U., et al., *In vivo differentiation potential of tracheal basal cells: evidence for multipotent and unipotent subpopulations.* Am J Physiol Lung Cell Mol Physiol, 2004. **286**(4): p. L643-9.
9. Hajj, R., et al., *Basal Cells of the Human Adult Airway Surface Epithelium Retain Transit-Amplifying Cell Properties.* Stem Cells, 2007. **25**(1): p. 139-148.
10. You, Y., et al., *Role of f-box factor foxj1 in differentiation of ciliated airway epithelial cells.* Am J Physiol Lung Cell Mol Physiol, 2004. **286**(4): p. L650-7.
11. Rawlins, E.L., et al., *Lung development and repair: contribution of the ciliated lineage.* Proc Natl Acad Sci U S A, 2007. **104**(2): p. 410-7.
12. Toskala, E., et al., *Temporal and spatial distribution of ciliogenesis in the tracheobronchial airways of mice.* Am J Physiol Lung Cell Mol Physiol, 2005. **289**(3): p. L454-459.
13. Park, K.-S., et al., *Transdifferentiation of Ciliated Cells during Repair of the Respiratory Epithelium.* Am. J. Respir. Cell Mol. Biol., 2006. **34**(2): p. 151-157.
14. Evans, M.J., et al., *Renewal of the terminal bronchiolar epithelium in the rat following exposure to NO2 or O3.* Lab Invest, 1976. **35**(3): p. 246-57.
15. Van Winkle, L.S., et al., *Early events in naphthalene-induced acute Clara cell toxicity: comparison of membrane permeability and ultrastructure.* Am J Respir Cell Mol Biol, 1999. **21**(1): p. 44-53.

16. Boers, James E., Anton W. Ambergen, and Frederik B.J.M. Thunnissen, *Number and Proliferation of Clara Cells in Normal Human Airway Epithelium.* Am. J. Respir. Crit. Care Med., 1999. **159**(5): p. 1585-1591.
17. Knight, D.A. and S.T. Holgate, *The airway epithelium: Structural and functional properties in health and disease.* Respirology, 2003. **8**(4): p. 432-446.
18. Linnoila, R.I., *Functional facets of the pulmonary neuroendocrine system.* Lab Invest, 2006. **86**(5): p. 425-444.
19. Reynolds, S.D., et al., *Conditional clara cell ablation reveals a self-renewing progenitor function of pulmonary neuroendocrine cells.* Am J Physiol Lung Cell Mol Physiol, 2000. **278**(6): p. L1256-63.
20. Peake, J.L., et al., *Alteration of pulmonary neuroendocrine cells during epithelial repair of naphthalene-induced airway injury.* Am J Pathol, 2000. **156**(1): p. 279-86.
21. Reynolds, S.D., et al., *Neuroepithelial bodies of pulmonary airways serve as a reservoir of progenitor cells capable of epithelial regeneration.* Am J Pathol, 2000. **156**(1): p. 269-78.
22. Stevens, T.P., et al., *Cell proliferation contributes to PNEC hyperplasia after acute airway injury.* Am J Physiol, 1997. **272**(3 Pt 1): p. L486-93.
23. Wine, J.J. and N.S. Joo, *Submucosal glands and airway defense.* Proc Am Thorac Soc, 2004. **1**(1): p. 47-53.
24. Hays, S.R. and J.V. Fahy, *Characterizing Mucous Cell Remodeling in Cystic Fibrosis: Relationship to Neutrophils.* Am. J. Respir. Crit. Care Med., 2006. **174**(9): p. 1018-1024.
25. Oppenheimer, E.H. and J.R. Esterly, *Pathology of cystic fibrosis review of the literature and comparison with 146 autopsied cases.* Perspect Pediatr Pathol, 1975. **2**: p. 241-78.
26. Jeffery, P.K., *Comparative morphology of the airways in asthma and chronic obstructive pulmonary disease.* Am J Respir Crit Care Med, 1994. **150**(5 Pt 2): p. S6-13.
27. Young, H.W.J., et al., *Central Role of Muc5ac Expression in Mucous Metaplasia and Its Regulation by Conserved 5' Elements.* Am. J. Respir. Cell Mol. Biol., 2007: p. 2005-0460OC.
28. Evans, C.M., et al., *Mucin is produced by clara cells in the proximal airways of antigen-challenged mice.* Am J Respir Cell Mol Biol, 2004. **31**(4): p. 382-94.
29. Zhu, Z., et al., *Pulmonary expression of interleukin-13 causes inflammation, mucus hypersecretion, subepithelial fibrosis, physiologic abnormalities, and eotaxin production.* J. Clin. Invest., 1999. **103**(6): p. 779-788.
30. Tyner, J.W., et al., *Blocking airway mucous cell metaplasia by inhibiting EGFR antiapoptosis and IL-13 transdifferentiation signals.* J. Clin. Invest., 2006. **116**(2): p. 309-321.
31. Takeyama, K., et al., *Epidermal growth factor system regulates mucin production in airways.* PNAS, 1999. **96**(6): p. 3081-3086.
32. Burgel, P.R. and J.A. Nadel, *Roles of epidermal growth factor receptor activation in epithelial cell repair and mucin production in airway epithelium.* Thorax, 2004. **59**(11): p. 992-996.
33. Homer, R.J., et al., *Differential expression of chitinases identify subsets of murine airway epithelial cells in allergic inflammation.* Am J Physiol Lung Cell Mol Physiol, 2006. **291**(3): p. L502-511.
34. Verkman, A.S., M.A. Matthay, and Y. Song, *Aquaporin water channels and lung physiology.* Am J Physiol Lung Cell Mol Physiol, 2000. **278**(5): p. L867-879.

35. Coyne, C.B., et al., *Role of claudin interactions in airway tight junctional permeability.* Am J Physiol Lung Cell Mol Physiol, 2003. **285**(5): p. L1166-1178.
36. Coyne, C.B., et al., *Regulation of airway tight junctions by proinflammatory cytokines.* Mol Biol Cell, 2002. **13**(9): p. 3218-34.
37. Bals, R. and P.S. Hiemstra, *Innate immunity in the lung: how epithelial cells fight against respiratory pathogens.* Eur Respir J, 2004. **23**(2): p. 327-333.
38. Singh, G. and S.L. Katyal, *Clara Cell Proteins.* Ann NY Acad Sci, 2000. **923**(1): p. 43-58.
39. Yoshikawa, S., et al., *Clara cell secretory protein and phospholipase A2 activity modulate acute ventilator induced lung injury in mice.* J Appl Physiol, 2004.
40. Watson, T.M., et al., *Altered lung gene expression in CCSP-null mice suggests immunoregulatory roles for Clara cells.* Am J Physiol Lung Cell Mol Physiol, 2001. **281**(6): p. L1523-30.
41. Cohen, G.M., *Pulmonary metabolism of foreign compounds: its role in metabolic activation.* Environ Health Perspect, 1990. **85**: p. 31-41.
42. Buckpitt, A., et al., *Relationship of cytochrome P450 activity to Clara cell cytotoxicity. IV. Metabolism of naphthalene and naphthalene oxide in microdissected airways from mice, rats, and hamsters.* Mol Pharmacol, 1995. **47**(1): p. 74-81.
43. Chichester, C.H., et al., *Characterization of the cytochrome P-450 monooxygenase system in nonciliated bronchiolar epithelial (Clara) cells isolated from mouse lung.* Am J Respir Cell Mol Biol, 1991. **4**(2): p. 179-86.
44. Fanucchi, M.V., et al., *Pulmonary cytochrome P450 monooxygenase and Clara cell differentiation in mice.* Am J Respir Cell Mol Biol, 1997. **17**(3): p. 302-14.
45. Hukkanen, J., O. Pelkonen, and H. Raunio, *Expression of xenobiotic-metabolizing enzymes in human pulmonary tissue: possible role in susceptibility for ILD.* Eur Respir J, 2001. **18**(32_suppl): p. 122S-126.
46. Puchelle, E., et al., *Airway epithelial repair, regeneration, and remodeling after injury in chronic obstructive pulmonary disease.* Proc Am Thorac Soc, 2006. **3**(8): p. 726-33.
47. Blanpain, C., V. Horsley, and E. Fuchs, *Epithelial Stem Cells: Turning over New Leaves.* Cell, 2007. **128**(3): p. 445.
48. Alison, M.R., et al., *An introduction to stem cells.* J Pathol, 2002. **197**(4): p. 419-23.
49. Stripp, B.R., et al., *Plasticity of airway cell proliferation and gene expression after acute naphthalene injury.* Am J Physiol, 1995. **269**(6 Pt 1): p. L791-9.
50. Eblaghie, M.C., et al., *Evidence that autocrine signaling through Bmpr1a regulates the proliferation, survival and morphogenetic behavior of distal lung epithelial cells.* Developmental Biology, 2006. **291**(1): p. 67.
51. Hong, K.U., et al., *Clara cell secretory protein-expressing cells of the airway neuroepithelial body microenvironment include a label-retaining subset and are critical for epithelial renewal after progenitor cell depletion.* Am J Respir Cell Mol Biol, 2001. **24**(6): p. 671-81.
52. Yamashita, Y.M., M.T. Fuller, and D.L. Jones, *Signaling in stem cell niches: lessons from the Drosophila germline.* J Cell Sci, 2005. **118**(4): p. 665-672.
53. Goodell, M.A., et al., *Isolation and functional properties of murine hematopoietic stem cells that are replicating in vivo.* J Exp Med, 1996. **183**(4): p. 1797-806.
54. Tumbar, T., et al., *Defining the Epithelial Stem Cell Niche in Skin.* Science, 2004. **303**(5656): p. 359-363.

55. Potten, C.S. and M. Loeffler, *Stem cells: attributes, cycles, spirals, pitfalls and uncertainties. Lessons for and from the crypt.* Development, 1990. **110**(4): p. 1001-20.
56. Giangreco, A., S.D. Reynolds, and B.R. Stripp, *Terminal bronchioles harbor a unique airway stem cell population that localizes to the bronchoalveolar duct junction.* Am J Pathol, 2002. **161**(1): p. 173-82.
57. Krause, D.S., et al., *Multi-organ, multi-lineage engraftment by a single bone marrow-derived stem cell.* Cell, 2001. **105**(3): p. 369-77.
58. Coulombel, L., *Identification of hematopoietic stem/progenitor cells: strength and drawbacks of functional assays.* Oncogene, 2004. **23**(43): p. 7210-22.
59. Kim, C.F., et al., *Identification of bronchioalveolar stem cells in normal lung and lung cancer.* Cell, 2005. **121**(6): p. 823-35.
60. Giangreco, A., et al., *Molecular phenotype of airway side population cells.* Am J Physiol Lung Cell Mol Physiol, 2004. **286**(4): p. L624-30.
61. Evans, M.J., et al., *The Attenuated Fibroblast Sheath of the Respiratory Tract Epithelial-Mesenchymal Trophic Unit.* Am. J. Respir. Cell Mol. Biol., 1999. **21**(6): p. 655-657.
62. McMillan, S.J., G. Xanthou, and C.M. Lloyd, *Manipulation of allergen-induced airway remodeling by treatment with anti-TGF-beta antibody: effect on the Smad signaling pathway.* J Immunol, 2005. **174**(9): p. 5774-80.
63. Araya, J., et al., *Integrin-Mediated Transforming Growth Factor-{beta} Activation Regulates Homeostasis of the Pulmonary Epithelial-Mesenchymal Trophic Unit.* Am J Pathol, 2006. **169**(2): p. 405-415.
64. Mustoe, T.A., et al., *Accelerated healing of incisional wounds in rats induced by transforming growth factor-beta.* Science, 1987. **237**(4820): p. 1333-6.
65. Ashcroft, G.S., et al., *Mice lacking Smad3 show accelerated wound healing and an impaired local inflammatory response.* Nat Cell Biol, 1999. **1**(5): p. 260-6.
66. Neurohr, C., S.L. Nishimura, and D. Sheppard, *Activation of Transforming Growth Factor-beta by the Integrin {alpha}vbeta8 Delays Epithelial Wound Closure.* Am. J. Respir. Cell Mol. Biol., 2006. **35**(2): p. 252-259.
67. Fjellbirkeland, L., et al., *Integrin {alpha}v{beta}8-Mediated Activation of Transforming Growth Factor-{beta} Inhibits Human Airway Epithelial Proliferation in Intact Bronchial Tissue.* Am J Pathol, 2003. **163**(2): p. 533-542.
68. Boxall, C., S.T. Holgate, and D.E. Davies, *The contribution of transforming growth factor-{beta} and epidermal growth factor signalling to airway remodelling in chronic asthma.* Eur Respir J, 2006. **27**(1): p. 208-229.
69. Leask, A. and D.J. Abraham, *TGF-{beta} signaling and the fibrotic response.* FASEB J., 2004. **18**(7): p. 816-827.
70. Hu, B., Z. Wu, and S.H. Phan, *Smad3 Mediates Transforming Growth Factor-{beta}-Induced {alpha}-Smooth Muscle Actin Expression.* Am. J. Respir. Cell Mol. Biol., 2003. **29**(3): p. 397-404.
71. Zhao, J., et al., *Smad3 deficiency attenuates bleomycin-induced pulmonary fibrosis in mice.* Am J Physiol Lung Cell Mol Physiol, 2002. **282**(3): p. L585-593.
72. Ramirez, A.M., et al., *Smad3 deficiency ameliorates experimental obliterative bronchiolitis in a heterotopic tracheal transplantation model.* Am J Pathol, 2004. **165**(4): p. 1223-32.
73. Le, A.V., et al., *Inhibition of allergen-induced airway remodeling in Smad 3-deficient mice.* J Immunol, 2007. **178**(11): p. 7310-6.

74. Holgate, S.T., *Epithelial damage and response.* Clin Exp Allergy, 2000. **30 Suppl 1**: p. 37-41.
75. Holgate, S.T., et al., *Epithelial-mesenchymal interactions in the pathogenesis of asthma.* J Allergy Clin Immunol, 2000. **105**(2 Pt 1): p. 193-204.
76. Davies, D.E., et al., *Airway remodeling in asthma: new insights.* J Allergy Clin Immunol, 2003. **111**(2): p. 215-25; quiz 226.
77. Howat, W.J., S.T. Holgate, and P.M. Lackie, *TGF-beta isoform release and activation during in vitro bronchial epithelial wound repair.* Am J Physiol Lung Cell Mol Physiol, 2002. **282**(1): p. L115-123.
78. Douglas, I.S., et al., *Beta-catenin in the fibroproliferative response to acute lung injury.* Am J Respir Cell Mol Biol, 2006. **34**(3): p. 274-85.
79. Steel, M.D., et al., *[beta]-Catenin/T-cell factor-mediated transcription is modulated by cell density in human bronchial epithelial cells.* The International Journal of Biochemistry & Cell Biology, 2005. **37**(6): p. 1281.
80. Dvorak, H.F., *Tumors: wounds that do not heal. Similarities between tumor stroma generation and wound healing.* N Engl J Med, 1986. **315**(26): p. 1650-9.
81. Perryman, S.V. and K.G. Sylvester, *Repair and regeneration: opportunities for carcinogenesis from tissue stem cells.* Journal of Cellular and Molecular Medicine, 2006. **10**(2): p. 292-308.
82. Haddow, A., *Molecular repair, wound healing, and carcinogenesis: tumor production a possible overhealing?* Adv Cancer Res, 1972. **16**: p. 181-234.
83. Mazieres, J., et al., *Wnt signaling in lung cancer.* Cancer Lett, 2005. **222**(1): p. 1-10.
84. Pinto, D. and H. Clevers, *Wnt, stem cells and cancer in the intestine.* Biol Cell, 2005. **97**(3): p. 185-96.
85. van de Wetering, M., et al., *The beta-catenin/TCF-4 complex imposes a crypt progenitor phenotype on colorectal cancer cells.* Cell, 2002. **111**(2): p. 241-50.
86. Korinek, V., et al., *Depletion of epithelial stem-cell compartments in the small intestine of mice lacking Tcf-4.* Nat Genet, 1998. **19**(4): p. 379-83.
87. Voynow, J.A., et al., *Basal-like Cells Constitute the Proliferating Cell Population in Cystic Fibrosis Airways.* Am. J. Respir. Crit. Care Med., 2005. **172**(8): p. 1013-1018.
88. Leigh, M.W., et al., *Cell proliferation in bronchial epithelium and submucosal glands of cystic fibrosis patients.* Am J Respir Cell Mol Biol, 1995. **12**(6): p. 605-12.
89. Hajj, R., et al., *Human airway surface epithelial regeneration is delayed and abnormal in cystic fibrosis.* J Pathol, 2007. **211**(3): p. 340-50.
90. Ordonez, C., et al., *Epithelial Desquamation in Asthma . Artifact or Pathology?* Am. J. Respir. Crit. Care Med., 2000. **162**(6): p. 2324-2329.
91. Cohen, L., et al., *Epithelial Cell Proliferation Contributes to Airway Remodeling in Severe Asthma.* Am. J. Respir. Crit. Care Med., 2007. **176**(2): p. 138-145.
92. Ricciardolo, F.L., et al., *Proliferation and inflammation in bronchial epithelium after allergen in atopic asthmatics.* Clin Exp Allergy, 2003. **33**(7): p. 905-11.
93. McDyer, J.F., *Human and Murine Obliterative Bronchiolitis in Transplant.* Proc Am Thorac Soc, 2007. **4**(1): p. 37-43.
94. Cordier, J.-F., *Challenges in pulmonary fibrosis {middle dot} 2 : Bronchiolocentric fibrosis.* Thorax, 2007. **62**(7): p. 638-649.
95. Visscher, D.W. and J.L. Myers, *Bronchiolitis: The Pathologist's Perspective.* Proc Am Thorac Soc, 2006. **3**(1): p. 41-47.

96. Kuo, E., et al., *Role of Airway Epithelial Injury in Murine Orthotopic Tracheal Allograft Rejection.* The Annals of Thoracic Surgery, 2006. **82**(4): p. 1226-1233.
97. Jaramillo, A., et al., *Anti-HLA class I antibody binding to airway epithelial cells induces production of fibrogenic growth factors and apoptotic cell death: a possible mechanism for bronchiolitis obliterans syndrome.* Human Immunology, 2003. **64**(5): p. 521-529.
98. Kreiss, K., et al., *Clinical Bronchiolitis Obliterans in Workers at a Microwave-Popcorn Plant.* N Engl J Med, 2002. **347**(5): p. 330-338.
99. Feng, X.-H. and R. Derynck, *SPECIFICITY AND VERSATILITY IN TGF-β SIGNALING THROUGH SMADS.* Annual Review of Cell and Developmental Biology, 2005. **21**(1): p. 659-693.
100. Shi, Y. and J. Massague, *Mechanisms of TGF-beta signaling from cell membrane to the nucleus.* Cell, 2003. **113**(6): p. 685-700.
101. Massague, J., J. Seoane, and D. Wotton, *Smad transcription factors.* Genes Dev, 2005. **19**(23): p. 2783-810.
102. He, W., et al., *Hematopoiesis controlled by distinct TIF1gamma and Smad4 branches of the TGFbeta pathway.* Cell, 2006. **125**(5): p. 929-41.
103. Subramanian, G., et al., *Targeting Endogenous Transforming Growth Factor {beta} Receptor Signaling in SMAD4-Deficient Human Pancreatic Carcinoma Cells Inhibits Their Invasive Phenotype1.* Cancer Res, 2004. **64**(15): p. 5200-5211.
104. Biondi, C.A., et al., *Mice develop normally in the absence of Smad4 nucleocytoplasmic shuttling.* Biochem J, 2007. **404**(2): p. 235-245.
105. Dennler, S., et al., *Direct binding of Smad3 and Smad4 to critical TGF beta-inducible elements in the promoter of human plasminogen activator inhibitor-type 1 gene.* Embo J, 1998. **17**(11): p. 3091-100.
106. Hocevar, B.A., T.L. Brown, and P.H. Howe, *TGF-beta induces fibronectin synthesis through a c-Jun N-terminal kinase-dependent, Smad4-independent pathway.* Embo J, 1999. **18**(5): p. 1345-56.
107. Zhu, S., et al., *Activation of Mps1 Promotes Transforming Growth Factor-beta-independent Smad Signaling.* J Biol Chem, 2007. **282**(25): p. 18327-38.
108. Engel, M.E., et al., *Interdependent SMAD and JNK signaling in transforming growth factor-beta-mediated transcription.* J Biol Chem, 1999. **274**(52): p. 37413-20.
109. Edlund, S., et al., *Transforming growth factor-beta-induced mobilization of actin cytoskeleton requires signaling by small GTPases Cdc42 and RhoA.* Mol Biol Cell, 2002. **13**(3): p. 902-14.
110. Lin, X., et al., *PPM1A functions as a Smad phosphatase to terminate TGFbeta signaling.* Cell, 2006. **125**(5): p. 915-28.
111. Knockaert, M., et al., *Unique players in the BMP pathway: Small C-terminal domain phosphatases dephosphorylate Smad1 to attenuate BMP signaling.* PNAS, 2006. **103**(32): p. 11940-11945.
112. Chen, H.B., et al., *Identification of phosphatases for Smad in the BMP/DPP pathway.* Genes Dev., 2006. **20**(6): p. 648-653.
113. Itoh, S. and P. ten Dijke, *Negative regulation of TGF-[beta] receptor/Smad signal transduction.* Current Opinion in Cell Biology, 2007. **19**(2): p. 176.
114. Stadeli, R., R. Hoffmans, and K. Basler, *Transcription under the control of nuclear Arm/beta-catenin.* Curr Biol, 2006. **16**(10): p. R378-85.

115. Clevers, H., *Wnt/beta-catenin signaling in development and disease.* Cell, 2006. **127**(3): p. 469-80.
116. Korswagen, H.C., M.A. Herman, and H.C. Clevers, *Distinct beta-catenins mediate adhesion and signalling functions in C. elegans.* Nature, 2000. **406**(6795): p. 527-32.
117. Perez-Moreno, M. and E. Fuchs, *Catenins: keeping cells from getting their signals crossed.* Dev Cell, 2006. **11**(5): p. 601-12.
118. Gordon, M.D. and R. Nusse, *Wnt signaling: multiple pathways, multiple receptors, and multiple transcription factors.* J Biol Chem, 2006. **281**(32): p. 22429-33.
119. Logan, C.Y. and R. Nusse, *THE WNT SIGNALING PATHWAY IN DEVELOPMENT AND DISEASE.* Annual Review of Cell and Developmental Biology, 2004. **20**(1): p. 781-810.
120. Lei, S., et al., *The murine gastrin promoter is synergistically activated by transforming growth factor-beta/Smad and Wnt signaling pathways.* J Biol Chem, 2004. **279**(41): p. 42492-502.
121. Hu, M.C. and N.D. Rosenblum, *Smad1, beta-catenin and Tcf4 associate in a molecular complex with the Myc promoter in dysplastic renal tissue and cooperate to control Myc transcription.* Development, 2005. **132**(1): p. 215-25.
122. Hussein, S.M., E.K. Duff, and C. Sirard, *Smad4 and beta-catenin co-activators functionally interact with lymphoid-enhancing factor to regulate graded expression of Msx2.* J Biol Chem, 2003. **278**(49): p. 48805-14.
123. Labbe, E., A. Letamendia, and L. Attisano, *Association of Smads with lymphoid enhancer binding factor 1/T cell-specific factor mediates cooperative signaling by the transforming growth factor-beta and wnt pathways.* Proc Natl Acad Sci U S A, 2000. **97**(15): p. 8358-63.
124. Satterwhite, D.J. and K.L. Neufeld, *TGF-beta targets the Wnt pathway components, APC and beta-catenin, as Mv1Lu cells undergo cell cycle arrest.* Cell Cycle, 2004. **3**(8): p. 1069-73.
125. Cordray, P. and D.J. Satterwhite, *TGF-beta induces novel Lef-1 splice variants through a Smad-independent signaling pathway.* Dev Dyn, 2005. **232**(4): p. 969-78.
126. Delaney, J.R. and M. Mlodzik, *TGF-beta activated kinase-1: new insights into the diverse roles of TAK1 in development and immunity.* Cell Cycle, 2006. **5**(24): p. 2852-5.
127. Yamaguchi, K., et al., *Identification of a member of the MAPKKK family as a potential mediator of TGF-beta signal transduction.* Science, 1995. **270**(5244): p. 2008-11.
128. Ishitani, T., J. Ninomiya-Tsuji, and K. Matsumoto, *Regulation of lymphoid enhancer factor 1/T-cell factor by mitogen-activated protein kinase-related Nemo-like kinase-dependent phosphorylation in Wnt/beta-catenin signaling.* Mol Cell Biol, 2003. **23**(4): p. 1379-89.
129. Maeda, Y., V. Dave, and J.A. Whitsett, *Transcriptional control of lung morphogenesis.* Physiol Rev, 2007. **87**(1): p. 219-44.
130. Shannon, J.M., et al., *Mesenchyme specifies epithelial differentiation in reciprocal recombinants of embryonic lung and trachea.* Dev Dyn, 1998. **212**(4): p. 482-94.
131. Shannon, J.M. and B.A. Hyatt, *Epithelial-mesenchymal interactions in the developing lung.* Annu Rev Physiol, 2004. **66**: p. 625-45.
132. Zhao, J., et al., *Abrogation of Smad3 and Smad2 or of Smad4 gene expression positively regulates murine embryonic lung branching morphogenesis in culture.* Dev Biol, 1998. **194**(2): p. 182-95.

133. Zhao, J., et al., *Abrogation of Transforming Growth Factor-[beta] Type II Receptor Stimulates Embryonic Mouse Lung Branching Morphogenesis in Culture.* Developmental Biology, 1996. **180**(1): p. 242.
134. Serra, R., R.W. Pelton, and H.L. Moses, *TGF beta 1 inhibits branching morphogenesis and N-myc expression in lung bud organ cultures.* Development, 1994. **120**(8): p. 2153-2161.
135. Zhou, L., et al., *Arrested lung morphogenesis in transgenic mice bearing an SP-C-TGF-beta 1 chimeric gene.* Dev Biol, 1996. **175**(2): p. 227-38.
136. Bragg, A.D., H.L. Moses, and R. Serra, *Signaling to the epithelium is not sufficient to mediate all of the effects of transforming growth factor beta and bone morphogenetic protein 4 on murine embryonic lung development.* Mech Dev, 2001. **109**(1): p. 13-26.
137. Bellusci, S., et al., *Evidence from normal expression and targeted misexpression that bone morphogenetic protein (Bmp-4) plays a role in mouse embryonic lung morphogenesis.* Development, 1996. **122**(6): p. 1693-1702.
138. Weaver, M., et al., *Bmp signaling regulates proximal-distal differentiation of endoderm in mouse lung development.* Development, 1999. **126**(18): p. 4005-15.
139. Weaver, M., N.R. Dunn, and B.L. Hogan, *Bmp4 and Fgf10 play opposing roles during lung bud morphogenesis.* Development, 2000. **127**(12): p. 2695-704.
140. Shi, W., et al., *Gremlin negatively modulates BMP-4 induction of embryonic mouse lung branching morphogenesis.* Am J Physiol Lung Cell Mol Physiol, 2001. **280**(5): p. L1030-1039.
141. Shi, W., et al., *Overexpression of Smurf1 negatively regulates mouse embryonic lung branching morphogenesis by specifically reducing Smad1 and Smad5 proteins.* Am J Physiol Lung Cell Mol Physiol, 2004. **286**(2): p. L293-300.
142. Chen, C., et al., *Smad1 expression and function during mouse embryonic lung branching morphogenesis.* Am J Physiol Lung Cell Mol Physiol, 2005. **288**(6): p. L1033-9.
143. Chen, H., et al., *Abnormal mouse lung alveolarization caused by Smad3 deficiency is a developmental antecedent of centrilobular emphysema.* Am J Physiol Lung Cell Mol Physiol, 2005. **288**(4): p. L683-691.
144. Colarossi, C., et al., *Lung alveolar septation defects in Ltbp-3-null mice.* Am J Pathol, 2005. **167**(2): p. 419-28.
145. Bonniaud, P., et al., *Smad3 Null Mice Develop Airspace Enlargement and Are Resistant to TGF-{beta}-Mediated Pulmonary Fibrosis.* J Immunol, 2004. **173**(3): p. 2099-2108.
146. Wang, X., et al., *Dysregulation of TGF-beta1 receptor activation leads to abnormal lung development and emphysema-like phenotype in core fucose-deficient mice.* Proc Natl Acad Sci U S A, 2005. **102**(44): p. 15791-6.
147. Tebar, M., et al., *Expression of Tcf/Lef and sFrp and localization of [beta]-catenin in the developing mouse lung.* Mechanisms of Development, 2001. **109**(2): p. 437.
148. Okubo, T. and B.L. Hogan, *Hyperactive Wnt signaling changes the developmental potential of embryonic lung endoderm.* J Biol, 2004. **3**(3): p. 11.
149. Shu, W., et al., *Wnt/[beta]-catenin signaling acts upstream of N-myc, BMP4, and FGF signaling to regulate proximal-distal patterning in the lung.* Developmental Biology, 2005. **283**(1): p. 226.
150. Wang, Z., et al., *Wnt7b activates canonical signaling in epithelial and vascular smooth muscle cells through interactions with Fzd1, Fzd10, and LRP5.* Mol Cell Biol, 2005. **25**(12): p. 5022-30.

151. Shu, W., et al., *Wnt7b regulates mesenchymal proliferation and vascular development in the lung.* Development, 2002. **129**(20): p. 4831-42.
152. Mucenski, M.L., et al., *{beta}-Catenin Is Required for Specification of Proximal/Distal Cell Fate during Lung Morphogenesis.* J. Biol. Chem., 2003. **278**(41): p. 40231-40238.
153. De Langhe, S.P., et al., *Dickkopf-1 (DKK1) reveals that fibronectin is a major target of Wnt signaling in branching morphogenesis of the mouse embryonic lung.* Developmental Biology, 2005. **277**(2): p. 316.
154. Li, C., et al., *Wnt5a Participates in Distal Lung Morphogenesis.* Developmental Biology, 2002. **248**(1): p. 68.
155. Li, C., et al., *Wnt5a regulates Shh and Fgf10 signaling during lung development.* Developmental Biology, 2005. **287**(1): p. 86.
156. Kerr, K.M., *Pulmonary preinvasive neoplasia.* J Clin Pathol, 2001. **54**(4): p. 257-71.
157. Colby, T.V., Wistuba, II, and A. Gazdar, *Precursors to pulmonary neoplasia.* Adv Anat Pathol, 1998. **5**(4): p. 205-15.
158. Linnoila, R.I., et al., *The role of CC10 in pulmonary carcinogenesis: from a marker to tumor suppression.* Ann N Y Acad Sci, 2000. **923**: p. 249-67.
159. Meuwissen, R. and A. Berns, *Mouse models for human lung cancer.* Genes Dev, 2005. **19**(6): p. 643-64.
160. Evans, M.J., L.J. Cabral-Anderson, and G. Freeman, *Role of the Clara cell in renewal of the bronchiolar epithelium.* Lab Invest, 1978. **38**(6): p. 648-53.
161. Borthwick, D.W., et al., *Evidence for stem-cell niches in the tracheal epithelium.* Am J Respir Cell Mol Biol, 2001. **24**(6): p. 662-70.
162. Marshman, E., C. Booth, and C.S. Potten, *The intestinal epithelial stem cell.* Bioessays, 2002. **24**(1): p. 91-8.
163. Vessey, C.J. and P.M. de la Hall, *Hepatic stem cells: a review.* Pathology, 2001. **33**(2): p. 130-41.
164. Cotsarelis, G., T.T. Sun, and R.M. Lavker, *Label-retaining cells reside in the bulge area of pilosebaceous unit: implications for follicular stem cells, hair cycle, and skin carcinogenesis.* Cell, 1990. **61**(7): p. 1329-37.
165. Cotsarelis, G., et al., *Existence of slow-cycling limbal epithelial basal cells that can be preferentially stimulated to proliferate: implications on epithelial stem cells.* Cell, 1989. **57**(2): p. 201-9.
166. Lehrer, M.S., T.T. Sun, and R.M. Lavker, *Strategies of epithelial repair: modulation of stem cell and transit amplifying cell proliferation.* J Cell Sci, 1998. **111 (Pt 19)**: p. 2867-75.
167. Giangreco, A., S.D. Reynolds, and B.R. Stripp, *Terminal Bronchioles Harbor a Unique Airway Stem Cell Population That Localizes to the Bronchoalveolar Duct Junction.* Am J Pathol, 2002. **161**(1): p. 173-182.
168. Giangreco, A., et al., *Molecular Phenotype of Airway Side Population Cells.* Am J Physiol Lung Cell Mol Physiol, 2003.
169. Huelsken, J., et al., *beta-Catenin controls hair follicle morphogenesis and stem cell differentiation in the skin.* Cell, 2001. **105**(4): p. 533-45.
170. Moles, J.P. and F.M. Watt, *The epidermal stem cell compartment: variation in expression levels of E-cadherin and catenins within the basal layer of human epidermis.* J Histochem Cytochem, 1997. **45**(6): p. 867-74.

171. Wong, M.H., et al., *Selection of multipotent stem cells during morphogenesis of small intestinal crypts of Lieberkuhn is perturbed by stimulation of Lef-1/beta-catenin signaling.* J Biol Chem, 2002. **277**(18): p. 15843-50.
172. Reya, T., et al., *A role for Wnt signalling in self-renewal of haematopoietic stem cells.* Nature, 2003. **423**(6938): p. 409-14.
173. Eaves, C.J., *Manipulating hematopoietic stem cell amplification with Wnt.* Nat Immunol, 2003. **4**(6): p. 511-2.
174. Love, R., *Beta-catenin, brains, and beyond.* Lancet Neurol, 2002. **1**(5): p. 272.
175. DasGupta, R. and E. Fuchs, *Multiple roles for activated LEF/TCF transcription complexes during hair follicle development and differentiation.* Development, 1999. **126**(20): p. 4557-68.
176. Gat, U., et al., *De Novo hair follicle morphogenesis and hair tumors in mice expressing a truncated beta-catenin in skin.* Cell, 1998. **95**(5): p. 605-14.
177. Niemann, C., et al., *Expression of DeltaNLef1 in mouse epidermis results in differentiation of hair follicles into squamous epidermal cysts and formation of skin tumours.* Development, 2002. **129**(1): p. 95-109.
178. Watt, F.M., *The stem cell compartment in human interfollicular epidermis.* J Dermatol Sci, 2002. **28**(3): p. 173-80.
179. Hatsell, S., et al., *Beta-catenin and Tcfs in mammary development and cancer.* J Mammary Gland Biol Neoplasia, 2003. **8**(2): p. 145-58.
180. Moon, R.T., et al., *The promise and perils of Wnt signaling through beta-catenin.* Science, 2002. **296**(5573): p. 1644-6.
181. Niemann, C., et al., *Indian hedgehog and beta-catenin signaling: role in the sebaceous lineage of normal and neoplastic mammalian epidermis.* Proc Natl Acad Sci U S A, 2003. **100 Suppl 1**: p. 11873-80.
182. Wagenaar, R.A., H.C. Crawford, and L.M. Matrisian, *Stabilized beta-catenin immortalizes colonic epithelial cells.* Cancer Res, 2001. **61**(5): p. 2097-104.
183. Posthaus, H., et al., *beta-Catenin is not required for proliferation and differentiation of epidermal mouse keratinocytes.* J Cell Sci, 2002. **115**(Pt 23): p. 4587-95.
184. Kuhnert, F., et al., *Essential requirement for Wnt signaling in proliferation of adult small intestine and colon revealed by adenoviral expression of Dickkopf-1.* Proc Natl Acad Sci U S A, 2004. **101**(1): p. 266-71.
185. van den Brink, G.R., et al., *Indian Hedgehog is an antagonist of Wnt signaling in colonic epithelial cell differentiation.* Nat Genet, 2004. **36**(3): p. 277-82.
186. Sato, N., et al., *Maintenance of pluripotency in human and mouse embryonic stem cells through activation of Wnt signaling by a pharmacological GSK-3-specific inhibitor.* Nat Med, 2004. **10**(1): p. 55-63.
187. DasGupta, R., H. Rhee, and E. Fuchs, *A developmental conundrum: a stabilized form of beta-catenin lacking the transcriptional activation domain triggers features of hair cell fate in epidermal cells and epidermal cell fate in hair follicle cells.* J Cell Biol, 2002. **158**(2): p. 331-44.
188. Brault, V., et al., *Inactivation of the beta-catenin gene by Wnt1-Cre-mediated deletion results in dramatic brain malformation and failure of craniofacial development.* Development, 2001. **128**(8): p. 1253-64.

189. Chomczynski, P. and N. Sacchi, *Single-step method of RNA isolation by acid guanidinium thiocyanate-phenol-chloroform extraction.* Anal Biochem, 1987. **162**(1): p. 156-9.
190. Reynolds, S.D., et al., *Molecular and functional properties of lung SP cells.* Am J Physiol Lung Cell Mol Physiol, 2007. **292**(4): p. L972-83.
191. Heid, C.A., et al., *Real time quantitative PCR.* Genome Res, 1996. **6**(10): p. 986-94.
192. Taswell, C., *Limiting dilution assays for the determination of immunocompetent cell frequencies. I. Data analysis.* J Immunol, 1981. **126**(4): p. 1614-9.
193. Ji, H., et al., *K-ras activation generates an inflammatory response in lung tumors.* Oncogene, 2006. **25**(14): p. 2105-12.
194. Simon, D.M., et al., *Epithelial cell PPARgamma is an endogenous regulator of normal lung maturation and maintenance.* Proc Am Thorac Soc, 2006. **3**(6): p. 510-1.
195. Soriano, P., *Generalized lacZ expression with the ROSA26 Cre reporter strain.* Nat Genet, 1999. **21**(1): p. 70-1.
196. Mucenski, M.L., et al., *beta-Catenin is required for specification of proximal/distal cell fate during lung morphogenesis.* J Biol Chem, 2003. **278**(41): p. 40231-8.
197. Harada, N., et al., *Intestinal polyposis in mice with a dominant stable mutation of the beta-catenin gene.* Embo J, 1999. **18**(21): p. 5931-42.
198. Batlle, E., et al., *Beta-catenin and TCF mediate cell positioning in the intestinal epithelium by controlling the expression of EphB/ephrinB.* Cell, 2002. **111**(2): p. 251-63.
199. Bienz, M. and H. Clevers, *Linking colorectal cancer to Wnt signaling.* Cell, 2000. **103**(2): p. 311-20.
200. Ohgaki, H., et al., *APC mutations are infrequent but present in human lung cancer.* Cancer Lett, 2004. **207**(2): p. 197-203.
201. Schmidt, G.H., D.J. Winton, and B.A. Ponder, *Development of the pattern of cell renewal in the crypt-villus unit of chimaeric mouse small intestine.* Development, 1988. **103**(4): p. 785-90.
202. Watt, F.M., *Epidermal stem cells: markers, patterning and the control of stem cell fate.* Philos Trans R Soc Lond B Biol Sci, 1998. **353**(1370): p. 831-7.
203. Jamora, C., et al., *Links between signal transduction, transcription and adhesion in epithelial bud development.* Nature, 2003. **422**(6929): p. 317-22.
204. Barker, N., et al., *Restricted high level expression of Tcf-4 protein in intestinal and mammary gland epithelium.* Am J Pathol, 1999. **154**(1): p. 29-35.
205. Pinto, D., et al., *Canonical Wnt signals are essential for homeostasis of the intestinal epithelium.* Genes Dev, 2003. **17**(14): p. 1709-13.
206. Shu, W., et al., *Wnt/beta-catenin signaling acts upstream of N-myc, BMP4, and FGF signaling to regulate proximal-distal patterning in the lung.* Dev Biol, 2005. **283**(1): p. 226-39.
207. Warburton, D., et al., *The molecular basis of lung morphogenesis.* Mech Dev, 2000. **92**(1): p. 55-81.
208. Dean, C.H., et al., *Canonical Wnt signaling negatively regulates branching morphogenesis of the lung and lacrimal gland.* Dev Biol, 2005. **286**(1): p. 270-86.
209. Derynck, R. and Y.E. Zhang, *Smad-dependent and Smad-independent pathways in TGF-beta family signalling.* Nature, 2003. **425**(6958): p. 577-84.
210. Saika, S., et al., *Expression of Smad7 in Mouse Eyes Accelerates Healing of Corneal Tissue after Exposure to Alkali.* Am J Pathol, 2005. **166**(5): p. 1405-1418.

211. Yang, X., et al., *Generation of Smad4/Dpc4 conditional knockout mice.* Genesis, 2002. **32**(2): p. 80-1.
212. Hoyle, G.W., et al., *Hyperinnervation of the airways in transgenic mice overexpressing nerve growth factor.* Am J Respir Cell Mol Biol, 1998. **18**(2): p. 149-57.
213. Bhaskaran, M., et al., *Trans-differentiation of Alveolar Epithelial Type II Cells to Type I Cells Involves Autocrine Signaling by Transforming Growth Factor beta1 through the Smad Pathway.* J Biol Chem, 2007. **282**(6): p. 3968-76.
214. Chu, G.C., et al., *Differential requirements for Smad4 in TGFbeta-dependent patterning of the early mouse embryo.* Development, 2004. **131**(15): p. 3501-12.
215. Li, W., et al., *Squamous cell carcinoma and mammary abscess formation through squamous metaplasia in Smad4/Dpc4 conditional knockout mice.* Development, 2003. **130**(24): p. 6143-53.
216. Bardeesy, N., et al., *Smad4 is dispensable for normal pancreas development yet critical in progression and tumor biology of pancreas cancer.* Genes Dev, 2006. **20**(22): p. 3130-46.
217. Wang, R.H., et al., *A role of SMAD4 in iron metabolism through the positive regulation of hepcidin expression.* Cell Metab, 2005. **2**(6): p. 399-409.
218. Massague, J. and R.R. Gomis, *The logic of TGF[beta] signaling.* FEBS Letters, 2006. **580**(12): p. 2811.
219. Sapkota, G., et al., *Dephosphorylation of the Linker Regions of Smad1 and Smad2/3 by Small C-terminal Domain Phosphatases Has Distinct Outcomes for Bone Morphogenetic Protein and Transforming Growth Factor-beta Pathways.* J. Biol. Chem., 2006. **281**(52): p. 40412-40419.
220. Massague, J., *Integration of Smad and MAPK pathways: a link and a linker revisited.* Genes Dev, 2003. **17**(24): p. 2993-7.
221. Howe, J.R., et al., *The prevalence of MADH4 and BMPR1A mutations in juvenile polyposis and absence of BMPR2, BMPR1B, and ACVR1 mutations.* J Med Genet, 2004. **41**(7): p. 484-91.
222. Schneider, G. and R.M. Schmid, *Genetic alterations in pancreatic carcinoma.* Mol Cancer, 2003. **2**: p. 15.
223. Alberici, P., et al., *Smad4 haploinsufficiency in mouse models for intestinal cancer.* Oncogene, 2006. **25**(13): p. 1841-51.
224. Yang Kang, J.M.M.J.A.T.W.M.B.A.D.L.M.W.S.B.J., *Enhanced tumorigenesis and reduced transforming growth factor-? type II receptor in lung tumors from mice with reduced gene dosage of transforming growth factor-?1.* Molecular Carcinogenesis, 2000. **29**(2): p. 112-126.
225. Borczuk, A.C., et al., *Lung Adenocarcinoma Global Profiling Identifies Type II Transforming Growth Factor-{beta} Receptor as a Repressor of Invasiveness.* Am. J. Respir. Crit. Care Med., 2005. **172**(6): p. 729-737.
226. Munoz, N.M., et al., *Transforming growth factor beta receptor type II inactivation induces the malignant transformation of intestinal neoplasms initiated by Apc mutation.* Cancer Res, 2006. **66**(20): p. 9837-44.
227. Forrester, E., et al., *Effect of conditional knockout of the type II TGF-beta receptor gene in mammary epithelia on mammary gland development and polyomavirus middle T antigen induced tumor formation and metastasis.* Cancer Res, 2005. **65**(6): p. 2296-302.

228. Chytil, A., et al., *Conditional inactivation of the TGF-beta type II receptor using Cre:Lox.* Genesis, 2002. **32**(2): p. 73-5.
229. Li, D., et al., *Bronchial and peripheral murine lung carcinomas induced by T790M-L858R mutant EGFR respond to HKI-272 and rapamycin combination therapy.* Cancer Cell, 2007. **12**(1): p. 81-93.
230. Ten Have-Opbroek, A.A. and E.C. De Vries, *Clara cell differentiation in the mouse: ultrastructural morphology and cytochemistry for surfactant protein A and Clara cell 10 kD protein.* Microsc Res Tech, 1993. **26**(5): p. 400-11.
231. Besnard, V., et al., *Stage-specific regulation of respiratory epithelial cell differentiation by Foxa1.* Am J Physiol Lung Cell Mol Physiol, 2005. **289**(5): p. L750-9.
232. Massaro, G.D., L. Davis, and D. Massaro, *Postnatal development of the bronchiolar Clara cell in rats.* Am J Physiol, 1984. **247**(3 Pt 1): p. C197-203.
233. Reynolds, S.D., et al., *Secretoglobins SCGB3A1 and SCGB3A2 define secretory cell subsets in mouse and human airways.* Am J Respir Crit Care Med, 2002. **166**(11): p. 1498-509.
234. Pilette, C., et al., *Reduced epithelial expression of secretory component in small airways correlates with airflow obstruction in chronic obstructive pulmonary disease.* Am J Respir Crit Care Med, 2001. **163**(1): p. 185-94.
235. Reynolds, S.D., et al., *Airway injury in lung disease pathophysiology: selective depletion of airway stem and progenitor cell pools potentiates lung inflammation and alveolar dysfunction.* Am J Physiol Lung Cell Mol Physiol, 2004. **287**(6): p. L1256-65.
236. Rodrigo, L., et al., *Immunohistochemical evidence for the expression and induction of paraoxonase in rat liver, kidney, lung and brain tissue. Implications for its physiological role.* Chem Biol Interact, 2001. **137**(2): p. 123-37.
237. Janmohamed, A., et al., *Cell-, tissue-, sex- and developmental stage-specific expression of mouse flavin-containing monooxygenases (Fmos).* Biochemical Pharmacology, 2004. **68**(1): p. 73.
238. Terao, M., et al., *Cloning of the cDNAs Coding for Two Novel Molybdo-flavoproteins Showing High Similarity with Aldehyde Oxidase and Xanthine Oxidoreductase.* J. Biol. Chem., 2000. **275**(39): p. 30690-30700.
239. Van Itallie, C.M., et al., *Two splice variants of claudin-10 in the kidney create paracellular pores with different ion selectivities.* Am J Physiol Renal Physiol, 2006. **291**(6): p. F1288-99.
240. Inai, T., et al., *Heterogeneity in expression and subcellular localization of tight junction proteins, claudin-10 and -15, examined by RT-PCR and immunofluorescence microscopy.* Arch Histol Cytol, 2005. **68**(5): p. 349-60.
241. Weston, W.M., et al., *Differential Display Identification of plunc, a Novel Gene Expressed in Embryonic Palate, Nasal Epithelium, and Adult Lung.* J. Biol. Chem., 1999. **274**(19): p. 13698-13703.